Environmental management in semi-enclosed seas
（閉鎖性海域における環境管理）

学位取得年月 2019 年 09 月

王 峰

List of Contents

Acknowledgments

This research on environmental management in semi-enclosed seas would have been impossible without the help of many excellent people. It takes a whole village to raise a graduate student should be a common saying. The people thanked below are only a few who made it that.

To my advisors, Professor Satoshi Nakai and Professor Nishijima Wataru, I cannot express how grateful I am for your guidance, generosity, patience and consistent encouragement for the past 3 years. Thank you for providing me with opportunities to pursue multiple academic interests at Hiroshima University. I am honored to be your student and have learned so much from both of you. Your positive outlook and unwavering faith in this research and my ability to complete the work were invaluable.

To the rest of my PhD committee: Professor Sakai, Professor Fukui and Professor Goto for their time reviewing this thesis and valuable advice and comments on this research.

To staff and members of Environmental Research and Management Center (ERMC): Ohno Sensei, Umehara Sensei, Hashimoto Sensei, Shibata Sense, Yagi San, Sakashita San, Shimogori San and Koumoto San for helping me preparing various important documents related to my life and study in Hiroshima University and many other invaluable science and life advice and instrument help along the way. Umehara Sensei deserves a special thanks for generously sharing his time and valuable insights, helping search for information related to my research, all of these led me to a better understanding on filed survey, lab experiments in Japan and my work.

To Marine Research Class members, Umehara Sensei, Sekito San, Miyagawa San, Yoshimori San, Yota San, Yoshihara San and Harada San for all the help during my research. Thank you for the accompany, statistical knowledge and advice, positive and entertaining comments and great help in my Japanese study. I will miss our various academic seminars.

To other past and current members of Green Process Engineering Lab, Nakawatase San, Uchita San, Nishimoto San, Kubota San, Marushima San, Onzuka San, Miura San - thank you for all your help and support over the years.

To faculty and staff of the Graduate School of Engineering at Hiroshima University, for their generous support. I'll always be grateful for the incredible opportunities they provided me. To staff of Student Plaza for their kind help in my international conferences.

To Japan Student Support Office (JASSO) for their scholarship from October 2016 to March 2017 and from April 2019 to September 2019.

Last, but definitely not least, to my family, for all their love, immeasurable support and encouragement throughout this process. Your many contributions made my Ph.D. study in Japan possible.

This work was supported by grant from the Environment Research and Technology Development Fund of the Ministry of the Environment, Japan (S-13). I am grateful to the Ministry of the Environment and the Ministry of Land, Infrastructure, Transport and Tourism, Japan, for supplying data from their investigation of Tokyo Bay, Ise Bay and the Seto Inland Sea in Chapter 2, Chapter 3 and Chapter 4; to Fisheries & Marine Technology Center, Hiroshima Prefectural Technology Research Institute for supplying data from their investigation of Hiroshima Bay; to Environmental Consultants for Ocean and Human Corporation for providing the nutrient loading data of the Seto Inland Sea in Chapter 4 and high resolution Secchi depth in Chapter 5; to the Hydrographic and Oceanographic Department, Japan Coast Guard for providing the high resolution water depth in Chapter 5.

Feng Wang

June 2019

Abstract

Eutrophication has become a primary threat to many coastal ecosystems since the second half of last century. Following three or four decades of effort to revert this issue, evidences of ecosystem recovery are growing. Nevertheless, many ecosystems have not met their recovery potential yet. What's more, new problems have emerged in recent years, for instance, reductions in the annual fishery landings in some ecosystems due to decrease in the primary production. All of these suggest that our environmental managements need to be reviewed. The question of why different ecosystems response differently to nutrient loading reductions also need to be answered. Here we explored the region-specific water clarity and phytoplankton biomass baselines in the context of anthropogenic nutrient loading reductions in some semi-encolsed seas to obtain better environmental management targets. In addition, we assessed the potential of eelgrass bed recovery and its effectiveness in controlling phytoplankton in an eutrophic estuarine area.

Region-specific background Secchi depth (BSD) provides valuable information on light availability in aquatic ecosystems. We estimated BSD in Tokyo Bay and Ise Bay and the Seto Inland Sea based on monitoring data collected in the period 1981–2015. BSD values were successfully obtained in 89–96%, 67–94% and 19-67% of monitoring sites in Tokyo Bay, Ise Bay and the Seto Inland Sea, respectively. Low BSD values were obtained in the innermost regions of these semi-enclosed seas, adjacent to the estuaries of large rivers. BSD was positively correlated with salinity in these seas, indicating that river-supplied substances, including tripton and/or colored dissolved organic matter, strongly influenced BSD values. Although the highest chlorophyll *a* concentrations were measured in the innermost sectors of these seas, the proportional contribution of phytoplankton to light attenuation was surprisingly low in comparison with other sectors. Moreover, the average estimated proportional light attenuation of phytoplankton was <40% in all these seas, indicating that background factors played a dominant role even in these highly eutrophic waters. Determinations of Secchi depth, BSD, and the proportional contributions of phytoplankton and background factors to light attenuation will improve understanding of the aquatic light environment, which in turn will inform the development of rational coastal management practices.

Water quality had been improved in most areas of the Seto Inland Sea, harmful algal blooms were still frequently observed in some regions of the sea. Based on a nonlinear perspective and an empirical approach with several natural environmental factors, a novel indicator, vulnerable index, was established to estimate surface chlorophyll *a* (Chl.*a*) concentration in the Seto Inland Sea with long-term monitoring records during the period 2003–2012. Results suggested that models that included both salinity and water clarity were more predictive than that did not. The inclusion of distance to coast or water stability resulted in further improvement of model performance, whereas the improvements were limited. Highest Vulnerable Index were observed in the coastal regions of Osaka bay, Harima Nada, Hiroshima Bay and lowest Vulnerable Index in Aki Nada, Iyo Nada, offshore area of Suo Nada and two channels connecting the Pacific Ocean. We also found that the coastal areas with highest Vulnerable Index coincide with the areas adjacent to highly populated watersheds, indicating that high natural potential for phytoplankton growth as well as high anthropogenic nutrient input from neighboring residences combined to result in the frequent red tide occurrence in the areas mentioned above. Vulnerable Index provide a simple and clearly defined way to identify vulnerable coastal zone in nature to phytoplankton growth. We suggest that vulnerable index be incorporated in future decision-making process and different management measures be implemented according to the property of VI in different water bodies of the Seto Inland Sea.

Water quality data from 1981–2015 were used to elucidate the spatiotemporal distributions of Chl.*a* concentration and Secchi depth in the west-central Seto Inland Sea, Japan. The results revealed that salinity and distance from the northern coastline were the main factors for predicting Chl.*a* concentration and Secchi depth, respectively. Significant differences in both of these were observed between subareas in spring, summer and autumn; differences were insignificant in winter. Chl.*a* concentrations have decreased for the past 35 years, while their extent differed in the subareas. A greater rate of decrease in Chl.*a* concentration was observed in the innermost Hiroshima Bay in spring, compared with other subareas, while no significant difference in different subareas was found in other seasons. Secchi depth has increased for the past 35 years, but no significant difference in its rate of increase was found among different subareas in all seasons. Total nitrogen (TN) loading better explained changes in mean Chl.*a* concentration than total phosphorus (TP) throughout the west-central Seto Inland Sea. Phytoplankton’s contributions to light attenuation were low in the west-central Seto Inland Sea, indicating that the nutrient loading reduction programme has been of limited effectiveness in improving water clarity.

Eelgrass beds are highly productive and support diverse faunal assemblages; they also take in nutrients from the water and prevent excessive phytoplankton growth in eutrophic coastal waters through the reduction of available nutrients. Despite its importance, the global distribution of eelgrass has declined worldwide. In eutrophic areas with high Chl.*a* concentrations, natural recovery of eelgrass beds after eutrophication is possible. To facilitate this, sufficient water clarity can be reached after a large enough decrease in phytoplankton concentration. In this study, we proposed a novel indicator for the maximum possible Secchi depth (MPSD), defined as the Secchi depth when the Chl.*a* concentration is equal to a reference Chl.*a* concentration. We applied the MPSD to evaluate water clarity improvements through the reduction of terrigenous anthropogenic nutrient loading. We found that phytoplankton did not control water clarity in the study area, which was instead controlled by background factors. Therefore, improvements in water clarity would not be expected after reducing terrigenous anthropogenic nutrient loading. The habitat of *Zostera marina* is determined by light availability, so we investigated a potential area with ≥20% surface irradiance and *Z. marina* existed in 27% of it (100–373 ha). The maximum recovery by Secchi depth improvements to the MPSD was estimated at 36 ha. The impact of eelgrass recovery and expansion on phytoplankton growth from May to September was evaluated by a mathematical model under two scenarios: the current eelgrass distribution (100 ha) and potential maximum eelgrass distribution (370 ha). The decrease in Chl.*a* concentration to 1.0–3.0 μg l^{-1} was achieved in an area originally with 4.0 to 7.0 μg l^{-1} of Chl.*a* from May to July; this improvement decreased with time. These evaluation methods and findings could help us gain a better understanding of the nutrient management in seagrass-vegetated semi-enclosed seas subjected to anthropogenic nutrient input.

List of Tables

Chapter 2

Chapter 3

Chapter 4

Chapter 5

List of Figures

Chapter 1

Chapter 2

Chapter 3

Chapter 4

Chapter 5

Chapter 1: Preface

1.1 Introduction

Coastal areas are home to around one third of the world's population and over 70% of the world's mega-cities (> 8 million inhabitants) are located in coastal areas (Vandeweerd et al. 2002, http://population.city/world/, Figure 1.1). Estuaries and coastal seas have long been the focal points of marine resource use. They provide more values and services related to human well-being than any other ecosystem type (Millennium Ecosystem Assessment 2005). Coastal ecosystems habitat almost 80% of known marine fish species and yield 90% of global fisheries (Vandeweerd et al. 2002). In addition, a range of coastal ecosystems (e.g. sand beaches, marshes, mangroves, coral reefs, and seagrass beds) provide many other important ecosystems services including shoreline protection, pollution control, nutrient cycling and carbon storage (Orth et al. 2006, Barbier et al. 2011).

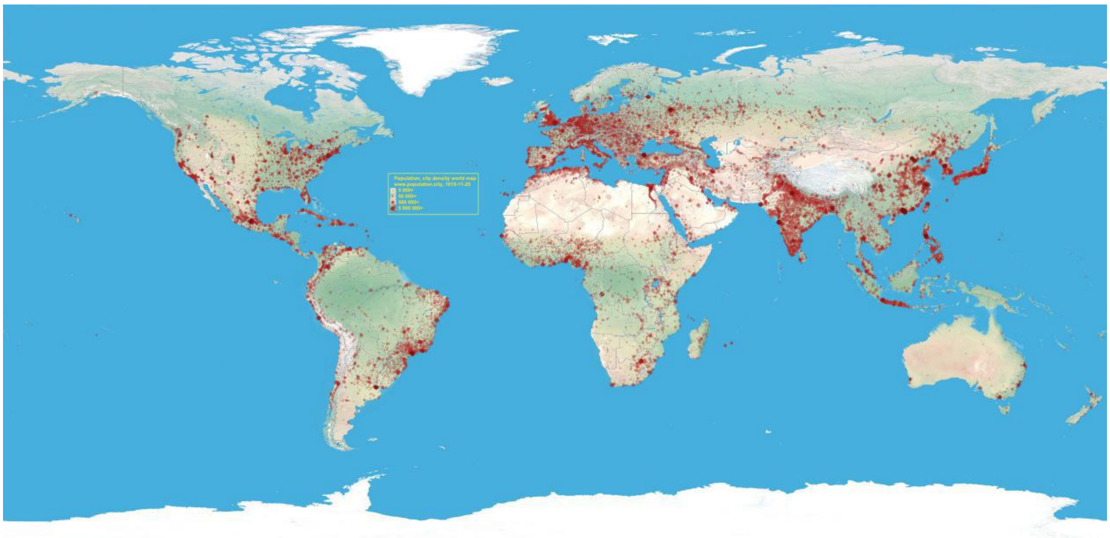

Figure 1.1 World Population map (http://population.city/world/)

Despite the importance of coastal ecosystems, many human activities, including nutrient pollution, shoreline construction and trawling fisheries, have lead to widespread deterioration of these systems (Lotze et al. 2006, Halpern et al. 2008, Barbier et al. 2011). Globally, half of the salt marshes and one third of mangroves, coral reefs and seagrass beds have been either lost or degraded (Valiela et al. 2001, Millennium Ecosystem Assessment 2005, Waycott et al. 2009). Meanwhile, lots of associated ecosystem services they provide were lost.

Among the threats facing coastal ecosystems, eutrophication has been the primary one throughout the world (Smith 2003, Selman et al. 2008, Rablais et al. 2009, McCrackin et al. 2017, Figure 1.2). Eutrophication stimulates blooms of phytoplankton and macroalgae (Cloern 2001, Duarte et al. 2013), which affect the system in several ways. The elevated phytoplankton biomass reduce water clarity and light availability of the benthic environment, threatening the survival of growth of submerged aquatic vegetation and benthic microalgae (Kraufvelin et al. 2006, Lefcheck et al. 2018). As the phytoplankton and macroalgae die and decompose, dissolved oxygen was consumed, which could adversely impact the local fauna both directly and indirectly via accumulation of toxic hydrogen sulfide (Gray et al. 2002). Besides, some phytoplankton species produce toxins that can pose health threats to wildlife and humans (Anderson et al. 2002, Imai et al. 2006, Chen et al. 2019).

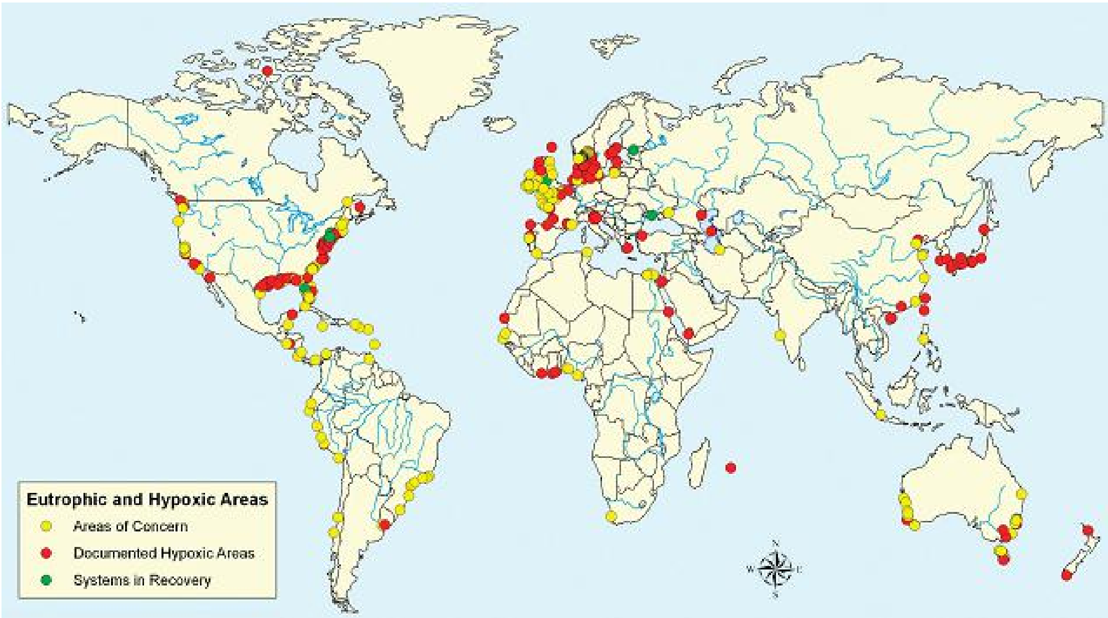

Figure 1.2 World eutrophic and hypoxic area (Selman et al. 2008)

Reducing anthropogenic nutrient input has been considered as the necessary first step to address eutrophication (McCrackin et al. 2017). A variety of national and international nutrient management projects have been implemented following the eutrophication in coastal waters, such as the Action Plan for the Aquatic Environment in relation to Danish coastal waters (Riemann et al. 2016), a Total Pollutant Load Control System (TPLCS) in Japanese enclosed waters including the Seto Inland Sea (Nakai et al. 2018), the Baltic Sea Action Plan (BSAP) in the Baltic Sea (Backer et al.

2010) and European Water Framework Directives in European coastal waters (Kallis and Butler 2001). Evidences of ecosystem recovery are growing after three decades of efforts to revert widespread eutrophication. Alleviation of eutrophication, that is, improvement in nutrients, Chl.*a*, dissolved oxygen concentrations and seagrass cover, have appeared (Riemann et al. 2016, Andersen et al. 2017, Lefcheck et al. 2018, Nishijima et al. 2018), that are direct consequence of long-term efforts to reduce nutrient inputs. In Tampa Bay, USA, total nitrogen, Chl.a concentration, dissolved oxygen, water clarity and seagrass coverage improved greatly following continuing nutrient management actions and the above water quality indicators were approaching conditions observed before large human population increase in the 1950s (Greening et al. 2014). In Chesapeake Bay, long-term nutrient reductions, had enlarged the seagrass coverage to 17,000 ha, the highest cover in almost half a century (Lefcheck et al. 2017). In Danish coastal waters, reductions in nutriment input from land resulted in parallel declines in nutrient, Chl.a concentrations and increased coverage of seagrass and macroalgae in deeper waters (Riemann et al. 2016). Effects of nutrient reductions had also appeared in the Seto Inland Sea, Japan. Harmful algal blooms have been controlled to a large extent in most coastal area and annual red tide frequency has declined from 299 in 1976 to around 100 after 1990 (Imai et al. 2006). Water clarity was improved from 6.4 m in the 1980s to 7.3 m in the 2000s (Nishijima et al. 2015).

Despite the efforts to mitigate the influence of anthropogenic inputs and restore lost ecosystem functionality, many ecosystems have not met their recovery potential yet (Figure 1.3, Duarte et al. 2013). In addition, due to the scarce of long-term, large-scale and effective restoration to validate ongoing management actions, the recommendation are often guided more by theory than empirical evidence, which sometimes leads to less-than desirable outcomes. Existing studies found that eutrophication and recovery following different non-linear pathways (Duarte et al. 2013) and once the ecosystem is altered by eutrophication, the nature of feedbacks is altered and difficult to re-establish (Kemp et al. 2005, Moksnes et al. 2018). Moreover, cumulative pressures have developed in parallel to eutrophication, which counteract the efforts to mitigate eutrophication to some extent (Carstensen et al. 2011, Duarte and Krause-Jensen 2018). These additional pressures include global warming, ocean acidification and increased runoff (Sinha et al. 2017, Duarte and Krause-Jensen 2018). What's more, following the implementation of nutrient loading reduction projects, new problems have become public concerns in recent years, for instance, discoloration of Nori and Wakame seaweed and reductions in the annual fishery landings in the Seto Inland Sea (Fisheries Agency of Japan, 2016). Since nitrogen and phosphorus are essential nutrients for the growth of primary producers, such as phytoplankton, macroalgae and seagrass, increases and decreases in primary producers would produce direct and indirect effects on fishery landings in coastal areas (Yamamoto 2003). These suggest that the nutrient management projects need to be reviewed.

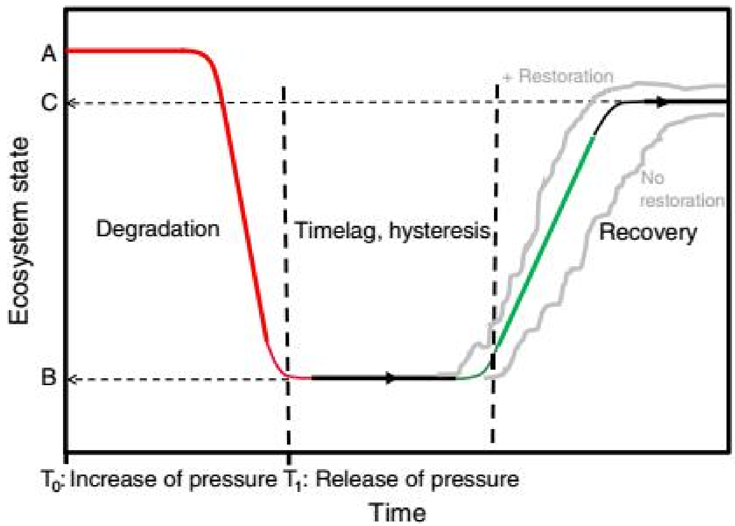

Figure 1.3 Changes in ecosystem state (A: pre-disturbance state, B: degraded state, C: recovered state) with increase and release of pressures (Duarte et al. 2015)

Enclosed or semi-enclosed seas are featured by high primary and fish productivity. Whereas, due to poor exchange of water, they are also more sensitive to anthropogenic stress than other kinds of open coastal ecosystems. Here we present the data-driven analysis and predictions on the environmental management in three semi-enclosed sea: Tokyo Bay and Ise Bay and the Seto Inland Sea (Figure 1.4), which are among the most consistently studied and managed coastal regions in the world. The management of semi-enclosed seas have undergone a major and positive shift from water quality control to environmental remediation and restoration of habitat, which aimed at realizing a beautiful and bountiful sea (Nakai et al., 2018). Under the new management framework, restoration of seagrass and seaweed beds constituted an important part, which would rely much on the improvement of water clarity. Secchi depth is a traditional metric of water clarity and has been widely used in various aquatic systems. It is also used as a metric of eutrophication due to its relationship to phytoplankton biomass because of its relationship to the depth of euphotic zone (HELCOM 2006). Furthermore, Secchi depth has also been related to maximum depth of submerged aquatic vegetation (Dennison et al. 1993). Therefore, Secchi depth has been considered as an importance indicator of the status of aquatic systems. Nevertheless, water clarity and light attenuation are affected not only by phytoplankton but also by suspended sestons, chromophoric dissolved organic matter and the water (Devlin et al. 2008). The latter ones are little influenced by the changes of eutrophication. Therefore, alleviation of eutrophication achieved by the reductions in anthropogenic nutrient loadings and consequent reduction in phytoplankton biomass do not result in a significant improvement in water clarity in shallow coastal areas (Riemann et al. 2016). Hence we require a new indicator to determine the improvement potential of water clarity with alleviation of eutrophication in coastal areas.

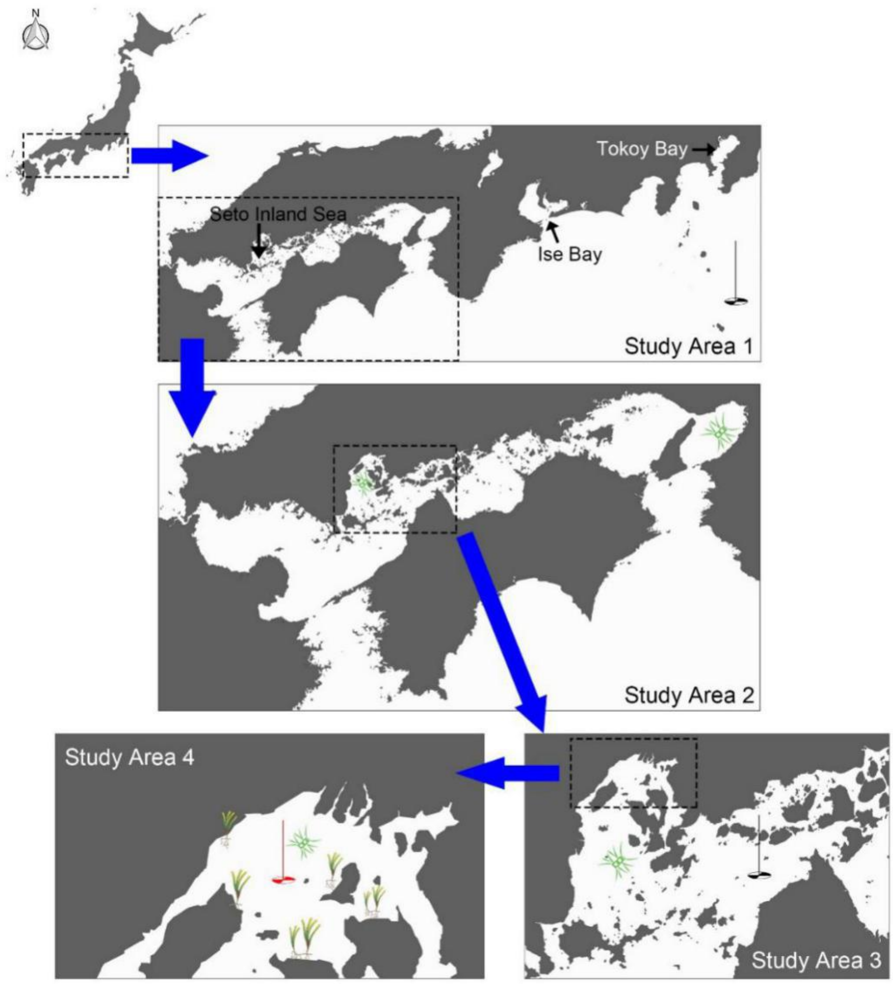

Figure 1.4 Study area in different chapters of this dissertation

Another issues with changes in eutrophication is the marked changes in primary producers and primary production. Stable and appropriate primary production is essential to sustain the healthy functioning of ecosystems and the sustainable supply of fishery resources. However, excessive phytoplankton growth must be controlled or reduced due to its huge detriment to the whole ecosystem mentioned before. Despite the significant reductions in anthropogenic nutrient loading, red tides still frequently occur in some nearshore areas of the semi-enclosed seas, implying that some natural factors play important roles in the outbreaks of phytoplankton bloom and determine the baseline phytoplankton biomass in these areas. The baseline phytoplankton biomass that could be supported by a subarea should be studied for both a better understanding on the region-specific phytoplankton growth potential and more scientific coastal management practice.

Eelgrass beds are highly productive and support diverse faunal assemblages by providing ideal habitats for many commercial fishes and reducing the vulnerability of juveniles to piscivorous predators. They could prevent excessive phytoplankton growth in eutrophic coastal waters through the competition of available nutrients. These above crucial ecosystem services provided by eelgrass beds keep them in focus of many coastal management projects. The reduction in nutrient loadings is expected to aid the recovery of eelgrass beds due to a projected improvement in water clarity. However, management plans for eutrophic coastal waters need to be constructed with careful assessment on the potential for eelgrass recovery and extension through the improvement of light availability of the water column. Moreover, the impact of eelgrass recovery and expansion on control of the growth of phytoplankton after nutrient reduction should be evaluated.

1.2 Objectives

This research aims to:

1. determine the improvement potential of water clarity by nutrient loading management and the phytoplankton's contribution to light attenuation for helping evaluate the effectiveness of nutrient loading reduction on water clarity improvement via reducing phytoplankton biomass in Tokyo Bay, Ise Bay and the Seto Inland Sea;
2. establish a vulnerable index to determine the baseline phytoplankton biomass and help identify the management priority coastal regions that are easily influenced by

eutrophication and red tides and access how phytoplankton in different coastal waters responses to natural factors and facilitate future assessment, monitoring and management of the Seto Inland Sea and other coastal seas in the world;

3. identify the primary factors regulating Chl.a concentration and Secchi depth in the west-central Seto Inland Sea (Hiroshima Bay and Aki Nada), as well as their decadal changes with decreasing anthropogenic nutrient loadings;

4. determine the maximum possible water clarity that could be reached after the reduction of anthropogenic nutrient loadings and evaluate the impact of eelgrass beds recovery and expansion on control of phytoplankton growth in the northern Hiroshima Bay.

1.3 Research flow

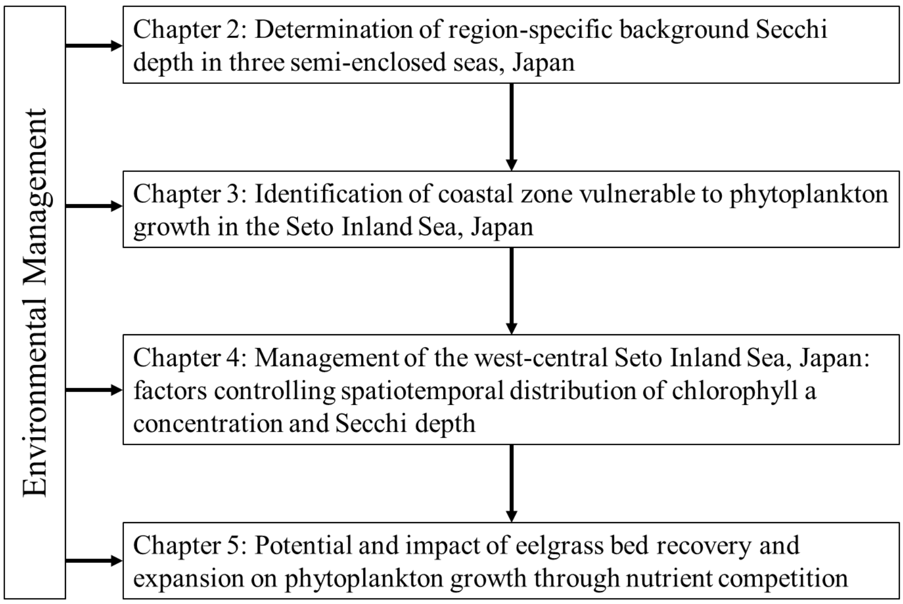

Figure 1.5 Schematic diagram of the research in this dissertation

Chapter 1 was the preface, which included a brief introduction on the 1) importance of coastal seas, 2) degradation of coastal seas, 3) progress in coastal recovery, 4) objectives of the research and 5) the research flow.

Chapter 2 determined the improvement potential of water clarity and the phytoplankton's contribution to light attenuation in several semi-enclosed seas with different nutrient loadings in order to evaluate the influence of nutrient management on light condition in these coastal ecosystems and obtain a proper light condition recovery target for management.

Chapter 3 established a novel index to identify definitive natural factors influencing phytoplankton growth and the coastal regions vulnerable to phytoplankton growth in the Seto Inland Sea for a better management resource allocation.

Based on vulnerable zone (management priority zone) identified from Chapter 3, we took west-central Seto Inland Sea as an example area for deep and regional environmental management methods development in Chapter 4 and Chapter 5.

Chapter 4 identified the primary factors regulating Chl.a concentration and Secchi depth in the west-central Seto Inland Sea, as well as their temporal changes in different subregions, from which we obtain the area demonstrating clear response to TPLCS and its underpinning mechanism.

Chapter 5 determined the maximum possible water clarity that could be reached after the relief of anthropogenic nutrient loadings and evaluated the effectiveness of eelgrass beds recovery and expansion on phytoplankton growth inhibition in the eutrophic northern Hiroshima Bay.

1.4 References

Andersen, J.H., Carstensen, J., Conley, D.J., Dromph, K., Fleming - Lehtinen, V., Gustafsson, B.G., Josefson, A.B., Norkko, A., Villnäs, A., Murray, C., 2017. Long - term temporal and spatial trends in eutrophication status of the Baltic Sea. Biological Reviews 92, 135-149.

Anderson, D.M., Glibert, P.M., Burkholder, J.M., 2002. Harmful algal blooms and eutrophication: nutrient sources, composition, and consequences. Estuaries 25, 704-726.

Backer, H., Leppänen, J.-M., Brusendorff, A.C., Forsius, K., Stankiewicz, M., Mehtonen, J., Pyhälä, M., Laamanen, M., Paulomäki, H., Vlasov, N., 2010. HELCOM Baltic Sea Action Plan–a regional programme of measures for the marine environment based on the ecosystem approach. Marine pollution bulletin 60, 642-649.

Barbier, E.B., Hacker, S.D., Kennedy, C., Koch, E.W., Stier, A.C., Silliman, B.R., 2011. The value of estuarine and coastal ecosystem services. Ecological monographs 81, 169-193.

Carstensen, J., Sánchez-Camacho, M., Duarte, C.M., Krause-Jensen, D., Marba, N., 2011. Connecting the dots: responses of coastal ecosystems to changing nutrient concentrations. Environmental Science & Technology 45, 9122-9132.

Chen, Z.-F., Zhang, Q.-C., Kong, F.-Z., Liu, Y., Zhao, Y., Zhou, Z.-X., Geng, H.-X., Dai, L., Zhou, M.-J., Yu, R.-C., 2019. Resolving phytoplankton taxa based on high-throughput sequencing during brown tides in the Bohai Sea, China. Harmful Algae 84, 127-138.

Cloern, J.E., 2001. Our evolving conceptual model of the coastal eutrophication problem. Marine ecology progress series 210, 223-253.

Dennison, W.C., Orth, R.J., Moore, K.A., Stevenson, J.C., Carter, V., Kollar, S., Bergstrom, P.W., Batiuk, R.A., 1993. Assessing water quality with submersed aquatic vegetation. BioScience 43, 86-94.

Devlin, M., Barry, J., Mills, D., Gowen, R., Foden, J., Sivyer, D., Tett, P., 2008. Relationships between suspended particulate material, light attenuation and Secchi depth in UK marine waters. Estuarine, Coastal and Shelf Science 79, 429-439.

Duarte, C.M., Krause-Jensen, D., 2018. Intervention options to accelerate ecosystem recovery from coastal eutrophication. Frontiers in Marine Science 5, 470.

Gray, J.S., Wu, R.S.-s., Or, Y.Y., 2002. Effects of hypoxia and organic enrichment on the coastal marine environment. Marine ecology progress series 238, 249-279.

Halpern, B.S., Walbridge, S., Selkoe, K.A., Kappel, C.V., Micheli, F., D'agrosa, C., Bruno, J.F., Casey, K.S., Ebert, C., Fox, H.E., 2008. A global map of human impact on marine ecosystems. Science 319, 948-952.

HELCOM., 2006. Development of tools for assessment of eutrophication in the Baltic Sea. Baltic Marine Environment Protection Commission-Helsinki Commission.

Imai, I., Yamaguchi, M., Hori, Y., 2006. Eutrophication and occurrences of harmful algal blooms in the Seto Inland Sea, Japan. Plankton and Benthos Research 1, 71-84.

Kallis, G., Butler, D., 2001. The EU water framework directive: measures and implications. Water policy 3, 125-142.

Kemp, W.M., Boynton, W.R., Adolf, J.E., Boesch, D.F., Boicourt, W.C., Brush, G., Cornwell, J.C., Fisher, T.R., Glibert, P.M., Hagy, J.D., 2005. Eutrophication of Chesapeake Bay: historical trends and ecological interactions. Marine Ecology Progress Series 303, 1-29.

Kraufvelin, P., Salovius, S., Christie, H., Moy, F.E., Karez, R., Pedersen, M.F., 2006. Eutrophication-induced changes in benthic algae affect the behaviour and fitness of the marine amphipod Gammarus locusta. Aquatic Botany 84, 199-209.

Lefcheck, J.S., Orth, R.J., Dennison, W.C., Wilcox, D.J., Murphy, R.R., Keisman, J., Gurbisz, C., Hannam, M., Landry, J.B., Moore, K.A., 2018. Long-term nutrient reductions lead to the unprecedented recovery of a temperate coastal region. Proceedings of the National Academy of Sciences 115, 3658-3662.

Lotze, H.K., Lenihan, H.S., Bourque, B.J., Bradbury, R.H., Cooke, R.G., Kay, M.C., Kidwell, S.M., Kirby, M.X., Peterson, C.H., Jackson, J.B., 2006. Depletion, degradation, and recovery potential of estuaries and coastal seas. Science 312, 1806-1809.

McCrackin, M.L., Jones, H.P., Jones, P.C., Moreno‐Mateos, D., 2017. Recovery of lakes and coastal marine ecosystems from eutrophication: A global meta‐analysis. Limnology and Oceanography 62, 507-518.

Millennium Ecosystem Assessment, M., 2005. Ecosystems and human well-being. Synthesis.

Moksnes, P.-O., Eriander, L., Infantes, E., Holmer, M., 2018. Local regime shifts prevent natural recovery and restoration of lost eelgrass beds along the Swedish west coast. Estuaries and coasts, 1-20.

Nakai, S., Soga, Y., Sekito, S., Umehara, A., Okuda, T., Ohno, M., Nishijima, W., Asaoka, S., 2018. Historical changes in primary production in the Seto Inland Sea, Japan, after implementing regulations to control the pollutant loads. Water Policy 20, 855-870.

Nishijima, W., Umehara, A., Okuda, T., Nakai, S., 2015. Variations in macrobenthic community structures in relation to environmental variables in the Seto Inland Sea, Japan. Marine pollution bulletin 92, 90-98.

Orth, R.J., Carruthers, T.J., Dennison, W.C., Duarte, C.M., Fourqurean, J.W., Heck, K.L., Hughes, A.R., Kendrick, G.A., Kenworthy, W.J., Olyarnik, S., 2006. A global crisis for seagrass ecosystems. Bioscience 56, 987-996.

Rabalais, N.N., Turner, R.E., Diaz, R.J., Justić, D., 2009. Global change and eutrophication of coastal waters. ICES Journal of Marine Science 66, 1528-1537.

Riemann, B., Carstensen, J., Dahl, K., Fossing, H., Hansen, J.W., Jakobsen, H.H., Josefson, A.B., Krause-Jensen, D., Markager, S., Stæhr, P.A., 2016. Recovery of

Danish coastal ecosystems after reductions in nutrient loading: a holistic ecosystem approach. Estuaries and Coasts 39, 82-97.

Sinha, E., Michalak, A., Balaji, V., 2017. Eutrophication will increase during the 21st century as a result of precipitation changes. Science 357, 405-408.

Smith, V.H., 2003. Eutrophication of freshwater and coastal marine ecosystems a global problem. Environmental Science and Pollution Research 10, 126-139.

Valiela, I., Bowen, J.L., York, J.K., 2001. Mangrove Forests: One of the World's Threatened Major Tropical Environments: At least 35% of the area of mangrove forests has been lost in the past two decades, losses that exceed those for tropical rain forests and coral reefs, two other well-known threatened environments. Bioscience 51, 807-815.

Vandeweerd, V., Bernal, P., Belfiore, S., Goldstein, K., Cicin-Sain, B., 2002. A Guide to Oceans, Coasts, and Islands at the World Summit on Sustainable Development.

Waycott, M., Duarte, C.M., Carruthers, T.J., Orth, R.J., Dennison, W.C., Olyarnik, S., Calladine, A., Fourqurean, J.W., Heck, K.L., Hughes, A.R., 2009. Accelerating loss of seagrasses across the globe threatens coastal ecosystems. Proceedings of the national academy of sciences 106, 12377-12381.

Yamamoto, T., 2003. The Seto Inland Sea—eutrophic or oligotrophic? Marine Pollution Bulletin 47, 37-42.

Chapter 2: Determination of region-specific background Secchi depth in three semi-enclosed seas, Japan

2.1 Introduction

Light availability is a critical factor for phytoplankton growth and primary production (Harrison et al., 2007; Domingues et al., 2011; Arteaga et al., 2014; Edwards et al., 2016). Reliable estimation of the primary production potential of phytoplankton in the water column requires information on shifts in underwater light attenuation and the factors responsible for changes in water clarity (Nakai et al., 2018). The factors determining underwater light attenuation, including suspended particulate matter, phytoplankton populations, colored dissolved organic matter (CDOM) and water molecules, have been well studied; the relative contributions of these factors to light attenuation in the water column vary spatially and temporally (Lund-Hansen, 2004; Devlin et al., 2008).

Reductions in water clarity due to eutrophication have been widely documented in a range of coastal regions such as the Baltic sea that is the largest body of brackish water with 377,000 km² and is an semi-enclosed sea connecting the North Sea through narrow and shallow Danish straits (Sandén & Håkansson, 1996), Chesapeake Bay that is a large (11500 km^2), semi-enclosed estuary with narrow (1 to 4 km) central channel confined by a sill at its seaward end (Kemp et al., 2005) and brackish Lake Nakaumi that is shallow coastal lagoon with an areas of 92.1 km^2 (Hiratsuka et al., 2007). Great efforts have been made to reduce anthropogenic nutrient loading in aquatic systems; however, the responses of phytoplankton and changes in water clarity in enclosed and semi-enclosed seas following reductions in nutrient loading are frequently region specific. For example, light transmittance and/or Secchi depth (SD) increased when nutrient loads were reduced (due to decreases in chlorophyll *a* concentrations) in the semi-enclosed waters of coastal Denmark (Riemann et al., 2016) and the Seto Inland Sea that is the largest semi-enclosed sea in Japan with an area of 23,000 km^2 and connects Pacific Ocean through two wide and deep channels (Nishijima et al., 2018). However, in other areas where anthropogenic nutrient loading was less significant initially, reductions in phytoplankton populations and increases in water clarity were much smaller following efforts to reduce nutrient inputs (Williams et al., 2010; Taylor et al., 2011). Even in regions with major anthropogenic nutrient loading, reductions in inputs have little effect on light attention by phytoplankton when there is substantial sediment re-suspension or major suspended particulate matter input from inflowing rivers. Thus, regional, geographic and hydrographic conditions determine changes in light attenuation when nutrient inputs are reduced.

SD has been routinely documented for several decades in many coastal areas of the world ocean. However, it is an optical metrics reflecting the overall influence of both phytoplankton and other region-specific background factors, including tripton, CDOM and sea water. To know and compare both SD and its background levels we especially policymakers and coastal managers can precisely understand the current optical condition and the degree and the limit of improvement of the optical condition through the control of phytoplankton growth by reducing anthropogenic nutrient input. Nishijima et al. (2016) proposed a novel concept, that is, background Secchi depth (BSD), which they defined as a region-specific Secchi depth excluding the contribution of phytoplankton by analyzing 40 years of monitoring data for Secchi depth and chlorophyll a concentration in the Suo Nada Basin of the Seto Inland Sea, Japan. BSD has not been tested extensively in other waters, where the effects of reductions in nutrient loading on phytoplankton growth and other factors influencing light attenuation may be more marked than in mainly oligotrophic Suo Nada. The BSD procedure also requires testing under a range of local geographic and hydrographic conditions.

In this study, we compiled water quality data (including chlorophyll *a* concentrations and SDs) for the period 1981–2015 in sectors of Tokyo Bay, Ise Bay and the Seto Inland Sea, Japan (Figure 1) that differed in geographic and hydrographic conditions (e.g. topography, bathymetry, connectivity to the outer ocean and freshwater input; detailed description could be seen in following 2.1. Study sites) to obtain estimates of BSD and the proportional phytoplankton contribution to light attenuation. With these data, we aimed to determine the improvement potential of water clarity by nutrient loading management and the proportional phytoplankton contribution to light attenuation for helping evaluate the effectiveness of nutrient loading reduction on water clarity improvement via reducing phytoplankton biomass in Tokyo Bay, Ise Bay and the Seto Inland Sea.

2.2 Materials and methods

2.2.1. Study sites

Tokyo Bay, Ise Bay and the Seto Inland Sea are semi-enclosed seas located in central Japan (Figure 2.1). All these bays are connected to the Pacific Ocean to the south: Tokyo Bay through the Uraga Channel, Ise Bay through the Irago Strait and the Seto Inland Sea through Bungo Channel and Kii Channel. Tokyo Bay is surrounded by Japan's most industrialized zone; it has an area of 1380 km^2, and a mean depth of 38.6 m. The watersheds of Tokyo Bay support a human population of 30.96 million. Ise Bay is the largest bay on the Japanese coast (2342 km^2). It has a mean depth 16.8 m; 10.89 million people live within the watersheds of this bay. Harbors occupy 20.7% of the area of Ise Bay and 40.6% of the area of Tokyo Bay.

The Seto Inland Sea is classified as a semi-enclosed sea connected to the Pacific Ocean through the Kii Channel in the southeastern side and the Bungo Channel in the southwestern side as well as to the Sea of Japan through the narrow Kanmon Strait (Figure 2.1). The Seto Inland Sea is large (area 23,203 km2) and shallow (mean depth of 38.0 m) with a variety of geographic features including 12 basins, which are divided by islands and peninsulas.

More than 80% of the freshwater inputs flow into the northern shores of Tokyo Bay and Ise Bay. In Ise Bay, the annual average tidal current velocity in the inner region is ~0.1 m s^{-1}. In the Irago Strait at the mouth of the bay, the velocity can exceed 0.8 m s^{-1} during spring (Fujiwara et al., 2002). In Tokyo Bay, the tidal velocity increases from ~0.05 m s^{-1} in the innermost sector to >0.77 m s^{-1} off Cape Kannonzaki–Futtsu, which is located at the mouth of the bay (Japan Coast Guard, 2002). In the Seto Inland Sea, the high amplitudes of the tidal currents are observed in the narrow straits and the maximum tidal speeds in some straits approach 5 m s-1 in spring tides.

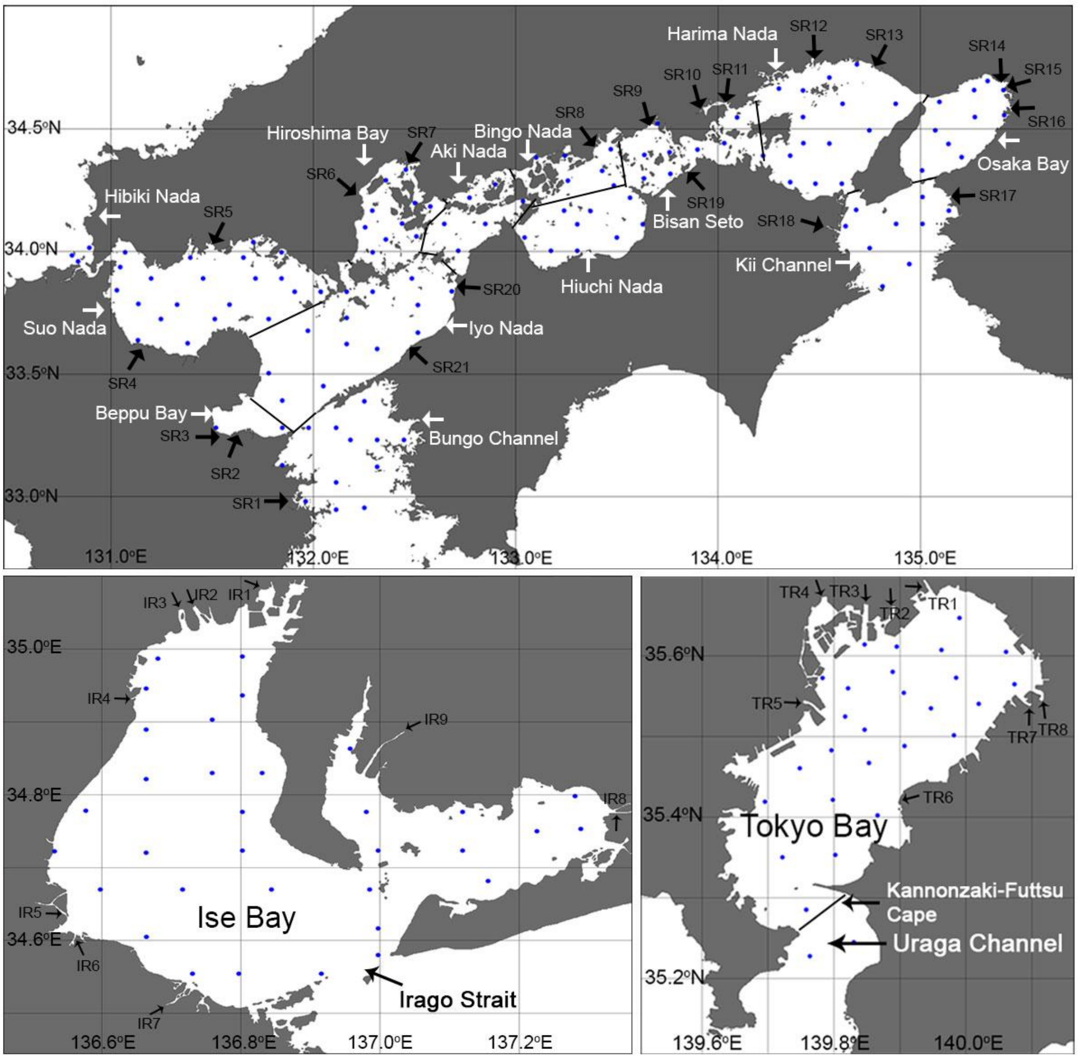

Figure 2.1 Location of the study area. Filled blue circles indicate positions of the monitoring sites. TR1 - TR8 refer to the Edogawa, Nakagawa, Arakawa, Sumidagawa, Tamagawa, Obitsugawa, Yorogawa, and Muratagawa Rivers, respectively. IR1 - IR9 refer to the Shonaigawa, Kisogawa, Ibigawa, Suzukagawa, Kumozugawa, Tarudagawa, Miyagawa, Toyogawa, and Yahagigawa Rivers, respectively. SR1-SR21 refer to the Banjogawa, Ohnogawa, Oitagawa, Yamakunigawa, Sabagawa, Ozegawa, Ohtagawa, Ashidagawa, Takahashigawa, Asahigawa, Yoshiigawa, Ibogawa, Kakogawa, Inagawa, Yodogawa, Yamatogawa, Kinokawa, Yoshinogawa, Dokigawa, Shigenobugawa and Hijikawa, respectively.

Tokyo Bay, Ise Bay and the Seto Inland Sea have suffered severe eutrophication since the 1970s and late 1950s, respectively (Han and Furuya, 2000; Kasai et al., 2004). A Total Pollutant Load Control System (TPLCS) has been in place since 1979 to improve water quality (Ministry of the Environment of Japan, 2011). Chemical oxygen demand (COD), total nitrogen (TN), and total phosphorus (TP) have steadily declined since then. Between 1979 and 2009, loadings of TN and TP into Ise Bay were reduced from 88.3 kg N km^{-2} d^{-1} to 55.4 kg N km^{-2} d^{-1} and from 11.5 kg P km^{-2} d^{-1} to 4.2 kg P km^{-2} d^{-1}; the respective reductions in Tokyo Bay were from 263.8 kg N km^{-2} d^{-1} to 134.1 kg N km^{-2} d^{-1} and from 29.9 kg P km^{-2} d^{-1} to 9.4 kg P km^{-2} d^{-1}. In the Seto Inland Sea, TN and TP declined from 27.7 kg-N km-2 d-1 to 16.7 kg-N km-2 d-1 (a 40% reduction) and from 2.63 kg-P km-2 d-1 to 1.03 kg-P km-2 d-1 (a 61% reduction). In recent years, harmful algal blooms have occurred ~30 times annually in Tokyo.Bay and Ise Bay and ~30 times in the Seto Inland Sea.

2.2.2 Water quality dataset

The Ministry of the Environment (MOE) of Japan provided seasonal water quality data for the period 1981–2015 for locations across Tokyo Bay (28 sites), Ise Bay (33 sites) and the Seto Inland Sea (124 sites). The field survey has been conducted once in each season for all the monitoring sites. We defined four seasons of the year as winter, extending from mid-January to early February; spring, during the month of May; summer, extending from July to early September; and fall, during the month of October in Ise Bay and the Seto Inland Sea and during the month of November in Tokyo Bay.

SD was measured with a 30-cm-diameter white disk. The SD measurement was carried out twice and the average of the two values was used in later analysis. Water samples were taken at 0.5 m below the surface. Water temperature, salinity, COD, TN, TP and chlorophyll *a* concentration were measured following the Guidelines for Marine Observations (Japan Meteorological Agency, 2000). Briefly, salinity and water temperature were measured by CTD (Sea Bird Electronic Inc., USA) in situ. Chlorophyll *a* was analyzed by the Welschmeyer method (Welschmeyer, 1994). TN and TP concentrations were colorimetrically determined by an autoanalyzer (e.g. SWAAT, BLTEC, Japan), following oxidation by potassium persulfate. COD was analyzed by the potassium permanganate oxidation method.

2.2.3 Estimation of background Secchi depth (BSD)

The strength of light attenuation in the water column is generally related to reciprocal of SD (Devlin et al., 2008), thus we used harmonic means for SD. Arithmetic means were used for other water quality parameters (e.g. water temperature, TN, TP and Chl.*a* concentrations). BSD was calculated for every monitoring site in each season of the 35-year sampling period. From the slopes of the linear regressions of the natural logarithm of the reciprocal of the SDs [*ln*(1/*SD*)] plotted against the chlorophyll *a* concentrations (Fig. 2.2), we calculated y-intercepts as the reciprocals of the BSDs [*ln*(1/*BSD*)], i.e., *ln*(1/*SD*), in the absence of phytoplankton effects (Nishijima et al., 2018).

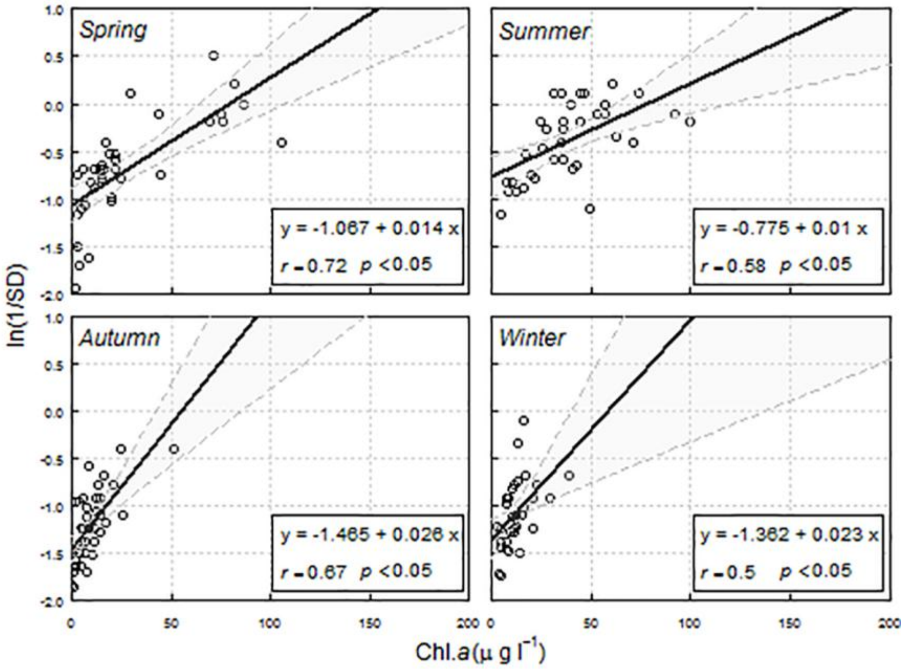

Figure 2.2 Sample linear regression plots of ln(1/SD) on chlorophyll a concentrations that were used to calculate ln(1/BSD) (data from Station 15 in Tokyo Bay). All correlations for all four seasons were significant (i.e., p < 0.05). When *p* exceeded 0.05 in other regressions, the estimated BSDs were considered unreliable and were not used in later analyses. SD, Secchi depth; BSD, background Secchi depth.

We estimated phytoplankton contribution to light attenuation, based on the concept of BSD, as follows (Eqs 1–7):

$$K_{\mathrm{d}} = K_{\mathrm{W}} + K_{\mathrm{CDOM}} + K_{\mathrm{tripton}} + K_{\mathrm{phyt}} \quad \text{Eq. 1}$$

$$K_{\mathrm{bg}} = K_{\mathrm{W}} + K_{\mathrm{CDOM}} + K_{\mathrm{tripton}} \quad \text{Eq. 2}$$

$$K_{\mathrm{d}} = K_{\mathrm{bg}} + K_{\mathrm{phyt}} \quad \text{Eq. 3}$$

$$K_{\mathrm{d}} = a/SD \quad \text{Eq. 4}$$

$$K_{\mathrm{bg}} = a/BSD \quad \text{Eq. 5}$$

$$\mathrm{ph}yt\% = 100 \times (K_{bg} / K_{\mathrm{d}}) \quad \text{Eq. 6}$$

$$\mathrm{phyt}\% = 100 \times (1 - SD/BSD) \quad \text{Eq. 7}$$

In Eq. 1, K_d is the total light attenuation coefficient for the water column, and K_w, K_{CDOM}, $K_{tripton}$ and K_{phyt} are partial light attenuation by water, chromophoric dissolved organic matters (CDOM), tripton and phytoplankton, respectively. In Eq. 2, K_{bg} is the attenuation caused by background factors, which is the sum of K_w, K_{CDOM} and $K_{tripton}$ in Eq. 1 (Nishijima et al. 2018). In Eqs 4 and 5, *SD* is Secchi depth and *BSD* is the background Secchi depth. The coefficient *a* is the product of K_d and *SD* or the product of K_{bg} and *BSD*. In Eqs 6 and 7 phyt% is phytoplankton contribution in light attenuation. The average phyt% at a monitoring site is then obtained from Eq. 9 when average *SD* is used.

2.2.4 Mapping and statistics

We mapped water quality parameters, BSD, and the phytoplankton contribution to light attenuation using Ocean Data View version 5.0.0 software (Schlitzer, 2018). Gridding (or gradation) was performed with the "DIVA gridding" built-In package in Ocean Data View software. Pearson's correlation coefficient *r* and its *p*-value were used to examine the relationships between BSD and diverse water parameters. For the determination of the relationship, we used the seasonal data set of BSD and water parameters in all monitoring sites. Non-parametric Kruskal–Wallis ANOVA tests and subsequent Dunn's tests for multiple comparisons were used to assess (i) BSD, (ii) chlorophyll *a* concentration, (iii) the regression slope of the plot of $ln(1/SD)$ on chlorophyll *a* concentration, and (iv) the phytoplankton's contribution to light attenuation. Bonferroni corrections were used for multiple comparisons. The Kruskal–Wallis test and Dunn's test were performed with R software (R Core Team 2015); *p*-values <0.05 were used to identify statistically significant effects.

2.3 Results

2.3.1. Spatial and seasonal variability in water quality

Seasonal patterns of water quality were similar between Tokyo Bay, Ise Bay and the Seto Inland Sea, despite their differences in geography and hydrography. The water temperatures in these seas were highest in summer and lowest in winter (Tables

Table 2.1 Secchi depths and water quality parameters in Tokyo Bay at 0.5 m depth during the period of 2006–2015. Table cells contain parameter means ± standard deviations and coefficients of variation for the monitoring sites (in parentheses). All the values are calculated from multiyear averages of each monitoring site (n = 28). TN, total nitrogen; TP, total phosphorus; COD, chemical oxygen demand; Chl.*a*, chlorophyll *a*

Season	Temp. (°C)	Chl.*a* (μg l^{-1})	Secchi depth (m)	Salinity	TN (mg l^{-1})	TP (mg l^{-1})	COD (mg l^{-1})
Spring	18.7 ± 0.8	8.3 ± 6.2	3.0 ± 0.3	27.2 ± 3.3	0.35 ± 0.12	0.032 ± 0.018	2.9 ± 0.8
	(0.04)	(0.75)	(0.09)	(0.12)	(0.33)	(0.58)	(0.28)
Summer	26.2 ± 1.0	12.6 ± 8.6	1.9 ± 0.2	21.6 ± 5.8	0.35 ± 0.13	0.042 ± 0.027	3.8 ± 1.0
	(0.04)	(0.68)	(0.11)	(0.27)	(0.38)	(0.64)	(0.25)
Autumn	21.8 ± 0.4	7.7 ± 4.9	3.4 ± 0.2	28.3 ± 2.0	0.32 ± 0.11	0.044 ± 0.016	2.5 ± 0.5
	(0.02)	(0.64)	(0.07)	(0.07)	(0.35)	(0.37)	(0.20)
Winter	8.8 ± 1.3	5.7 ± 4.9	5.0 ± 0.3	31.4 ± 1.0	0.28 ± 0.11	0.027 ± 0.007	1.8 ± 0.6
	(0.15)	(0.87)	(0.05)	(0.03)	(0.39)	(0.28)	(0.34)

Table 2.2 Secchi depths and water quality parameters in Ise Bay at 0.5 m depth during the period of 2006–2015. Table cells contain parameter means ± standard deviations and coefficients of variation for the monitoring sites (in parentheses). All the values are calculated from multiyear averages of each monitoring site (n = 33). TN, total nitrogen; TP, total phosphorus; COD, chemical oxygen demand; Chl.*a*, chlorophyll *a*

Season	Temp. (°C)	Chl.*a* (μg l^{-1})	Secchi depth (m)	Salinity	TN (mg l^{-1})	TP (mg l^{-1})	COD (mg l^{-1})
Spring	18.7 ± 0.8	8.3 ± 6.2	3.0 ± 0.3	27.2 ± 3.3	0.35 ± 0.12	0.032 ± 0.018	2.9 ± 0.8
	(0.04)	(0.75)	(0.09)	(0.12)	(0.33)	(0.58)	(0.28)
Summer	26.2 ± 1.0	12.6 ± 8.6	1.9 ± 0.2	21.6 ± 5.8	0.35 ± 0.13	0.042 ± 0.027	3.8 ± 1.0
	(0.04)	(0.68)	(0.11)	(0.27)	(0.38)	(0.64)	(0.25)
Autumn	21.8 ± 0.4	7.7 ± 4.9	3.4 ± 0.2	28.3 ± 2.0	0.32 ± 0.11	0.044 ± 0.016	2.5 ± 0.5
	(0.02)	(0.64)	(0.07)	(0.07)	(0.35)	(0.37)	(0.20)
Winter	8.8 ± 1.3	5.7 ± 4.9	5.0 ± 0.3	31.4 ± 1.0	0.28 ± 0.11	0.027 ± 0.007	1.8 ± 0.6
	(0.15)	(0.87)	(0.05)	(0.03)	(0.39)	(0.28)	(0.34)

Table 2.3 Secchi depths and water quality parameters in the Seto Inland Sea at 0.5 m depth during the period of 2006–2015. Table cells contain parameter means ± standard deviations and coefficients of variation for the monitoring sites (in parentheses). All the values are calculated from multiyear averages of each monitoring site (n = 124). TN, total nitrogen; TP, total phosphorus; COD, chemical oxygen demand; Chl.*a*, chlorophyll *a*

Season	Temp. (°C)	Chl.*a* (μg l^{-1})	Secchi depth (m)	Salinity	TN (mg l^{-1})	TP (mg l^{-1})	COD (mg l^{-1})
Spring	17.5 ± 1.0	2.1 ± 2.7	7.7 ± 3.3	32.3 ± 1.9	0.20 ± 0.12	0.018 ± 0.011	1.9 ± 0.6
	(0.06)	(1.28)	(0.42)	(0.06)	(0.64)	(0.60)	(0.34)
Summer	24.3 ± 1.3	3.6 ± 5.0	6.6 ± 2.5	30.8 ± 2.8	0.23 ± 0.14	0.022 ± 0.016	2.3 ± 0.8
	(0.05)	(1.41)	(0.39)	(0.09)	(0.63)	(0.72)	(0.35)
Autumn	23.5 ± 0.7	2.9 ± 2.7	6.7 ± 2.5	32.2 ± 1.2	0.22 ± 0.10	0.027 ± 0.012	1.9 ± 0.5
	(0.03)	(0.93)	(0.37)	(0.04)	(0.47)	(0.43)	(0.29)
Winter	11.6 ± 1.8	2.2 ± 1.7	7.5 ± 2.6	32.7 ± 1.4	0.21 ± 0.13	0.024 ± 0.009	1.6 ± 0.4
	(0.15)	(0.77)	(0.35)	(0.04)	(0.61)	(0.38)	(0.25)

2.1, 2.2 and 2.3). The chlorophyll *a* concentrations in the two bays were highest in summer and spring, and lowest in autumn and winter (Tables 2.1, 2.2 and 2.3). We attributed seasonal changes in chlorophyll *a* concentrations to seasonal changes in the water temperatures of these temperate coastal areas. SD was shallower in summer and spring than in autumn and winter.

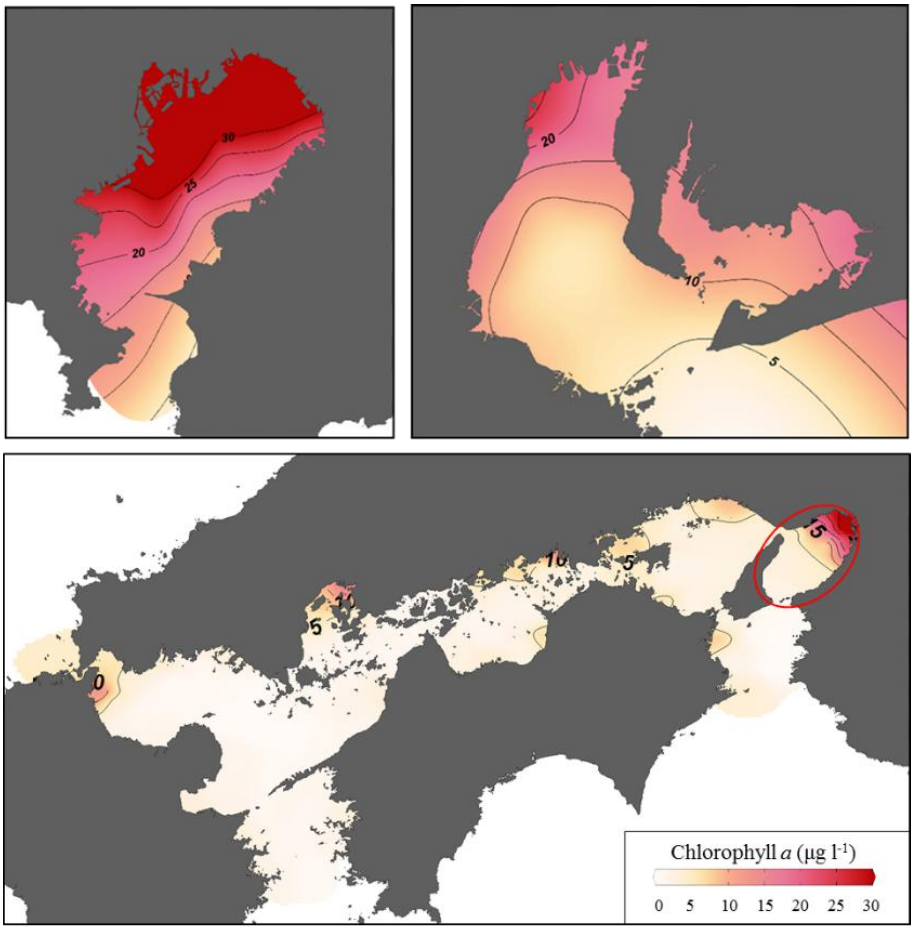

Figure 2.3 Spatial variation in chlorophyll a concentration in Tokyo Bay, Ise Bay and the Seto Inland Sea during summer during the period of 2006–2015. Contour lines demarcate 5 μg l^{-1}.

2.3.2. Secchi depth (SD) and background Secchi depth (BSD)

Phytoplankton cells reduce SD by increasing light attenuation, which is approximately proportional to the reciprocal of SD. As expected, the seasonal trend in SD was inversely related to that of chlorophyll *a* concentration in these seas (Tables 2.1, 2.2 and 2.3). Spatial variations in chlorophyll *a* concentration and SD in summer are depicted in Figure 2.3 and 2.4. SD were lowest in the innermost regions of Tokyo Bay (around the estuaries of the Nakagawa, Arakawa, and Sumidagawa Rivers), Ise

Bay (around the estuaries of the Shonaigawa, Kisogawa, and Ibigawa Rivers) and Osaka bay in the Seto Inland Sea (around the estuaries of Yodogawa and Inagawa). Conversely, the highest chlorophyll *a* concentrations occurred in the innermost parts of these seas, and the lowest values were measured around the bay mouths or the two channels of the Seto Inland Sea.

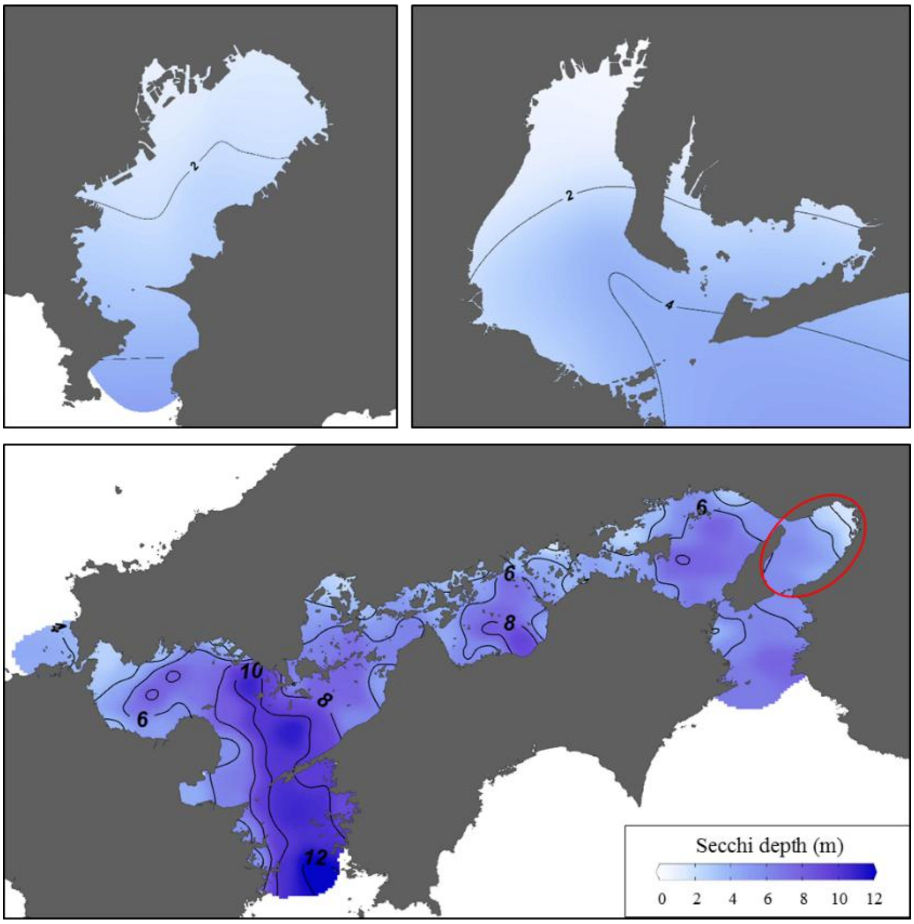

Figure 2.4 Spatial variation in SD in Tokyo Bay, Ise Bay and the Seto Inland Sea during summer during the period of 2006–2015. Contour lines demarcate 2m.

Values of BSD in these seas during summer were depicted in Figure 2.5. In Tokyo Bay, the regressions of ln(1/*SD*) against chlorophyll *a* concentration were statistically significant in 96%, 89%, 96%, and 89% of the 28 sites in spring, summer, autumn, and winter, respectively. In Ise Bay, we identified higher proportions of sites with reliable BSD in spring and winter (88% and 96%, respectively) than in summer and autumn (67% and 76%, respectively). In the Seto Inland Sea, reliable BSDs were obtained from 67% and 63% of the 124 total sites in spring and summer, respectively, and 37% and 19% of the total sites in autumn and winter. The high turbulence due to large fresh water input and occasional incidence of typhoons in the autumn and winter could drive markedly unstable tripton levels and make it difficult to determine an accurate BSD in these warm seasons in Ise Bay. BSD varied greatly by region and season. Spatially, BSD increased with proximity from the bay mouths to the inner parts where the estuaries were located (Figure 2.5). Seasonally, estimated BSD values tended to be lowest in summer, increased in spring and peaked in autumn and winter.

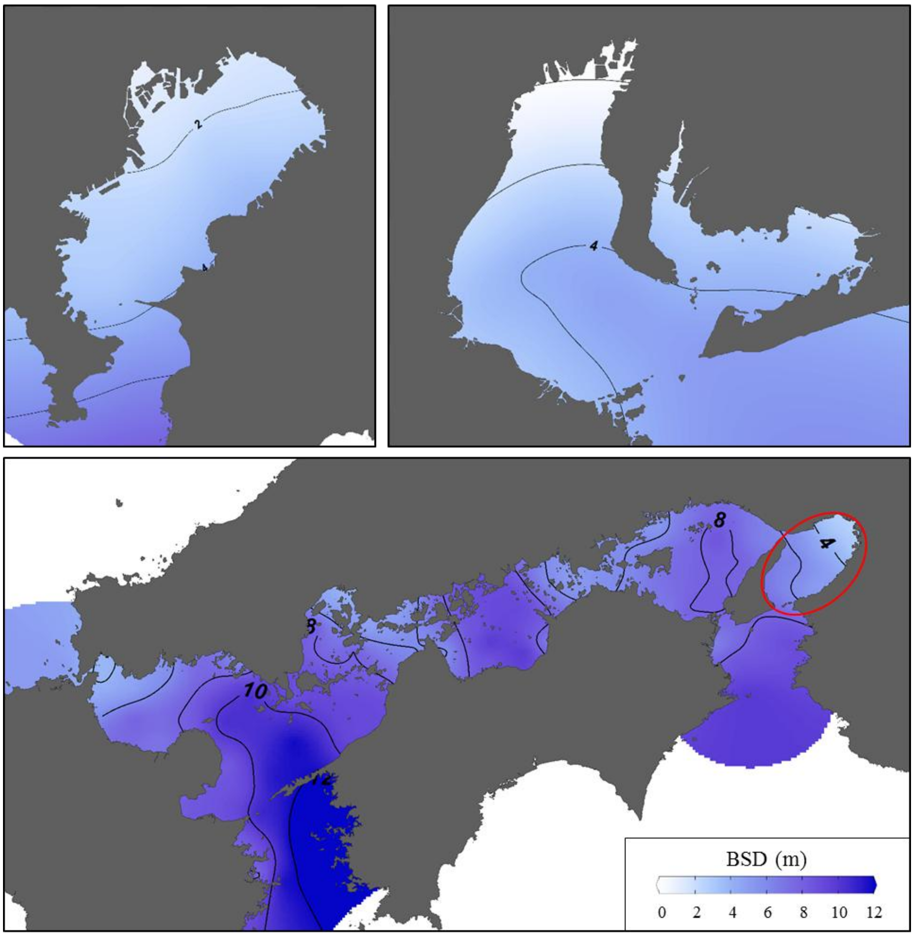

Figure 2.5 Spatial variation in BSD in Tokyo Bay, Ise Bay and the Seto Inland Sea during summer during the period of 2006–2015. Contour lines demarcate 2m.

2.3.3 Factors affecting background Secchi depth (BSD)

We performed correlation analyses to examine the relationships between estimated BSD and water quality parameters in Tokyo Bay, Ise Bay, Osaka Bay and the Seto Inland Sea (excluding Osaka Bay) using data from all four seasons. BSD was highly correlated with salinity (Table 2.4), indicating a major role for rivers in the supply of substances responsible for light attenuation, e.g., tripton and chromophoric dissolved organic matter. We also calculated significant but weaker correlations between BSD and water depth and temperature (Table 2.4). BSD and chlorophyll *a* concentration are, by definition, independent parameters. Nevertheless, they were highly correlated, likely because the rivers supplied nutrients to the sea, thereby enhancing plankton growth in low-salinity sectors of these seas.

Table 2.4 Pearson Pearson correlation coefficients for the relationships of BSD with water temperature, depth, salinity, chlorophyll *a* concentration (Chl.*a*) and SD

	Water temperature	Depth	Salinity	Chl.*a*	SD
Tokyo Bay	–0.43	0.56	0.73	–0.77	0.95
Ise Bay	–0.55	0.53	0.64	–0.62	0.96
Osaka Bay	-0.20	0.73	0.77	-0.77	0.98
Seto Inland Sea	-0.05	0.80	0.55	-0.60	0.97

$p < 0.05$ for all correlations except for BSD and water temperature in the Seto Inland Sea

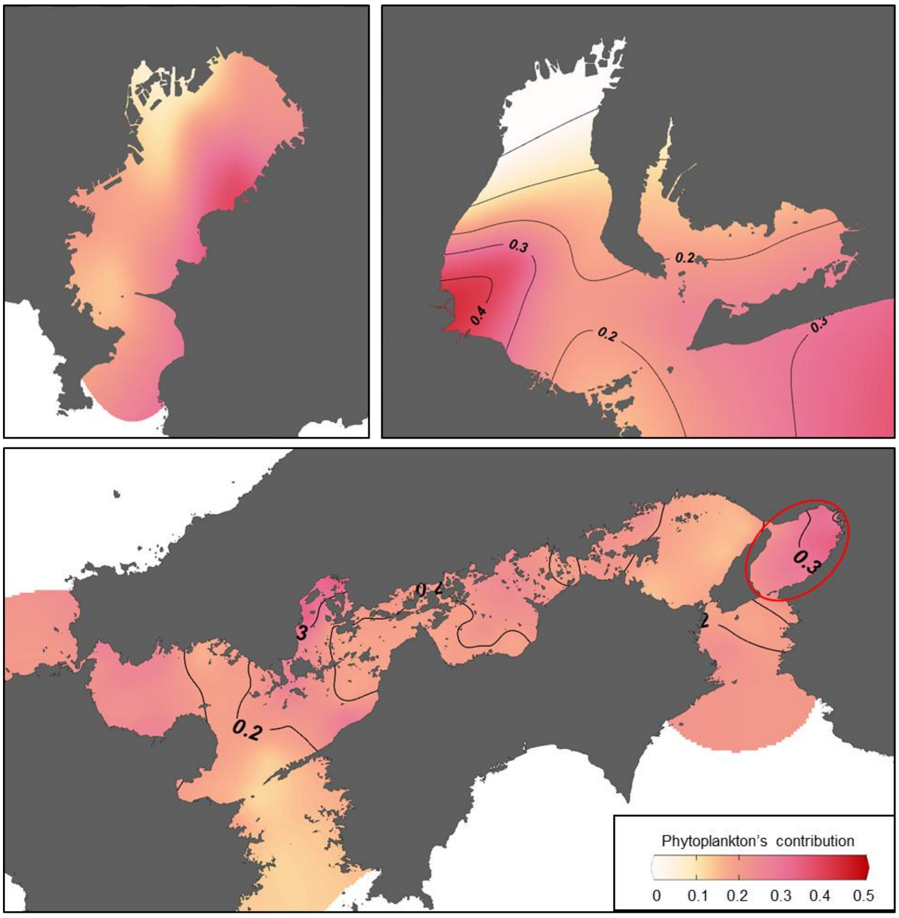

Figure 2.6 Spatial variation in the proportional contribution of phytoplankton to light attenuation in Tokyo Bay, Ise Bay and the Seto Inland Sea.

2.3.4 Phytoplankton proportional contributions to light attenuation

The contribution of the phytoplankton to light attenuation in the two bays is depicted in Figure 2.6. The contribution to light attenuation was generally higher in spring and summer than in autumn and winter. Although the highest chlorophyll *a* concentrations were measured in the innermost parts of Tokyo Bay and Ise Bay (Figure 2.3), the phytoplankton contribution to light attenuation was surprisingly low in these sectors (Figure 2.6). The result indicates that background factors were much more important for light attenuation.

2.4 Discussion

2.4.1 Seasonal and regional changes in water quality parameters

Tokyo Bay and Ise Bay exhibited a large seasonal change in salinity and chlorophyll *a* concentrations that are common in temperate coastal areas, e.g. Danish coastal ecosystems (Riemann et al., 2016) and the Seto Inland Sea (Nishijima et al., 2018). The strong north–south salinity gradient in both bays is probably explained by the major freshwater inputs by rivers on the northern shores: the Nakagawa, Arakawa, and Sumidagawa Rivers flowing into Tokyo Bay and the Shonaigawa, Kisogawa, and Ibigawa Rivers flowing into Ise Bay. The nutrient and tripton supply across the strong salinity gradient may be responsible for the gradient in phytoplankton biomass and SD. The ecosystem variability along salinity gradient found in Tokyo Bay and Ise Bay is similar to that found in San Francisco Bay, where salinity gradient play a fundamental role in structuring spatial patterns of physical properties and biota (Cloern et al., 2017). Because the inner sector of Tokyo Bay has a high degree of enclosure (Table 2.5), the tripton concentrations are readily influenced by seasonal changes in river runoff. On the contrary, Ise Bay has a relatively low degree of enclosure (i.e., strong influence of outer ocean waters), which may weaken the changes in river-derived nutrients and tripton. A recent study conducted in the coastal embayments of Buzzards Bay, Massachusetts also found that the embayment geomorphology strongly influenced the changes of water quality (Rheuban et al., 2016).

Table 2.5 Basic physicochemical data for Tokyo Bay, Ise Bay, Osaka Bay, and the Seto Inland Sea (excluding Osaka Bay)

	Area (km^2)	Mean Depth (m)	River discharge ($m^3\ km^{-3}\ s^{-1}$)	Degree of enclosure (-)	TN/TP loads ($kg\ km^{-2}\ d^{-1}$)
Seto Inland Sea	21,756	38	0.68	1.13	13.0/0.76
Osaka Bay	1447	28	7.53	2.61	71.7/4.90
Ise Bay	2342	17	17.48	1.52	55.4/4.23
Tokyo Bay	1380	39 (15)	3.46	4.34	134.1/9.4

Degree of enclosure = $\frac{\sqrt{S}}{W} \times \frac{D1}{D2}$ where S is area, W is the width of the bay (or sea) mouth, D1 is the maximum depth in the inner part of bay (or sea), and D2 is maximum depth at the mouth of the bay (or sea).
The value in parentheses in column 3 indicates the depth in the inner sector of Tokyo Bay (excluding Uraga Channel)

2.4.2 Comparison of background Secchi depths (BSDs) and light attenuation factors

The TPLCS has been implemented across Tokyo Bay, Ise Bay, and the Seto Inland Sea (Ministry of the Environment of Japan, 2011). Osaka Bay is managed separately from the other parts of the Seto Inland Sea because its environment has been more strongly impacted by human influence. The surface area of the Seto Inland Sea (not including Osaka Bay: 21,759 km^2) is much larger than the areas of Tokyo Bay (1380 km^2), Ise Bay (2342 km^2), and Osaka Bay (1447 km^2). Nutrient loadings from the surrounding land were highest in Tokyo Bay (8940.0 kg N $km^{-3}\ d^{-1}$ and 626.7 kg P $km^{-3}\ d^{-1}$), followed in rank order by Ise Bay (3258.8 kg N $km^{-3}\ d^{-1}$ and 248.8 kg P $km^{-3}\ d^{-1}$), Osaka Bay (2560.7 kg N $km^{-3}\ d^{-1}$ and 175.0 kg P $km^{-3}\ d^{-1}$), and the Seto Inland Sea (not including Osaka Bay: 342.1 kg N $km^{-3}\ d^{-1}$ and 20.0 kg P $km^{-3}\ d^{-1}$) (Ministry of the Environment of Japan, 2011). The large differences in nutrient loadings among water bodies may explain the marked differences in phytoplankton concentrations. Furthermore, the freshwater inputs and the degrees of enclosure differed among these four semi-enclosed water bodies (Table 2.5); these differences may have changed the interactions between abiotic and biotic factors in the different locations.

Nishijima et al., (2018) recently calculated BSDs in the Seto Inland Sea. However, reliable BSDs were not obtained in autumn or winter in many areas of this water body. Accordingly, we compared optical properties across the Tokyo Bay, Ise Bay, Osaka Bay, and the Seto Inland Sea (excluding Osaka Bay) in spring and summer. The estimated mean BSDs were highest in the Seto Inland Sea, followed in rank order by Osaka Bay, Ise Bay, and Tokyo Bay (Figure 2.7). The proportional difference between spring and summer BSDs in the Seto Inland Sea and Osaka Bay were similar (12 ± 9% and 14 ± 9%, respectively, calculated relative to values in spring). The proportional difference between spring and summer BSD values in Tokyo Bay and Ise Bay were relatively large (25 ± 9% and 18 ± 10%, respectively), which may be explained in part by the large seasonal differences in turbidity and tripton levels (Nakamura et al., 2005; Narita et al., 2006).

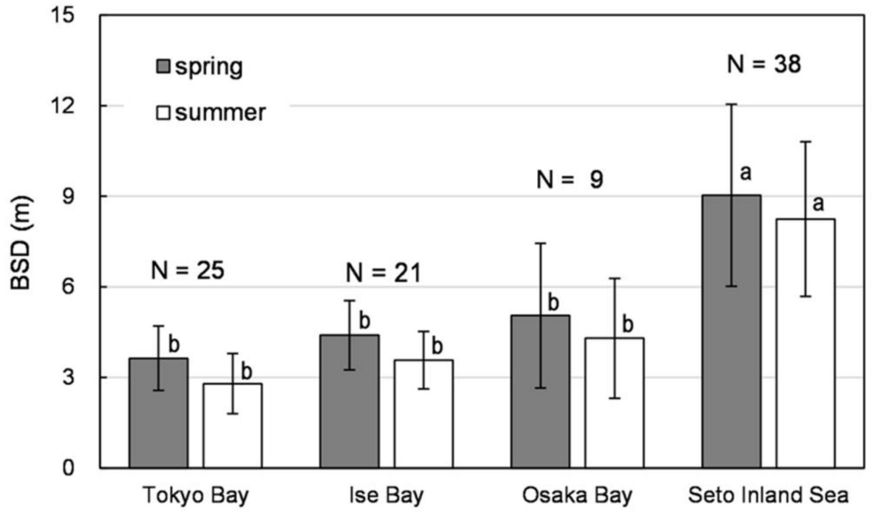

Figure 2.7 Region-specific BSDs in spring and summer in Tokyo Bay, Ise Bay, Osaka Bay and the Seto Inland Sea (excluding Osaka Bay). Values are means ± standard deviations. Different lowercase letters above the bars indicate significant pairwise differences ($p < 0.05$, Dunn's test) between water bodies during the same season.

The regression slopes for the plots of $ln(1/SD)$ on chlorophyll *a* concentration were much larger for the Seto Inland Sea (median: 0.105 and 0.073 in spring and summer, respectively) than for Osaka Bay (median: 0.045 and 0.014 in spring and summer, respectively), Ise Bay (median: 0.027 and 0.017 in spring and summer, respectively), and Tokyo Bay (median: 0.016 and 0.013 in spring and summer, respectively) (Figure 2.8). The differences in the slopes may be explained by differences in eutrophication and phytoplankton parameters among the four water bodies. Nutrient enrichment can increase phytoplankton cell size (Uitz et al., 2008; Cloern 2018), which decreases the amount of light absorbed per unit chlorophyll *a* concentration due to the package effect (Bricaud et al., 1995; Ciotti et al., 2002; Fujiki & Taguchi 2002).

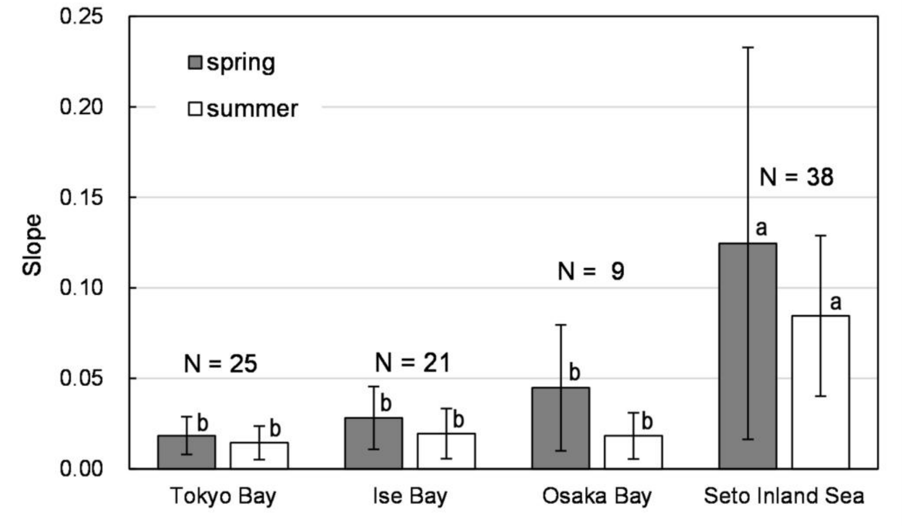

Figure 2.8 Regressions slopes for the plots of ln(1/SD) on chlorophyll a concentrations in spring and summer in Tokyo Bay, Ise Bay, Osaka Bay and the Seto Inland Sea (excluding Osaka Bay). Values are means ± standard deviations. Different lowercase letters above the bars indicate significant within-season pairwise differences ($p < 0.05$, Dunn's test) between water bodies.

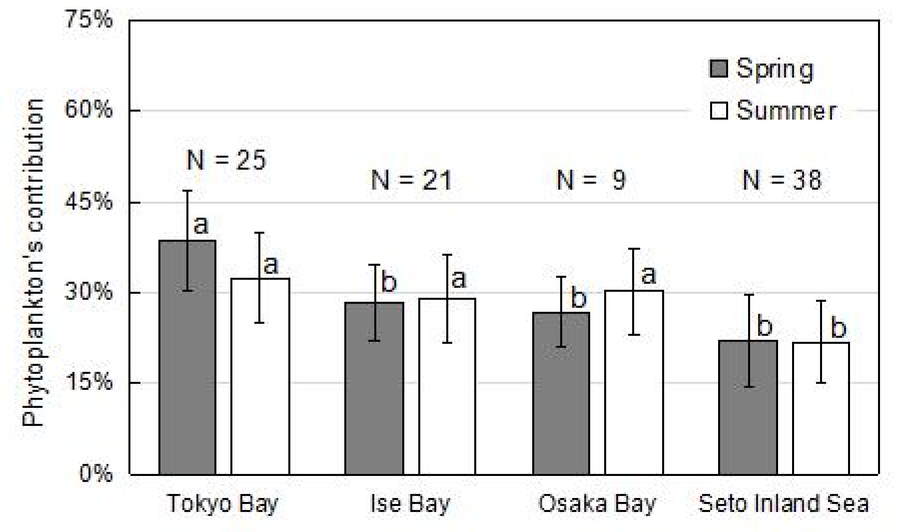

Figure 2.9 Proportional phytoplankton contributions to light attenuation in spring and summer in Tokyo Bay, Ise Bay, Osaka Bay and the Seto Inland Sea (excluding Osaka Bay). Values are means ± standard deviations. Different lowercase letters above the bars indicate significant within-season pairwise differences ($p < 0.05$, Dunn's test) between water bodies.

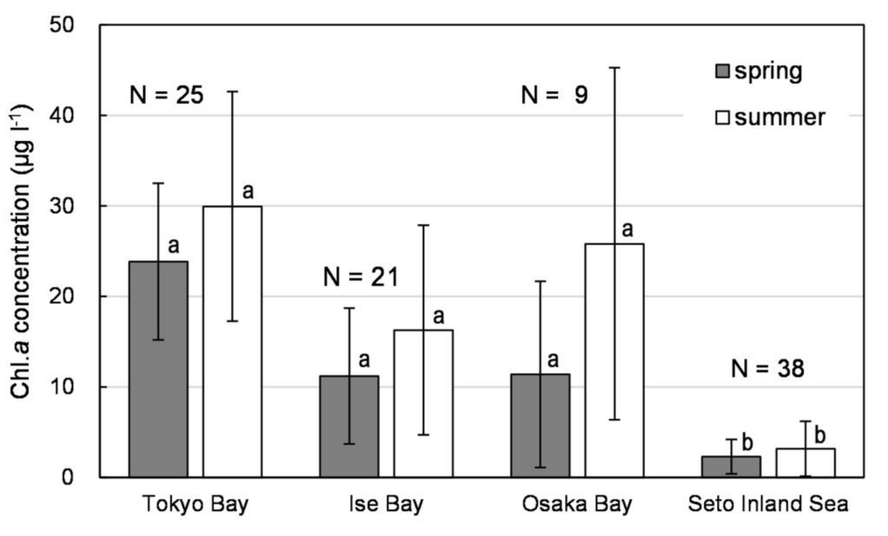

Figure 2.10 Mean chlorophyll a (Chl. a) concentrations in spring and summer in Tokyo Bay, Ise Bay, Osaka Bay and the Seto Inland Sea (excluding Osaka Bay). Values are means ± standard deviation. Different lowercase letters above the bars indicate significant within-season pairwise differences (p < 0.05, Dunn's test) between water bodies.

It is not surprising that the phytoplankton contribution to light attenuation was highest in Tokyo Bay (Figure 2.9) because the median chlorophyll *a* concentrations in this water body were so high (23.5 μg l^{-1} and 28.9 μg l^{-1} in spring and summer, respectively) compared to Osaka Bay (6.6 μg l^{-1} and 25.0 μg l^{-1}), Ise Bay (8.4 μg l^{-1} and 11.6 μg l^{-1}), and the Seto Inland Sea (1.7 μg l^{-1} and 2.1 μg l^{-1}) (Figure 2.10). The Seto Inland Sea comprises a series of sub-basins, most of which have low chlorophyll *a* concentrations (~2 μg l^{-1}). However, this pattern can be periodically disrupted in geographically semi-enclosed waters adjacent to highly populated watersheds (Nishijima et al., 2018). Although the chlorophyll *a* concentration in the Seto Inland Sea was lower than that for other water bodies, the phytoplankton contribution to light attenuation (~20%) was comparable to those for Osaka Bay, Ise Bay, and Tokyo Bay (Figure 2.9). The deep waters of the Seto Inland Sea and the relatively limited river discharges explain the low values of chlorophyll *a* and background factors, which together account for the elevated BSD estimates.

Relatively high phytoplankton contributions to light attenuation were calculated for Tokyo Bay, Ise Bay, and Osaka Bay. Nevertheless, the contributions were still <40% on average. Thus, the background factors were dominant even in semi-enclosed bays receiving very high nutrients loads from the land. Large river discharges are prevalent in these three bays. These discharges supply nutrients and suspended matter. The bays are shallow, and the bottoms are covered by mud or silt that is readily re-suspended (Yanagi et al., 2006; Rasmeemasmuang et al., 2008). Similarly, in the northern-central region of Florida Bay, an inner-shelf lagoon located off the southern tip of the Florida peninsula, phytoplankton was responsible for 31–34% of the total light attenuation with average chlorophyll *a* concentrations ranging from 14.5 to 18.4 μg l^{-1} (Phlips et al., 1995). In Chesapeake Bay, where the chlorophyll *a* concentrations could be up to around 50μg l^{-1} in the oligohaline region, phytoplankton only accounted for <25% of total light attenuation (Gallegos & Moore, 2000). Moreover, due to the low contribution of phytoplankton to light condition and marked variation in tripton levels in the oligohaline area of Chesapeake Bay, phytoplankton explained <1% of the total variability in total light attenuation (Xu et al., 2015). Likewise, in Manukau, a turbid estuary located in New Zealand, phytoplankton only caused 17–19% of total light attenuation with the chlorophyll *a* concentrations being up to 17.9 μg l^{-1} (Van 1990). These ecosystems receive substantial river input and support both high phytoplankton biomass and tripton levels. Common characteristics among these sites may reflect the general influence of eutrophication in all of them.

2.4.3 Using data on background Secchi depth (BSD), Secchi depth (SD), and the phytoplankton contribution to light attenuation to improve environmental management

Nutrient control is a common procedure for reducing excessive eutrophication. A reduction in nutrient supply decreases phytoplankton biomass, thereby improving water transparency. However, improvements in water transparency are limited, and the degree of limitation varies from region to region. BSD, which excludes the influence of phytoplankton, gives the upper limits that SD could reach. Consequently, we need measurements of current SD and BSD values simultaneous with estimations of the partial contributions of phytoplankton and background factors in light attenuation to determine the degree of improvement that can be expected by reducing chlorophyll *a* concentrations via reductions in nutrient loading in enclosed and semi-enclosed water bodies (Olesen 1996; Chen & Doering 2016; Nishijima et al., 2016; Nishijima et al., 2018).

2.5 Conclusions

BSD values were successfully obtained in 89–96%, 67–94% and 19-67% of monitoring sites in Tokyo Bay, Ise Bay and the Seto Inland Sea, respectively. We found only small differences in BSD between eutrophic Tokyo Bay, Ise Bay and Osaka Bay although their geographic and hydrographic conditions differed. BSD values were higher in autumn and winter than in spring and summer in 3 bays. Low BSD values were obtained in the innermost regions of these semi-enclosed seas, adjacent to the estuaries of large rivers. Estimated BSDs were positively correlated with salinity in these seas, indicating a major role for river input among the background factors. Although the highest chlorophyll *a* concentrations were measured in the innermost parts of Tokyo Bay, Ise Bay and Osaka Bay, the phytoplankton contribution to light attenuation was relatively low. Moreover, the average estimated proportional light attenuation of phytoplankton was <40% in all these seas, indicating that background factors were still dominant, even in eutrophic bays receiving very high nutrients loads from the land. Simultaneously compiled data on SD and BSD, along with estimates of the proportional contributions of phytoplankton and background factors to light attenuation, should facilitate the development of management plans that aim to improve water transparency by reducing phytoplankton biomass via reductions in nutrient loading.

2.6 References

Arteaga, L., Pahlow, M., Oschlies, A., 2014. Global patterns of phytoplankton nutrient and light colimitation inferred from an optimality - based model. Global Biogeochemical Cycles 28, 648-661.

Bricaud, A., Babin, M., Morel, A., Claustre, H., 1995. Variability in the chlorophyll - specific absorption coefficients of natural phytoplankton: Analysis and parameterization. Journal of Geophysical Research: Oceans 100, 13321-13332.

Chen, Z., Doering, P.H., 2016. Variation of light attenuation and the relative contribution of water quality constituents in the Caloosahatchee River Estuary. Florida Scientist, 93-108.

Ciotti, A.M., Lewis, M.R., Cullen, J.J., 2002. Assessment of the relationships between dominant cell size in natural phytoplankton communities and the spectral shape of the absorption coefficient. Limnology and Oceanography 47, 404-417.z

Cloern, J.E., 2018. Why large cells dominate estuarine phytoplankton. Limnology and Oceanography 63, S392-S409.

Cloern, J.E., Jassby, A.D., Schraga, T.S., Nejad, E. and Martin, C., 2017 Ecosystem variability along the estuarine salinity gradient: Examples from long - term study of San Francisco Bay. Limnology and Oceanography 62, S272-S291.

Devlin, M., Barry, J., Mills, D., Gowen, R., Foden, J., Sivyer, D., Tett, P., 2008. Relationships between suspended particulate material, light attenuation and Secchi depth in UK marine waters. Estuarine, Coastal and Shelf Science 79, 429-439.

Domingues, R.B., Anselmo, T.P., Barbosa, A.B., Sommer, U., Galvão, H.M., 2011. Light as a driver of phytoplankton growth and production in the freshwater tidal zone of a turbid estuary. Estuarine, Coastal and Shelf Science 91, 526-535.

Edwards, K.F., Thomas, M.K., Klausmeier, C.A., Litchman, E., 2016. Phytoplankton growth and the interaction of light and temperature: A synthesis at the species and community level. Limnology and Oceanography 61, 1232-1244.

Fujiki, T., Taguchi, S., 2002. Variability in chlorophyll a specific absorption coefficient in marine phytoplankton as a function of cell size and irradiance. Journal of Plankton Research 24, 859-874.

Fujiwara, T., Takahashi, T., Kasai, A., Sugiyama, Y., Kuno, M., 2002. The role of circulation in the development of hypoxia in Ise Bay, Japan. Estuarine, Coastal and Shelf Science 54, 19-31.

Gallegos, C.L., Moore, K., 2000. Factors contributing to water-column light attenuation.

Han, M-S., Furuya K., 2000. Size and species-specific primary productivity and community structure of phytoplankton in Tokyo Bay. Journal of Plankton Research 22: 1221-1235.

Harrison, W.G., Li, W.K., 2007. Phytoplankton growth and regulation in the Labrador Sea: light and nutrient limitation. J. Northw. Atl. Fish. Sci 39, 71-82.

Hiratsuka, J.-i., Yamamuro, M., Ishitobi, Y., 2007. Long-term change in water transparency before and after the loss of eelgrass beds in an estuarine lagoon, Lake Nakaumi, Japan. Limnology 8, 53-58.

Japan Coast Guard, 2000. Charts of Tidal Currents in Tokyo Wan, Tokyo.

Japan Meteorological Agency, 2000. Guidelines for Marine Observations. Tokyo.

Kasai, A., Fujiwara, T., Kimura, T., Yamada, H., 2004. Fortnightly shifts of intrusion depth of oceanic water into Ise Bay. Journal of oceanography, 60(5), 817-824.

Kemp, W.M., Boynton, W.R., Adolf, J.E., Boesch, D.F., Boicourt, W.C., Brush, G., Cornwell, J.C., Fisher, T.R., Glibert, P.M., Hagy, J.D., 2005. Eutrophication of Chesapeake Bay: historical trends and ecological interactions. Marine Ecology Progress Series 303, 1-29.

Lund-Hansen, L.C., 2004. Diffuse attenuation coefficients Kd (PAR) at the estuarine North Sea–Baltic Sea transition: time-series, partitioning, absorption, and scattering. Estuarine, Coastal and Shelf Science 61, 251-259.

Ministry of the Environment of Japan, 2011. Guidance for Introducing Total Pollutant Load Control System "TPLCS". http://www.env.go.jp/en/water/ecs/guidance_tplcs_summary.pdf (accessed August 2011)

Nakai, S., Soga, Y., Sekito, S., Umehara, A., Okuda, T., Ohno, M., Nishijima, W., Asaoka, S., 2018. Historical changes in primary production in the Seto Inland Sea, Japan, after implementing regulations to control the pollutant loads. Water Policy, wp2018093.

Nakamura T., Moriya K., Morita M., Koike T., 2005. Characteristics of spectral irradiance and turbidity in Ise Bay and its neighbouring waters. The Bulletin of the Faculty of Bioresources, Mie University 32:45–59 (in Japanese with English abstract).

Narita M., Arakawa H., Shimoda T., Morinaga T., 2006. Distribution of seawater turbidity due to dissolved organic matter and suspended matter in Tokyo Bay and the correlation with the contributing matter. Journal of the Tokyo University of Marine Science and Technology 2:35–46 (in Japanese with English abstract).

Nishijima, W., Umehara, A., Sekito, S., Okuda, T., Nakai, S., 2016. Spatial and temporal distributions of Secchi depths and chlorophyll a concentrations in the Suo Nada of the Seto Inland Sea, Japan, exposed to anthropogenic nutrient loading. Science of The Total Environment 571, 543-550.

Olesen, B., 1996. Regulation of light attenuation and eelgrass Zostera marina depth distribution in a Danish embayment. Marine Ecology Progress Series, 187-194.

Phlips, E., Lynch, T., Badylak, S., 1995. Chlorophyll a, tripton, color, and light availability in a shallow tropical inner-shelf lagoon, Florida Bay, USA. Marine Ecology Progress Series 127, 223-234.

R Core Team. R: A language and environment for statistical computing. 2015, Vienna, Austria.

Rasmeemasmuang, T., Sasaki, J., 2008. Modeling of mud accumulation and bed characteristics in Tokyo Bay. Coastal engineering journal 50, 277-307.

Riemann, B., J. Carstensen, K. Dahl, H. Fossing, J. W. Hansen, H. H. Jakobsen, A. B. Josefson, D. Krause-Jensen, S. Markager, and P. A. Stæhr. 2016. Recovery of Danish coastal ecosystems after reductions in nutrient loading: a holistic ecosystem approach. Estuaries and Coasts 39:82-97.

Rheuban, J.E., Williamson, S.C., Costa, J.E., Glover, D.M., Jakuba, R.W., McCorkle, D.C., Neill, C., Williams, T., Doney, S.C., 2016. Spatial and temporal trends in summertime climate and water quality indicators in the coastal embayments of Buzzards Bay Massachusetts. Biogeosciences 13, 253 – 265.

Sandén, P., Håkansson, B., 1996. Long – term trends in Secchi depth in the Baltic Sea. Limnology and Oceanography 41, 346-351.

Schlitzer, R., Ocean Data View, https://odv.awi.de, 2018.

Taylor, D.I., Oviatt, C.A., Borkman, D.G., 2011. Non-linear responses of a coastal aquatic ecosystem to large decreases in nutrient and organic loadings. Estuaries and Coasts 34, 745-757.

Uitz, J.U., Huot, Y., Bruyant, F., Babin, M., Claustre, H., 2008. Relating phytoplankton photophysiological properties to community structure on large scales. Limnology and Oceanography 53, 614-630.

Vant, W., 1990. Causes of light attenuation in nine New Zealand estuaries. Estuarine, Coastal and Shelf Science 31, 125-137.

Welschmeyer, N. A., 1994. Fluorometric analysis of chlorophyll a in the presence of chlorophyll b and pheopigments. Limnology and Oceanography 39, 1985–1992.

Williams, M.R., Filoso, S., Longstaff, B.J., Dennison, W.C., 2010. Long-term trends of water quality and biotic metrics in Chesapeake Bay: 1986 to 2008. Estuaries and Coasts 33, 1279-1299.

Xu, J., Hood, R. R., & Chao, S. Y., 2005. A simple empirical optical model for simulating light attenuation variability in a partially mixed estuary. *Estuaries*, *28*(4), 572-580.

Yamaguchi, H., Katahira, R., Ichimi, K., Tada, K., 2013. Optically active components and light attenuation in an offshore station of Harima Sound, eastern Seto Inland Sea, Japan. Hydrobiologia 714, 49-59.

Yamamoto, T., 2003. The Seto Inland Sea—eutrophic or oligotrophic? Marine Pollution Bulletin 47, 37-42.

Yanagi T, Hoshika A, Tsuji H. Changes in surface sediment characteristics and transport direction in Osaka Bay from 1982 to 2003. Oceanography in Japan 2006; 15:335–341 (in Japanese with English abstract).

Chapter 3: Identification of coastal zone vulnerable to phytoplankton growth in the Seto Inland Sea, Japan

3.1 Introduction

Classification or defining a typology of coastal waters or habitats was an important part in coastal management and had attracted the interest of marine policy makers, managers and scientists in recent years (Devlin et al. 2007, Halpern et al. 2012, Ramos et al. 2012, Delavenne et al. 2013). It could help us better understand the differences and similarities of among quantities of semi-discrete or discrete and identify candidate management units and prioritizing management efforts for the application of various regional or national regulations. Developing and application of effective analytical and operational tools which can facilitate the decision-making process, thus, had long been an interest to coastal water managers (Aguilera et al. 2001).

One important topic in coastal management was eutrophication and red tides or harmful algal blooms problems in coastal waters. Although red tides had been recorded in Bible and in the fossil record (Anderson 1997), it was until the middle of 20th century that this phenomena draw the attention of public due to their damage to coastal ecosystems and marine aquaculture and tourist industries on the global level (Imai et al. 2006, Álvarez-Salgado et al. 2008, Davidson et al. 2016). Thus, effective water quality assessment methods had always been in need to fulfill the requirements of legislation designed to monitor and protect coastal water bodies against degradation. Several methods of eutrophication status evaluation including Trophic Index (TRIX), US Environmental Protection Agency National Coastal Assessment Water Quality Index, HELCOM Eutrophication Assessment Tool (HEAT) and Statistical Trophic Index (STI) had been proposed and implemented around the world (Ferreira et al. 2011).

Choosing appropriate indicator(s) or parameter(s) was an important part in the assessment of water quality. Nutrients including dissolved inorganic nitrogen (DIN) and dissolved inorganic phosphorus (DIP), sometimes also total nitrogen (TN) and total phosphorus (TP), were important physico-chemical indicators in the assessment of trophic status of waters. Other physico-chemical indicators, such as dissolved oxygen (DO) and water clarity, and biological indicators including chlorophyll *a* (Chl.*a*) or macroalgae and seagrass were also involved in the trophic status assessment process (Ferreira et al. 2011).

Another important part in the water quality evaluation is the classification of water bodies based on selected indicators. Most researches performed the classification of coastal waters based on hierarchical agglomerative clustering (HAC) or a combination of self-organizing map and the k-means algorithm with several physical, chemical and biological indicators (Delavenne et al. 2013, Ramos et al. 2012). Bald et al. (2015) classified the Basque transitional and coastal waters in northern Spain by the Euclidean distance of sampling stations to the "bad" physico-chemical reference station in the three-dimensional space defined by factor analysis. Devlin et al. (2007) classified the UK marine waters by a new integrated index consisting of phytoplankton biomass, elevated phytoplankton abundance and seasonal succession of functional groups.

The present study took place in the Seto Inland Sea, which was the largest semi-enclosed sea located in western Japan. It was also a major fishing ground, marine aquaculture area and highly industrialized area in Japan. Severe environmental problems documented in the Seto Inland Sea in 1960s and 1970s due to heavy amounts of input of pollutants lead to the creation of the Provisional Law for Conservation of the Environment of the Seto Inland Sea in 1973 (this law was revised and renamed as Special Law for Conservation of the Environment of the Seto Inland Sea in 1978) (Akaha 1984, Imai et al. 2006). A series of studies were conducted on every aspect of the red tides (Imai et al. 1998, Nakamura 1995, Watanabe et al. 1995, Yanagi et al. 1995, Takeoka et al. 2002), which provided the basis for later prediction and mitigation of the adverse impacts on environment and various human activities. Nowadays harmful algal blooms have been controlled to a large extent in most coastal area and annual red tide frequency has declined from 299 in 1976 to around 100 after 1990 (Imai et al. 2006). As a result, the policy had been changed from water quality control to environment remediation and restoration of habitat (Nakai et al. 2018).

Current management strategy considers the Seto Inland Sea as a whole in spite of wide variation of environment in the area. However, we need to prioritize management efforts on vulnerable area to gain a better outcome. In this study, a novel indicator-vulnerable index (VI) is established to evaluate the natural phytoplankton growth potential and identify the vulnerable coastal zone of the Seto Inland Sea.

Furthermore, classification of the Seto Inland Sea water mass was performed based on the phytoplankton growth potential. The application of this new indicator would allow us to access how phytoplankton in different coastal waters responses to natural factors and could facilitate future assessment, monitoring and management of the Seto Inland Sea and other semi-enclosed seas in the world.

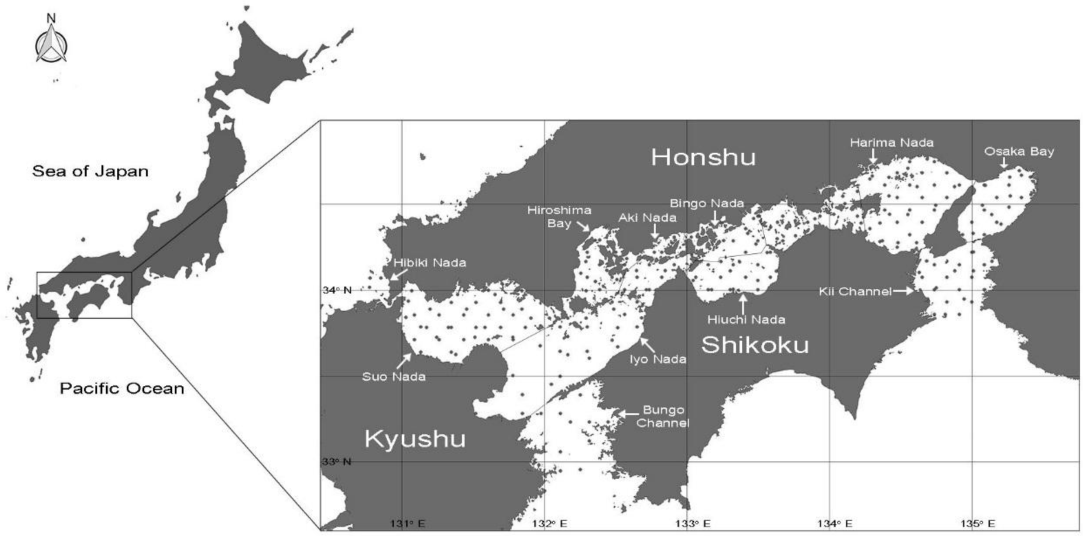

Figure 3.1 Map of the study area in the Seto Inland Sea. The boundaries between sub-areas are shown in black line. The dots indicate monitoring sites.

3.2 Materials and methods

3.2.1 Study area

The Seto Inland Sea is surrounded by Honshu, Kyushu and Shikoku in Japan and covers an area of ~23, 000 km^2 (Figure 3.1). Most of the area is less than 50 m deep with an average depth of 38 m. The Seto Inland Sea is composed of 12 water basins with different characteristics. A total of 664 rivers belonging to Class A and Class B flow into the Seto Inland Sea (Imai et al.2006). There is a growing urban population gradient from the western to eastern subsystems of the Seto Inland Sea (Miller et al. 2010). 19% of the TN and 28% of the total TP in Seto Inland Sea originates from the surrounding land (Yanagi & Ishii 2004).

3.2.2 Sample collection and analysis

Summer water quality data (July to early September) from 240 monitoring sites were provided by Ministry of the Environment (MOE, 119 monitoring sites) and Ministry of Land, Infrastructure, Transport and Tourism (MLIT, 121 monitoring sites) for the period 2003–2012. Secchi depth (SD) was measured with a 30-cm-diameter white disk. The measurement of SD was carried out twice and the average of the two values was used in later analysis. Water samples were taken at 0.5 m below the surface. Water temperature, salinity, Chl.a concentration and nutrient concentrations were measured following the Guidelines for Marine Observations (Japan Meteorological Agency, 2000). Briefly, salinity and water temperature were measured by CTD (Sea Bird Electronic Inc., USA) in situ. Chl.a was analyzed by the Welschmeyer method (Welschmeyer, 1994). DIN, DIP, TN and TP concentrations were colorimetrically determined by the autoanalyzer (e.g. SWAAT, BLTEC, Japan), following oxidation by potassium persulfate. Distance from the coastline was derived by ArcGIS 10.3 (ESRI 2011) for all monitoring sites.

3.2.3 Development of Vulnerable Index

3.2.3.1 Parameters selecting

Chl.a concentration is highest in summer, and summer is also the time when most red tides occur in Seto Inland Sea. Background Secchi depth (BSD) is the natural light condition of pelagic water bodies. Salinity and stability are also important natural factors influencing phytoplankton growth with no or very minor impact from human activities. Nutrients concentrations in Seto Inland Sea have been heavily influenced by human activities and cannot reflect the natural phytoplankton potential of a water body. In addition, population is the unit of phytoplankton bloom, and population growth is influenced by nutrients indirectly not directly via increased recruitment and (or) yield-dose relationships which influence population carrying capacity (Smayda 1997).

Method for calculation of waster stability (Brunt-Väisälä frequencies, N^2) was as based on the formula as follows:

$$N^2 = -\frac{g}{\rho} \times \frac{\partial \rho}{\partial z} \qquad \text{Eq. 1}$$

g is gravitational acceleration, ρ is sea water density at a water depth, $\partial\rho/\partial z$ is the change in density with depth.

Nishijima et al. (2018) separated the effects of non-phytoplankton components from total optical active components on light attenuation and proposed a new indicator background Secchi depth (BSD). It applies when the influence from phytoplankton is absent; that is, when Chl.a concentration equals 0. Based on the method described in Nishijima et al. (2018), BSD was calculated for each monitoring site used in the present study.

3.2.3.2 VI model establishment and selection

To select the optimal suite of explanatory variables to establish VI, salinity, $LogN^2$, BSD or SD, water depth and distance from coastline were screened.

$$VI = a_1 \times P_1 + a_2 \times P_2 + \cdots + a_i \times P_i \quad \text{Eq. 2}$$

In Eq. 2, each coefficient was limited in the range of 0–1 (namely, $0 \leq a_i \leq 1$) and the sum of coefficients (a_i) of different parameters were set as 1 for performance comparison of different combinations. Modified logistic regression models were used to predict the median summer Chl.a concentration with different VI derived from individual or several parameters mentioned above, namely, surface salinity, LogN2, BSD, water depth and distance from the coastline (hereafter referred to as distance) or their different combinations. The fitting of modified logistic regression models was conducted using the curve_fit function in SciPy library of Python programming language (Python Software Foundation):

$$Y = 1/(b_1 + b_2 \times \exp\,(b_3 \times VI) \quad \text{Eq. 3}$$

where Y is the median summer Chl.a concentration at a monitoring site, b_1, b_2 and b_3 are coefficients. b_1, b_2 and b_3 take positive values, moreover, b_1 was given the boundary of 0.005 and 0.05 to limit the modeled maximum Chl.a concentration in the range of 20–200 μg l^{-1}, a well-accepted maximum value in the Seto Inland Sea.

Linear fitting models were conducted with the OLS (a simple ordinary least squares model) class in StatsModels library of Python programming language (Python Software Foundation).

3.2.4 Mapping and date analysis

Spatial distribution of environmental factors and VI in the Seto Inland Sea was mapped with Ocean Data View version 5.0.0 software (Schlitzer 2018). Harmonic and arithmetic means were used for the Secchi depth and other water quality parameters, respectively. Standard deviation in the harmonic mean was calculated based on the method reported by Lam et al. (1985). Spearman correlation between Chl.*a* and environmental factors were performed with R software (R Core Team 2015); *p*-values < 0.05 were used to identify statistically significant effects.

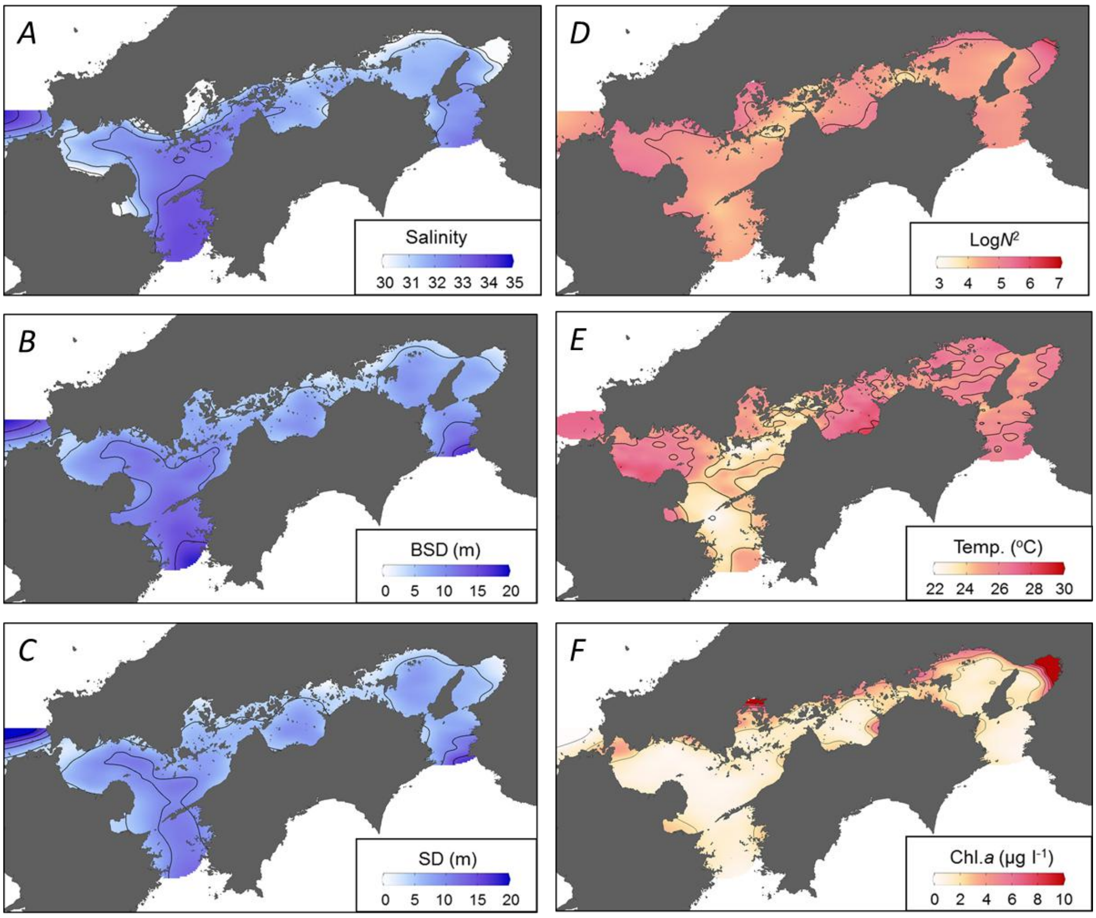

Figure 3.2 Spatial variation in mean salinity, BSD, SD, LogN^2, temperature and median Chl.*a* concentration in summer during the period 2003–2012. Contour lines demarcate 2 for salinity, 5 m for BSD and SD, 1 for LogN^2, 2 °C for temperature and 2 µg l^{-1} for Chl.*a* concentration. Temp. denotes temperature.

3.3 Results

3.3.1 Summer water quality in the Seto Inland Sea during the period of 2003-2012

Distributions of different water quality factors were shown in Figure 3.2. Salinity (31.41 ± 2.07, Mean ± sd) showed great spatial variability in the Seto Inland Sea, with lowest values of < 20 observed in geographically enclosed Osaka Bay and highest values of > 33 in the Kii Channel and Bungo Channel connected to the Pacific Ocean. SD (6.7 ± 0.2 m) and BSD (7.8 ± 0.2 m) showed similar spatial variation to that of salinity, with lower values measured in enclosed sub-basins facing highly populated watershed and some areas close to the coast. Water temperature ranged from 21.23 to 28.97 °C in the Seto Inland Sea, with an average of 25.55 °C. Surface Chl.*a* concentration in the Seto Inland Sea varied greatly with regard to locations, whereas in contrast to salinity and water clarity, highest Chl.*a* concentrations of > 10 μg l^{-1} were observed in some enclosed basins. 69% of the monitoring sites showed a median Chl.*a* concentration of < 2 μg l^{-1} and 93% of the monitoring sites showed a median Chl.*a* concentration of < 5 μg l^{-1}.

Table 3.1 Pearson correlation between Chl.a concentration and geographic or water quality factors in the Seto Inland Sea during the period 2003–2012.

	Salinity	LogN2	BSD	SD	Temp.	Depth	Dist.
LogN2	-0.59**						
BSD	0.47**	-0.21**					
SD	0.56**	-0.22**	0.86**				
Temp.	-0.14*	0.29**	-0.08	0.08			
Depth	0.48**	-0.54**	0.72**	0.57**	-0.37**		
Dist.	0.23**	-0.21**	0.36**	0.44**	-0.02	0.28**	
Chl.*a*	-0.72**	0.35**	-0.49**	-0.60**	-0.14*	-0.32**	-0.34**

Note: Temp. is water temperature, Dist. is distance from coast;
* is $p < 0.05$; ** is $p < 0.01$

The Spearman correlation coefficients between Chl.*a* and geographic and water quality parameters during the period 2003–2012 were summarized in Table 3.1. Significant correlations were obtained for nearly all the paired variables selected except for the relationship between water temperature and SD, BSD and distance ($p >$ 0.05). The median Chl.*a* concentration were best related to SD or BSD (r was –0.79

and –0.68, $p < 0.01$) and salinity (r: 0.58, $p < 0.01$). Salinity, water depth and LogN^2 was significant with all the other variables, indicating important effects of these geographic factors for characterizing the Seto Inland Sea.

3.3.2 Selection of model variables

Table 3.2 Performance of best linear fitting models derived from different parameters to predict chlorophyll *a*.

No. of Parameters	Parameters	R^2	AIC
1	Salinity	0.51	1369.12
2	Salinity+SD	0.57	1341.10
3	Salinity+SD+Depth	0.59	1332.29

Table 3.3 Performance of best logistic fitting models derived from different parameters to predict chlorophyll *a*.

No. of Parameters	Parameters	R^2	AIC
1	Salinity	0.51	1367.27
2	Salinity+SD	0.66	1278.66
3	Salinity+SD+LogN2	0.67	1277.80

Table 3.4 Performance of logistic fitting models to predict chlorophyll *a* with different forms of nutrients.

No.	Parameters	R^2	AIC
1	TN	0.22	1478.52
2	TP	0.30	1452.31
3	DIN	0.24	1471.02
4	DIP	0.05	1525.35

Tables 3.2 showed the performance of best linear fitting models derived from individual or different combination of two and three parameters. Salinity was the best parameter to predict surface Chl.a concentration ($R^2 = 0.51$, AIC (Akaike Information Criterion, Akaike 1974) = 1369.12). When two parameters were included in the model, salinity and SD ($R^2 = 0.57$, AIC = 1341.10) were the best combinations to predict Chl.*a* concentration. As for the three parameter models, inclusion of depth improved the R^2 of model, but the improvement (0.02) is rather limited.

Logistic fitting models performed equally to or better than linear fitting models (Tables 3.3, Figure 3.3). Salinity was also the best individual parameter to predict *C*hl.a concentration ($R^2 = 0.51$, AIC = 1367.27). Moreover, salinity and SD were the best 2 parameters combination ($R^2 = 0.66$, AIC = 1278.66). The inclusion of LogN^2

resulted in further improvement of model performance, whereas the improvement were rather limited with regard to R^2, being 0.01.

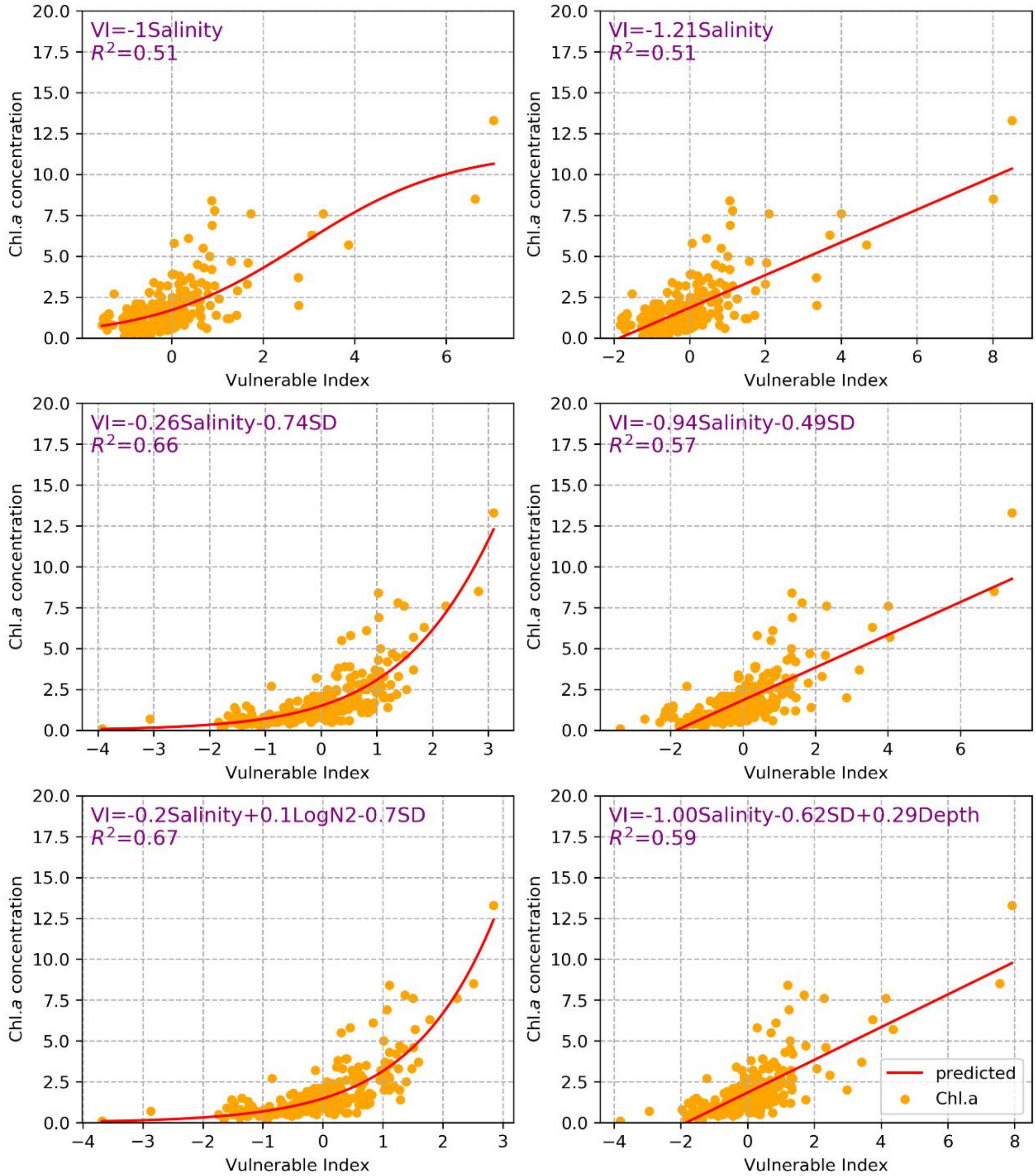

Figure 3.3 Comparison of different models to predict chlorophyll *a*.

Overall, the best combinations of parameters to predict Chl.a concentrations were salinity, LogN^2 and SD (Eq. 4 and Eq. 5). In particular, Eq. 5 reached the threshold of $R^2 \geq 0.65$ (Table 2.3), which were proposed to be the lower limit of valid goodness of fit (Moriasi et al. 2007, Ritter & Muñoz-Carpena 2013). In addition, VI is a better indicators for predicting Chl.*a* concentration than any form of nutrient ($R^2 \leq 0.30$, Table 3.4).

$$VI = -0.20Salinity + 0.10LogN^2 - 0.70SD \quad \text{Eq. 4}$$

$$Chl.a = 1/(0.005 + 0.671 \times \exp(-0.768VI)) \quad \text{Eq. 5}$$

3.3.3 Distribution of VI in the Seto Inland Sea

According to Eq. 4 and Eq. 5, the areas with lower water clarity and receiving higher freshwater runoff generated higher VI or could support higher surface Chl.*a* concentrations in the Seto Inland Sea and vice versa. Generally, VI deceased from geographically enclosed basins towards open basins or the outer ocean (Figure3.4). The coastal regions of Osaka bay, Harima Nada, Hiroshima Bay and part of Suo Nada had the highest VI. Whereas, the VI values of the Aki Nada, Iyo Nada, offshore area of Suo Nada, Bungo Channel and Kii Channel were very low.

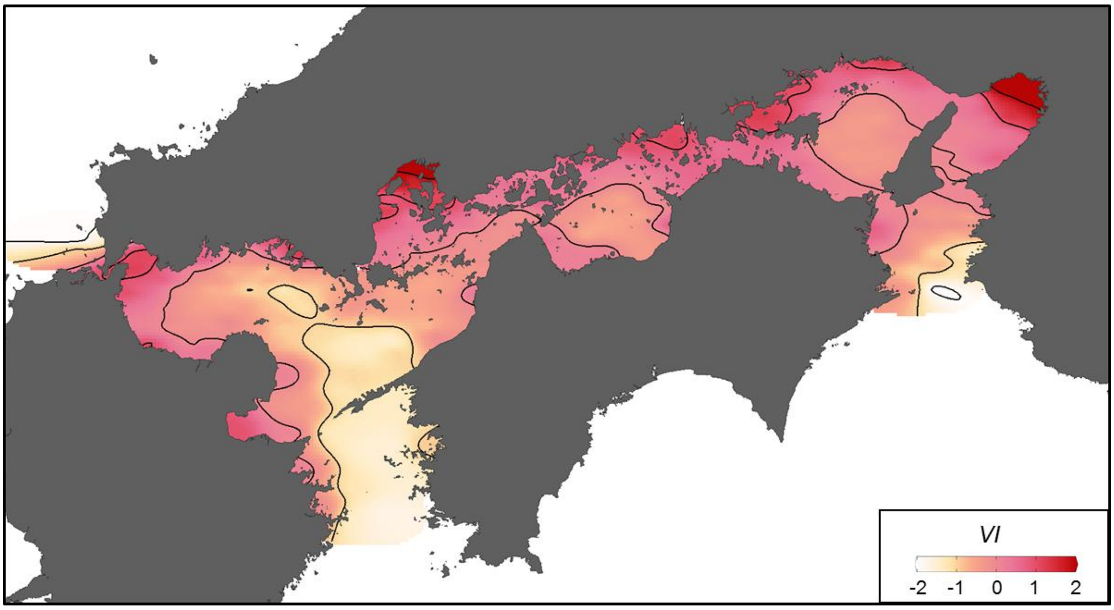

Figure 3.4 Distribution of Vulnerable Index derived from salinity, LogN^2 and SD in the Seto Inland Sea

Based on the best fit 3 parameter model (Eq. 4) and modified logistic regression (Eq. 5), the Seto Inland Sea was classified into 5 classes based on the estimated Chl.a concentration, that was C1 (0–2 μg l^{-1}), C2 (2–5 μg l^{-1}), C3 (5–10 μg l^{-1}), C4 (10–20 μg l^{-1}) and C5 (> 20 μg l^{-1}). The ratios of monitoring sites against total sites falling into above 5 classes were 69.20%, 27.43%, 2.11%, 0.84% and 0.42%, respectively, corresponding to 76.95%, 21.47%, 1.11%, 0.33% and 0.13% of the total area of the Seto Inland Sea (excluding the 3 monitoring sites in the Hibiki Nada).

3.4 Discussion

Previous attempts to understand phytoplankton dynamics in the Seto Inland Sea had not established a consistent mechanistic relationship between Chl.*a* concentration and environmental factors, especially the natural factors. Moreover, recent studies based on long-term data had proved that growth of phytoplankton biomass were nonlinear phenomena and the responses of Chl.*a* concentration to environmental drivers differed between normal phytoplankton dynamics and bloom conditions (McGowan et al. 2017, Nelson et al. 2017). Exploring the Seto Inland Sea data with a nonlinear perspective and an empirical approach provided us an ideal path for understanding the mechanisms related to phytoplankton dynamics by identifying causal environmental variables and their meaningful combinations. Moreover, any form of nutrient was not included in the screening process and establishment of vulnerable index, which gave us an insight into the influence of natural factors that were little influenced by anthropogenic activities on phytoplankton dynamics or bloom formation.

In the Seto Inland Sea, it was well known that low salinity was generally involved with large freshwater input, high LogN^2 and low water clarity (Figure 2), which provided an ideal condition for rapid phytoplankton growth and biomass accumulation in the surface layer of coastal water. Salinity was a better proxy for nutrient history than dissolved nitrogen or phosphorus that were rapidly accumulated into biomass. Firstly, similar dissolved nutrients concentrations could be related to opposite standing stock of phytoplankton, for example, low nitrate concentration could reflect 1) very low supply and low Chl.*a* concentration, 2) a balance between supply and uptake with high Chl.*a* concentration (McGowan et al. 2017). Secondly, total nutrient concentration might remain relatively stable during the stages of bloom initiation, expansion and ending, although the dissolved nutrients were nearly depleted after peak bloom biomass levels (Nelson et al. 2017). By contrast, (low) salinity could indicate a continuous supply of nutrients through freshwater input. As for water clarity, it indicated the levels of particulate matters or turbidity in the water column. In the surface layer (< 2 m), light availability was generally high enough to support phytoplankton growth. On the one hand, under high turbidity and low water clarity condition, phytoplankton cells were apt to migrate upwards in the water column, resulting in elevated Chl.*a* concentration in the water surface. On the other hand, high turbidity could also be related to resuspension of sedimented algae, turbulence-driven addition of nutrient rich porewater into the water column, namely, increased bottom-surface nutrient flux. It had been proved that in some coastal areas of the Seto Inland Sea, nutrient release from sediment contributed greatly to the nutrient pool of the water column in the warmer seasons (Lee et al. 2000).

Distance was a comprehensive indicator reflecting the influence of land on coastal waters (e.g. freshwater and nutrient input, increased water turbidity), which might influence the phytoplankton dynamics directly or indirectly. Our analysis also showed evidence for an effect of water stability in phytoplankton dynamics, an important mechanism for the onset of blooms in other areas (Strass & Nöthig 1996, Mouritsen & Richardson 2003, McGowan et al. 2017). However, the influence of water stability was limited, compared with salinity and water clarity. The improved phytoplankton growth was not because increased stratification per se (i.e. as physical growth promoters), but the increased nutrient, light condition and/or improved water quality conditions present in the boluses of stratified waters (Smayda 1997). These growth-facilitating microhabitats, with their entrained populations, would persist until nutrients were nearly exhausted, or the lenses were broken up by diffusion or increased turbulence (Smayda 1997).

While our model well predicted the variation of Chl.*a* concentration under different conditions, it did not capture everything. The estimated Chl.*a* concentration differed to the monitored values in some cases. This raised three possibilities: 1) the environmental factors involved were imperfect in the sense that different factors were highly correlated (e.g. salinity and LogN^2, salinity and SD) and might indicate the same proxies in some regions of the Seto Inland Sea, 2) phytoplankton community responded to environmental drivers not in the same way in different subareas with distinct geographic characteristics, 3) human activities, especially anthropogenic nutrient loading could have changed the nutrient balance in some coastal area where freshwater input were absent. In semi-enclosed coastal ecosystems receiving substantial freshwater input, salinity gradient played a fundamental role in structuring spatial patterns of physical properties (Cloern et al., 2017). Low salinity and low water clarity could both indicate high turbidity or freshwater input in the estuarine area. In addition, there had been field evidence that the importance of environmental factors to phytoplankton dynamics varied a lot in subareas with different characteristics (Nelson et al. 2017).

Based on the results in present study, 98.4% of the total area of the Seto Inland sea (Class 1 and 2) could only support phytoplankton biomass of less or equal to 5 μg l^{-1}, indicating a severe lack of the primary production and the need for sufficient nutrient. However, there was also 0.5% of the area (Class 4 and 5) that could support over 10 μg l^{-1}, in such area anthropogenic nutrient loading must be controlled to inhibit the excessive phytoplankton growth and accumulation and its negative influence on the whole ecosystem.

The significant and positive correlation between VI and nutrient concentrations ($p < 0.01$, Table 3) in the Seto Inland Sea suggested that there might be some linkage between the natural factors and anthropogenic factors facilitating phytoplankton growth in the Seto Inland Sea. The point source nutrient loading from human activities might be responsible for the deviation of some points to the relationship. Besides, it could also be inferred from above correlations that the TN concentration in the water was influenced to a larger extent than that of TP. A previous research on nutrient source of the Seto Inland Sea found that 19% of the TN and 28% of the TP in the Seto Inland Sea originated from the surrounding terrestrial zone, which might explain the smaller correlation coefficient between VI and TN (Yanagi & Ishii 2004). It was interesting that the coastal areas with highest VI values were consisting with the areas adjacent to highly populated watersheds (eastern Osaka Bay and northern Hiroshima Bay), which was as high as 19.34 million for eastern Osaka Bay and 1.80 million for Hiroshima Bay (Nishijima et al. 2018). Thus, the high natural potential for phytoplankton growth as well as high anthropogenic nutrient input from neighboring residences combined to result in the frequent red tide occurrence in the areas mentioned above (Imai et al. 2006). This was important in exploring the mechanisms underpinning the outbreak of red tides in different area within Seto Inland Sea and other coastal areas. Different measures should be taken according to the property of VI in different water bodies in future coastal management strategies.

3.5 Conclusions

Based on a nonlinear perspective and an empirical approach, this study proposed a novel indicator, vulnerable index derived from different natural environmental factors with long-term monitoring records of the Seto Inland Sea during the period

2003–2012. This index successfully predicted the baseline surface Chl.*a* concentration in the Seto Inland Sea . Results indicated that salinity was the best parameter to predict surface Chl.*a* concentration. When two parameters were included in the models, salinity and SD were the best combination to predict Chl.*a* concentration. As for the three parameter models, the inclusion of LogN^2 resulted in further improvement of VI model, whereas the improvements were limited.

Generally, VI deceased from geographically enclosed basins towards open basins or the outer ocean. Highest VI values were observed in the coastal regions of Osaka bay, Harima Nada, Hiroshima Bay and part of Suo Nada and lowest VI values in Aki Nada, Iyo Nada, offshore area of Suo Nada and two channels connecting the Pacific Ocean. The significant and positive correlation between VI and nutrient concentrations in the Seto Inland Sea suggested that there might be some linkage between the natural factors and anthropogenic factors facilitating phytoplankton growth in the Seto Inland Sea. The coastal areas with highest VI values were consisting with the areas adjacent to highly populated watersheds (eastern Osaka Bay and northern Hiroshima Bay), therefore, the high natural potential for phytoplankton growth as well as high anthropogenic nutrient input from neighboring residences united to result in the frequent red tide occurrence in some areas of the Seto Inland Sea. Based on above results, the natural property of local area must be taken into account in the process of policy-making and implementation of management measures.

3.6 References

Aguilera P, Frenich AG, Torres J, Castro H, Vidal JM, Canton M. Application of the Kohonen neural network in coastal water management: methodological development for the assessment and prediction of water quality. Water research 2001; 35: 4053-4062.

Akaha T. Conservation of the environment of the Seto Inland Sea. Coastal Management 1984; 12: 83-136.

Anderson DM. Turning back the harmful red tide. Nature 1997; 388: 513-514.

Chang P-H, Guo X, Takeoka H. A numerical study of the seasonal circulation in the Seto Inland Sea, Japan. Journal of oceanography 2009; 65: 721-736.

Davidson K, Anderson DM, Mateus M, Reguera B, Silke J, Sourisseau M, et al. Forecasting the risk of harmful algal blooms. Harmful Algae 2016; 53: 1-7.

Dekshenieks MM, Donaghay PL, Sullivan JM, Rines JE, Osborn TR, Twardowski MS. Temporal and spatial occurrence of thin phytoplankton layers in relation to physical processes. Marine Ecology Progress Series 2001; 223: 61-71.

Delavenne J, Marchal P, Vaz S. Defining a pelagic typology of the eastern English Channel. Continental Shelf Research 2013; 52: 87-96.

Devlin M, Best M, Coates D, Bresnan E, O'Boyle S, Park R, et al. Establishing boundary classes for the classification of UK marine waters using phytoplankton communities. Marine pollution bulletin 2007; 55: 91-103.

Ferreira JG, Andersen JH, Borja A, Bricker SB, Camp J, Da Silva MC, et al. Overview of eutrophication indicators to assess environmental status within the European Marine Strategy Framework Directive. Estuarine, Coastal and Shelf Science 2011; 93: 117-131.

Halpern BS, Longo C, Hardy D, McLeod KL, Samhouri JF, Katona SK, et al. An index to assess the health and benefits of the global ocean. Nature 2012; 488: 615-620.

Imai I, Kim MC, Nagasaki K, Itakura S, Ishida Y. Relationships between dynamics of red tide - causing raphidophycean flagellates and algicidal micro - organisms in the coastal sea of Japan. Phycological Research 1998; 46: 139-146.

Imai I, Yamaguchi M, Hori Y. Eutrophication and occurrences of harmful algal blooms in the Seto Inland Sea, Japan. Plankton and Benthos Research 2006; 1: 71-84.

Japan Meteorological Agency, 2000. Guidelines for Marine Observations. Tokyo.

Kirkpatrick B, Fleming LE, Squicciarini D, Backer LC, Clark R, Abraham W, et al. Literature review of Florida red tide: implications for human health effects. Harmful algae 2004; 3: 99-115.

Lee, I. and A. Hoshika. 2000. Seasonal variations in pollutant loads and water quality in Hiroshima Bay. Journal of Water Environment Society 23:367-373 (in Japanese with English abstract)

Lemos RT, Sansó B. Spatio - temporal variability of ocean temperature in the Portugal Current System. Journal of Geophysical Research: Oceans 2006; 111.

Miller TW, Omori K, Hamaoka H, Shibata J-y, Hidejiro O. Tracing anthropogenic inputs to production in the Seto Inland Sea, Japan–A stable isotope approach. Marine pollution bulletin 2010; 60: 1803-1809.

Mouritsen LT, Richardson K. Vertical microscale patchiness in nano-and microplankton distributions in a stratified estuary. Journal of Plankton Research 2003; 25: 783-797.

Nakamura Y, Suzuki S, Hiromi J. Population dynamics of heterotrophic dinoflagellates during a Gymnodinium mikimotoi red tide in the Seto Inland Sea. Marine Ecology Progress Series 1995; 125: 269-277.

Python Software Foundation. Python Language Reference, version 2.7. Available at http://www.python.org

Ramos E, Juanes JA, Galván C, Neto JM, Melo R, Pedersen A, et al. Coastal waters classification based on physical attributes along the NE Atlantic region. An approach for rocky macroalgae potential distribution. Estuarine, Coastal and Shelf Science 2012; 112: 105-114.

Richardson K, Visser A, Pedersen FB. Subsurface phytoplankton blooms fuel pelagic production in the North Sea. Journal of Plankton Research 2000; 22: 1663-1671.

Strass VH, Nöthig E-M. Seasonal shifts in ice edge phytoplankton blooms in the Barents Sea related to the water column stability. Polar Biology 1996; 16: 409-422.

Tada K, Monaka K, Morishita M, Hashimoto T. Standing stocks and production rates of phytoplankton and abundance of bacteria in the Seto Inland Sea, Japan. Journal of Oceanography 1998; 54: 285-295.

Takeoka H. Progress in Seto Inland sea research. Journal of oceanography 2002; 58: 93-107.

Watanabe M, Kohata K, Kimura T, Takamatsu T, Yamaguchi Si, Ioriya T. Generation of a Chattonella antiqua bloom by imposing a shallow nutricline in a mesocosm. Limnology and Oceanography 1995; 40: 1447-1460.

Yamamoto T. The Seto Inland Sea—eutrophic or oligotrophic? Marine Pollution Bulletin 2003; 47: 37-42.

Yanagi T, Ishii D. Open ocean originated phosphorus and nitrogen in the Seto Inland Sea, Japan. Journal of oceanography 2004; 60: 1001-1005.

Yanagi T, Yamamoto T, Koizumi Y, Ikeda T, Kamizono M, Tamori H. A numerical simulation of red tide formation. Journal of Marine Systems 1995; 6: 269-285.

Chapter 4: Management of the west-central Seto Inland Sea, Japan: factors controlling spatiotemporal distribution of chlorophyll a concentration and Secchi depth

4.1 Introduction

In recent decades, anthropogenically increased nutrient loading has led to undesirable changes in ecosystem structures and functions, including overgrowth of phytoplankton in various coastal areas around the world (Orth et al. 2006). Elevated Chl.*a* concentrations decrease light intensity in the water column and can adversely impact the growth and production of seagrasses and benthic microalgae (Orth et al. 2006). Excess sedimentation and subsequent mineralization of dead phytoplankton cells in the sediment results in the production of reductive sediment and hypoxia of bottom waters, and marked changes in the benthos (Nishijima et al. 2015).

A variety of nutrient reduction programmes have been implemented following the deterioration in coastal waters through phytoplankton overgrowth, such as the Grizzle-Figg Act in relation to Tampa Bay, Florida, USA (Greening et al. 2014), the Action Plan for the Aquatic Environment in relation to Danish coastal waters (Riemann et al. 2016), a ban on phosphate-based detergents and the use of biological nitrogen removal in Chesapeake Bay, USA (Williams et al. 2010) and a Total Pollutant Load Control System (TPLCS) in Japanese enclosed waters including the Seto Inland Sea (Nakai et al. 2018, Nishijima et al. 2018). The results, however, have been dependent on the nature of pressures (e.g. type, magnitude, frequency and timing), connectivity with adjacent systems and differing water quality parameters (Carstensen et al. 2011, Duarte et al. 2015). In successful cases, the improvement appeared in nutrients, Chl.*a*, dissolved oxygen concentrations and seagrass cover after implementation of the programme (Greening et al. 2014, Riemann et al. 2016, Nakai et al. 2018, Nishijima et al. 2018), whereas little improvement or even worsening were unfortunately reported too (Williams et al. 2010, Riemann et al. 2016).

On the other hand, stable and appropriate primary production by phytoplankton, as well as by seagrasses and benthic microalgae, is essential to sustain the healthy functioning of ecosystems and the sustainable supply of fishery resources (Takai et al.

2002, Hoshika et al. 2006, Nakai et al. 2018). Phytoplankton growth will directly respond to nutrient supply, whereas the growth and distribution of benthic macro- and microalgae will be determined by both nutrient supply and light availability; the latter will also be affected by nutrient supply through phytoplankton growth. Therefore, nutrient loading reductions should be managed to maintain and improve both appropriate phytoplankton growth and light availability, and the responses of these water quality parameters to nutrient loading reductions need to be understood.

One effect of TPLCS implementation on the Seto Inland Sea has appeared in certain ecosystem components (Yamamoto 2003, Nakai et al. 2018, Nishijima et al. 2018), although it varies in the subareas. The west-central Seto Inland Sea, including Hiroshima Bay and Aki Nada (Figure 1), receives substantial anthropogenic nutrient loading from its watersheds. Severe eutrophication in Hiroshima Bay (Seiki et al. 1991), especially the innermost region, is of great public concern because of its negative impact on ecosystem services. In addition, the west-central Seto Inland Sea is an archipelagic area, and the complex geographic conditions may significantly affect the characteristics of aquatic ecosystems, in which the responses to reduction of the anthropogenic loadings may vary.

In this study we constructed models estimating the spatiotemporal distributions of Chl.*a* and Secchi depth in the west-central Seto Inland Sea and identified the definitive factors of these two water quality parameters in considering geographic characteristics such as salinity, water depth and distance from coastline. Next, based on the definitive factors, we classified the west-central Seto Inland Sea into different subareas. We then assessed the effect of the TPLCS on Chl.*a* concentrations and Secchi depth in each subarea of the west-central Seto Inland Sea to allow better environmental management. This study will not only enrich the literature showing responses to reduced anthropogenic nutrient loadings in ecosystems, but also help us gain a better understanding of the factors dominating standing phytoplankton stocks and light availability in such a semi-enclosed coastal ecosystem.

4.2 Materials and Methods

4.2.1 Study area

The west-central Seto Inland Sea consists of Hiroshima Bay (1043 km^2) and Aki Nada (744 km^2) (Figure 4.1). Its southwestern part adjoins the Iyo Nada connected to the Pacific Ocean through the Bungo Channel. The Bingo Nada and Hiuchi Nada connect to the east-central part of the Seto Inland Sea. Several large rivers over 20 km in length (e.g. Yahata, Ohta, Seno, Kurose, Nishiki and Noro Rivers) flow into the west-central Seto Inland Sea on its northern coastline (Honshu). There is no large river over 10 km in length flowing into the west-central Seto Inland Sea on its southern coastline (Shikoku). A chain of islands: Miyajima, Eta-Noumijima, Kurahashijima, Kamikamagarijima, Osakikamijima, Osakishimojima and Omishima are located within 5–10 km of the coast of Honshu. Another chain of islands: Yashirojima, Nakashima and some small islands, constitute the southern border of the west-central Seto Inland Sea. Strong density stratification develops in warm seasons in the northwestern part of the area surrounded by the coast and the Miyajima and Eta-Noumijima islands. However, the waters in other parts mix well throughout the year (Asaoka et al. 2018).

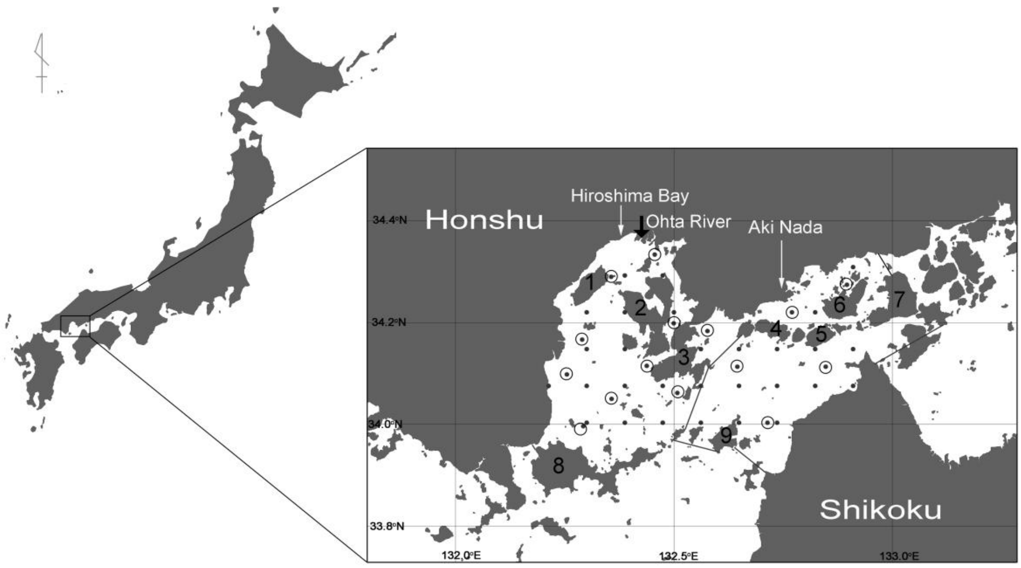

Figure 4.1 Map of the west-central Seto Inland Sea. Dots in circles are monitoring sites from MOE, dots without circles are monitoring sites from MLIT. Numbers show Miyajima, Eta-Noumijima, Kurahashijima, Kamikamagarijima, Osakikamijima, Osakishimojima, Omishima, Yashirojima and Nakashima in order.

4.2.2 Data set

Seasonal water quality data (winter: mid-January to early February, spring: May, summer: July to early September, autumn: October) were provided by the Ministry of the Environment (MOE, 15 monitoring sites) for the period of 1981–2015. The Ministry of Land, Infrastructure, Transport and Tourism (MLIT, 29 monitoring sites) provided information for the period 2000–2014. Chl.*a* concentrations were not monitored for 13 of the 29 MLIT sites. Secchi depth, nutrient concentration, water temperature and water depth data were available for all 44 sites. Distance from the coastline of Honshu was derived by ArcGIS 10.2 (ESRI 2011) for all monitoring sites.

The total nitrogen (TN) and total phosphorus (TP) loadings into the west-central Inland Sea were also provided by MOE. Loadings have been estimated by MOE as a part of the TPLCS every 5 years since 1979. The loading estimations took account of nutrient sources including industrial effluent, household discharges and agricultural wastewater.

4.2.3 Analysis

Secchi depth was twice measured with a 30-cm-diameter white disc by both MLIT and MOE and the average of two records was used for data analysis. Water samples were taken at depths of 0.5 m and 2.0 m in the MOE and MLIT observations, respectively. Analyses of water temperature, salinity, nutrients (NH_4^+, NO_2^-, NO_3^-, TN, PO_4^{3-}, TP), and Chl.*a* were conducted in accordance with the Guidelines for Marine Observations (Japan Meteorological Agency, 2000).

4.2.4 Factors influencing Chl.a concentration and Secchi depth

Distance from coastline and salinity is closely related with seston and nutrient levels in the water column, since freshwater discharged from the land is a carrier of particles and nutrients. Water depth is an important indicator of resuspension of sediment particles, which play important roles in the variations in light conditions or Chl.*a* concentration in the water column. The effect of distance from the island coastlines, and from those of the southern margins (Shikoku), however, are much less important than that from the coastline of Honshu (the northern coastline). This is because there are no (or only small) rivers, and no significant point sources of nutrients, in the islands and the southern area of land (Figure 4.2). Therefore, we chose the distance from the nearest northern coastline as a geographic parameter. Spearman rank correlation coefficients were used to determine the degree of correlation between distance, salinity, water depth, water temperature, Chl.*a* concentration and Secchi depth.

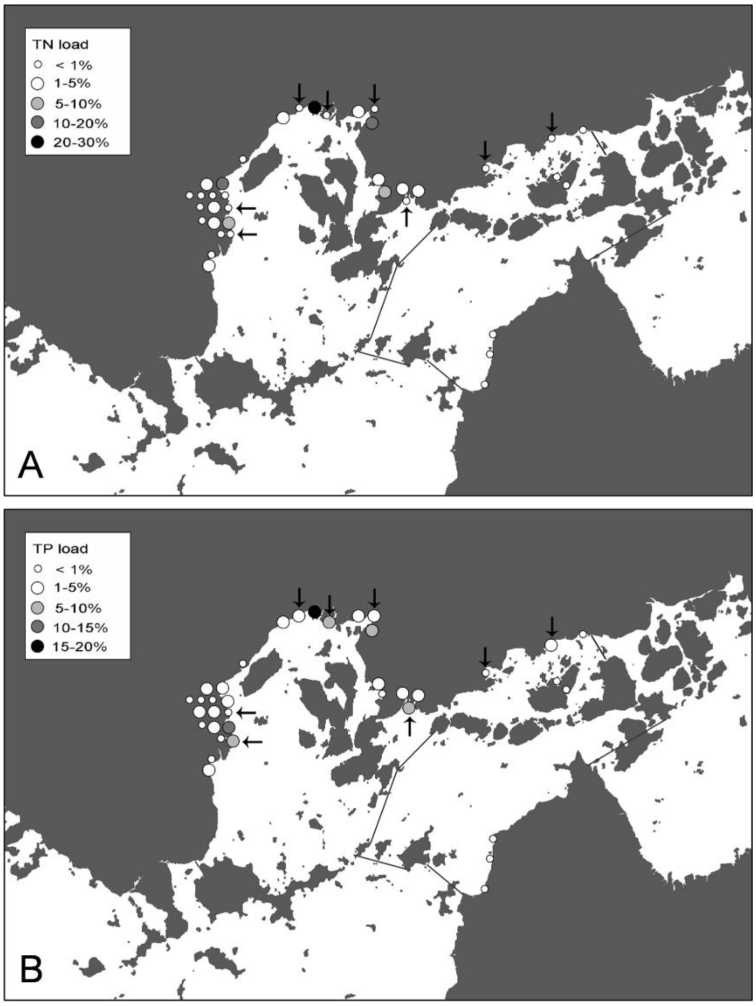

Figure 4.2 Distribution of total nitrogen (A) and total phosphorus (B) loads on the coastline of west-central Seto Inland Sea, percent is the ratio of nutrient loads in a site to the sum of nutrient loads in the whole area (Ministry of the Environment of Japan 2016). Arrows denote nutrient loads from rivers.

Logistic curve or logistic growth curve had been successfully used for predicting continuous variables with thresholds (e.g. Zwietering et al. 1990, Kucharavy & De Guio 2015). Eq. 1 (Figure 4.3 as an example) and Eq. 2 based on Zwietering et al. (1990) and Hara (1999) were used to predict the Secchi depth or Chl.*a* concentration with distance from the northern coastline, water depth and surface salinity (hereafter referred to as distance from coastline, depth and salinity, respectively) using the "lsqcurvefit" function (https://ww2.mathworks.cn/help/optim/ug/lsqcurvefit.html) of MATLAB R2014b (MathWorks, Inc., Natick, Massachusetts, USA):

$$A = 1/(b_1 + b_2 \times \exp(b_3 \times x)) \quad \text{Eq. 1}$$

$$A = 1/(b_1 + b_2 \times \exp(b_3 \times x_1 + b_4 \times x_2)) \quad \text{Eq. 2}$$

where A was SD or Chl.*a*, x was normalized distance, salinity or depth (z-score normalization based on mean and standard deviation). x_1 and x_2 were two factors from normalized distance, salinity and depth. b_1, b_2, b_3 and b_4 were coefficients. Eq. 1 was used to find the best determinant factor to predict Secchi depth or Chl.*a* concentration. Eq. 2 was used to find the best combination of factors to predict these two.

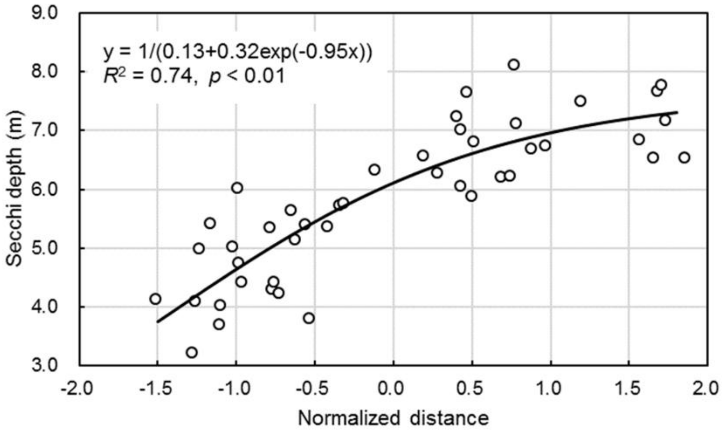

Figure 4.3 Example of modified logistic regression by which Secchi depth was plotted against normalized distance.

The best combination of distance from coastline, salinity and depth derived from the above equations was then used to classify the 31 monitoring sites with Chl.*a* concentration data into classes based on the results of agglomerative hierarchical clustering. The agglomerative hierarchical clustering of Euclidean distance was conducted with average linkage criteria method using R software (R Core Team 2015). Distance from the northern coastline and salinity (results from later analysis) were used after square-root-transformed and normalized for the clustering analysis. Then the monitoring sites were classified using the dendrogram obtained by the clustering.

4.2.5 Estimation of phytoplankton contribution to light attenuation

Nishijima et al. (2018) separate the roles of non-phytoplankton components from total optical active components contributing to light attenuation and propose a novel indicator background Secchi depth (BSD). BSD applies when the influence from phytoplankton is absent; that is, when Chl.a concentration equals 0. We estimated phytoplankton contribution to light attenuation, based on the concept of BSD, as follows (Eqs 3–9):

$$K_{\mathrm{d}} = K_{\mathrm{W}} + K_{\mathrm{CDOM}} + K_{\mathrm{tripton}} + K_{\mathrm{phyt}} \quad \text{Eq. 3}$$

$$K_{\mathrm{bg}} = K_{\mathrm{W}} + K_{\mathrm{CDOM}} + K_{\mathrm{tripton}} \quad \text{Eq. 4}$$

$$K_{\mathrm{d}} = K_{\mathrm{bg}} + K_{\mathrm{phyt}} \quad \text{Eq. 5}$$

$$K_{\mathrm{d}} = a/SD \quad \text{Eq. 6}$$

$$K_{\mathrm{bg}} = a/BSD \quad \text{Eq. 7}$$

$$\mathrm{ph}yt\% = 100 \times (K_{bg} / K_{\mathrm{d}}) \quad \text{Eq. 8}$$

$$\mathrm{phyt}\% = 100 \times (1 - SD/BSD) \quad \text{Eq. 9}$$

In Eq. 3, K_{d} is the total light attenuation coefficient for the water column, and K_{w}, K_{CDOM}, K_{tripton} and K_{phyt} are partial light attenuation by water, chromophoric dissolved organic matters (CDOM), tripton and phytoplankton, respectively. In Eq. 4, K_{bg} is the attenuation caused by background factors, which is the sum of K_{w}, K_{CDOM} and K_{tripton} in Eq. 3 (Nishijima et al. 2018). In Eqs 6 and 7, *SD* is Secchi depth and *BSD* is the background Secchi depth. The coefficient *a* is the product of K_{d} and *SD* or the product of K_{bg} and *BSD*. In Eqs 8 and 9 phyt% is phytoplankton contribution in light attenuation. The average phyt% at a monitoring site is then obtained from Eq. 9 when average *SD* is used.

4.2.6 Statistical analysis

Harmonic and arithmetic means were used for the Secchi depth and other water quality parameters, respectively. Standard deviation in the harmonic mean was calculated based on the method reported by Lam et al. (1985). Kruskal–Wallis ANOVA tests and subsequent Dunn's tests for multiple comparisons were used to compare Chl.a concentration and Secchi depth in different subareas. Bonferroni corrections were used for multiple comparisons. Chl.a and Secchi depth data from MOE during the period 1981–2015 were analysed for monotonously increasing or decreasing trends with linear regression. Influencers of the linear regression model were identified and removed by DFFITS (difference in fits, Belsley et al. 1980). Tukey's HSD test was used for a multiple comparison of regression slopes of linear models in different seasons of each subarea of west-central Seto Inland Sea. The Kruskal–Wallis test, Dunn's test and Tukey's HSD test were performed with R software (R Core Team 2015). A $p < 0.05$ was considered to be statistically significant in these tests.

4.3 Results

4.3.1 Spatial distribution of Secchi depth and Chl.a concentration, 2000–2014

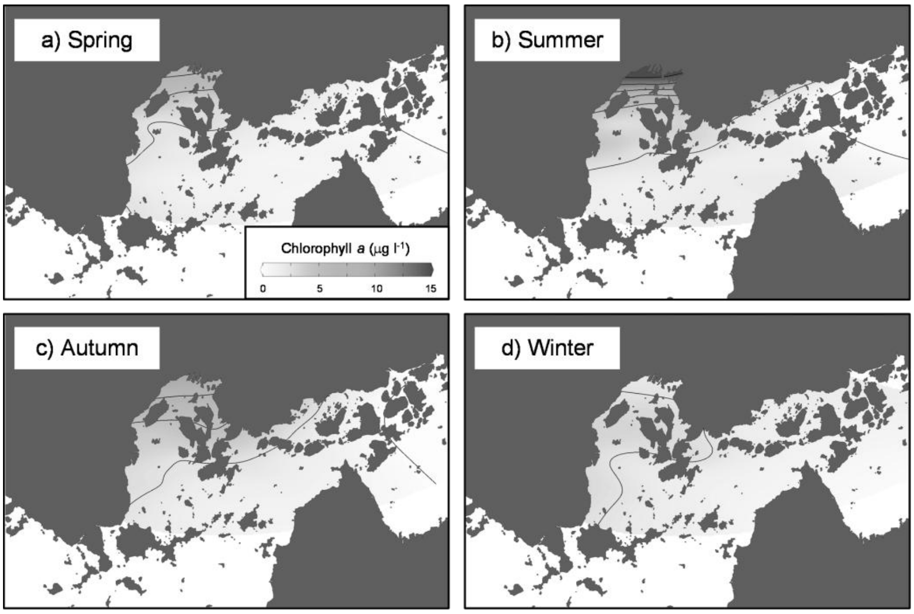

Figure 4.4 Seasonal and spatial distribution of mean chlorophyll a concentration, 2000–2014. Shading indicates chlorophyll a in μg l−1 and contour lines demarcate 2.5-μg l−1 intervals.

Water temperatures in the west-central Seto Inland Sea showed a typical seasonal variability. The mean water temperatures at the 44 monitoring sites were 10.2–12.6 °C (winter), 15.3–18.8 °C (spring), 22.1–26.2 °C (summer) and 22.3–23.7 °C (autumn). Salinity was the lowest in summer (22.7–32.9) and the highest in winter (31.2–33.6). Chl.*a* concentration at the surface of the west-central Seto Inland Sea varied greatly by seasons and locations (Figure 4.4). The values peaked in summer (1.1–14.5 μg l^{-1}), declined in autumn (1.0–8.7 μg l^{-1}) and winter (0.8–3.5 μg l^{-1}), and rose in spring (0.6–6.9 μg l^{-1}). Secchi depth in the west-central

Seto Inland Sea ranged from 2.0 to 8.4 m (Figure 4.5) with higher values observed in winter (4.0–8.4 m) and lower values in summer (2.1–7.6 m).

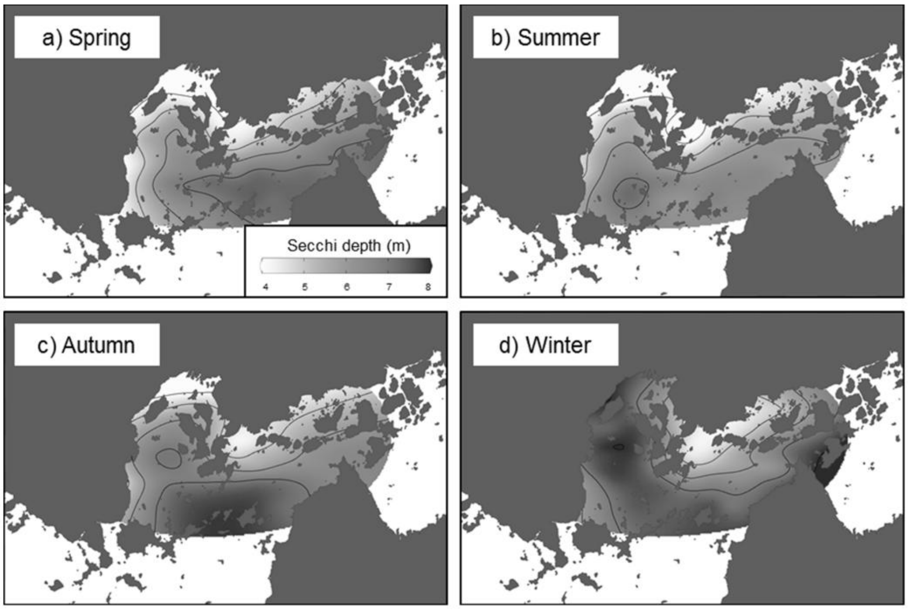

Figure 4.5 Seasonal and spatial distribution of mean Secchi depth, 2000–2014. Shading indicates Secchi depth in metres and contour lines demarcate 1-m intervals.

Table 4.1 Spearman correlation coefficients for the relationship among distance, depth, salinity, water temperature, chlorophyll *a* (Chl.*a*) and Secchi depth, 2000–2014.

Item	Season	Distance	Depth	Salinity	Temp.	DIN	DIP	Chl.*a*
Chl.*a*	Spring	-0.57**	-0.45*	-0.82**	0.80*	0.41*	-0.50*	
	Summer	-0.45*	-0.20	-0.48**	0.45**	0.16	-0.15	
	Autumn	-0.80**	-0.52*	-0.89**	-0.03	0.01	0.02	
	Winter	-0.61**	-0.60*	-0.55**	-0.45**	-0.42*	-0.50*	
Secchi	Spring	0.82**	0.56*	0.57**	-0.56*	-0.25	0.11	-0.68**
	Summer	0.78**	0.38*	0.40*	-0.23	-0.34	0.03	-0.66**
	Autumn	0.79**	0.37*	0.65**	-0.01	-0.19	0.07	-0.66**
	Winter	0.36*	0.41*	0.13	0.06	-0.08	-0.21	0.01

Note: Temp. is water temperature; * is $p < 0.05$; ** is $p < 0.01$

The Spearman correlation coefficients between Chl.*a*, Secchi depth and other geographic and water quality parameters, including distance from the northern coastline, salinity, water depth, dissolved inorganic nitrogen (DIN) and dissolved inorganic phosphorus (DIP), in different seasons during the period 2000–2014 are summarized in Table 4.1. The Chl.*a* concentrations were best related to salinity (r: –0.89 to –0.48, $p < 0.01$) and distance from the northern coastline (r: 0.45 to 0.80, $p < 0.05$), while the Secchi depth was best related to distance from the northern coastline (r: 0.36 to 0.82, $p < 0.05$) and depth (r: 0.37 to 0.56, $p < 0.05$). Secchi depth was also significant correlated with salinity except for winter when the variation of salinity was smaller than that in other seasons due to smaller river flow into the study area. Significant correlations were also found between Chl.*a* concentration and Secchi depth in spring, summer and autumn (r: 0.66 to 0.68, $p < 0.01$). Although DIN and DIP are the important factors in the control of Chl.*a* concentration, they did not show a positive relationship with Chl.*a* concentration except for spring (r: 0.41, $p < 0.05$).

4.3.2 Factors determining Chl.a concentration and Secchi depth

Table 4.2 Detailed results of logistic curve fitting to predict chlorophyll *a* with different combinations of distance from coast, water depth and salinity.

Parameter	Season	b_1	b_2	b_3	b_4	R^2	RMSE
Distance	Spring	0.01	0.61	0.48	-	0.25	1.27
	Summer	0.01	0.42	0.59	-	0.19	2.50
	Autumn	0.01	0.40	0.51	-	0.41	1.45
	Winter	0.20	0.31	0.44	-	0.40	0.64
Depth	Spring	0.01	0.55	0.17	-	0.04	1.45
	Summer	0.01	0.36	0.11	-	0.01	2.77
	Autumn	0.15	0.23	0.34	-	0.09	1.79
	Winter	0.05	0.46	0.28	-	0.34	0.67
Salinity	Spring	0.01	0.64	0.51	-	0.90	0.46
	Summer	0.01	0.47	0.64	-	0.90	0.87
	Autumn	0.05	0.36	0.53	-	0.81	0.82
	Winter	0.20	0.30	0.31	-	0.22	0.73
Distance + Depth	Spring	0.11	0.50	0.62	-0.10	0.26	1.29
	Summer	0.01	0.41	0.61	-0.11	0.20	2.54
	Autumn	0.01	0.40	0.52	-0.02	0.41	1.47
	Winter	0.20	0.31	0.32	0.24	0.48	0.60
Distance + Salinity	Spring	0.01	0.65	0.08	0.49	0.91	0.46
	Summer	0.01	0.48	0.11	0.61	0.91	0.87
	Autumn	0.01	0.41	0.23	0.36	0.86	0.72
	Winter	0.20	0.31	0.38	0.10	0.42	0.64
Salinity + Depth	Spring	0.01	0.64	0.04	0.51	0.91	0.46
	Summer	0.01	0.48	0.10	0.65	0.92	0.83
	Autumn	0.04	0.38	0.10	0.50	0.83	0.80
	Winter	0.20	0.31	0.35	0.23	0.44	0.63

We tried to find factors determining the Chl.*a* concentration and Secchi depth in the west-central Seto Inland Sea. The results of logistic curve fitting are shown in Tables 4.2 and 4.3. Salinity was the best individual predictor of Chl.*a* concentrations, especially from spring to autumn (R^2: 0.81–0.90). The supply of nutrients through freshwater will contribute to phytoplankton growth, but nutrients were also supplied from adjacent waters connecting to the study waters. The contribution of Pacific Ocean to TN and TP loadings into the study area was estimated to be about 80%–90% and about 75%, respectively (Ishii and Yanagi 2004). Therefore, the significant relationship between Chl.*a* concentration and salinity would not mean simply that Chl.*a* concentration was controlled by nutrients from the land. Low salinity areas are mainly located on shallow coasts, suggesting that salinity represents not only the nutrient supply from the land, but also the various effects of the land.

Table 4.3 Detailed results of logistic curve fitting to predict Secchi depth with different combinations of distance from coast, water depth and salinity.

Parameter	Season	b_1	b_2	b_3	b_4	R^2	RMSE
Distance	Spring	0.13	0.03	-0.95	-	0.74	0.65
	Summer	0.15	0.01	-1.58	-	0.58	0.85
	Autumn	0.13	0.02	-1.16	-	0.65	0.71
	Winter	0.14	0.01	-1.00	-	0.20	1.11
Depth	Spring	0.14	0.03	-0.59	-	0.20	1.16
	Summer	0.17	0.01	-1.43	-	0.11	1.23
	Autumn	0.15	0.00	-2.25	-	0.17	1.09
	Winter	0.15	0.00	-3.93	-	0.11	1.16
Salinity	Spring	0.12	0.05	-0.38	-	0.32	1.07
	Summer	0.13	0.05	-0.50	-	0.43	0.98
	Autumn	0.12	0.04	-0.35	-	0.29	1.00
	Winter	0.12	0.03	0.12	-	0.02	1.22
Distance + Depth	Spring	0.13	0.03	-0.91	-0.13	0.75	0.65
	Summer	0.15	0.01	-1.57	-0.04	0.58	0.86
	Autumn	0.13	0.02	-1.16	-0.01	0.65	0.72
	Winter	0.14	0.01	-1.03	-0.72	0.23	1.09
Distance + Salinity	Spring	0.13	0.03	-0.89	-0.09	0.75	0.65
	Summer	0.15	0.01	-1.35	-0.38	0.68	0.75
	Autumn	0.13	0.02	-1.10	-0.11	0.66	0.70
	Winter	0.12	0.02	-0.89	0.70	0.45	0.93
Salinity + Depth	Spring	0.14	0.03	-0.54	-0.48	0.43	0.99
	Summer	0.16	0.01	-0.78	-0.94	0.49	0.94
	Autumn	0.14	0.01	-0.82	-0.63	0.39	0.94
	Winter	0.12	0.03	-0.27	0.18	0.09	1.19

Distance was the best individual predictor of Secchi depth in the study area (Table 3.3, R^2: 0.58–0.74) in spring, summer and autumn, whereas salinity showed low correlation with Secchi depth (Table 3.3, R^2: 0.02–0.43). Moreover, depth was weakly correlated with Secchi depth even though the Chl.*a* concentration was not related to depth. Hibino and Matsumoto (2006) reported that sediment was covered with 1−6 cm of thin floating mud in the wide area of the northern part of Hiroshima Bay. In addition, suspended solids in the waterbody were supplied from floating mud on sediment near the coastline and transported southward (Lee et al. 2001). This might be the reason for the good correlation between the distance from the northern coastline and Secchi depth.

Since the combinational use of distance from the northern coastline and salinity in the logistic curves successfully predicted the Chl.*a* concentration and Secchi depth, these were used to explore the mechanisms underpinning Chl.*a* and Secchi depth distribution regime in the west-central Seto Inland Sea. The whole west-central Seto Inland Sea was divided into three classes by the agglomerative hierarchical clustering method (Figure 4.6). The monitoring sites belonging to Class 1, characterized by low salinity and short distance from coastline, were located in the innermost part of Hiroshima Bay. The monitoring sites in Class 2, with median salinity and at a short distance from the coastline, were distributed in western coastal Hiroshima Bay and northern coastal Aki Nada. The monitoring sites in Class 3 were distributed in the area far away from the northern coastline.

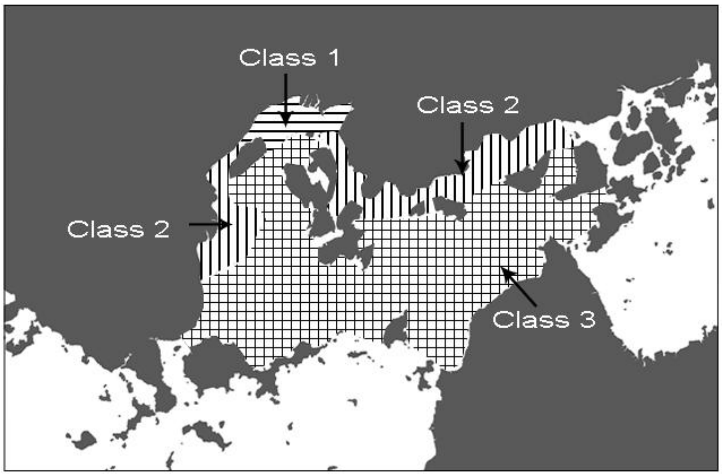

Figure 4.6 Classification of the west-central Seto Inland Sea based on distance from the northern coastline and salinity.

4.3.3 Spatial and historical changes in Chl.a concentration and Secchi depth in the west-central Seto Inland Sea

The seasonal mean Chl.*a* concentration and Secchi depth during the period 2000–2014 in the classified subareas of the west-central Seto Inland Sea are shown in Figure 4.7. A significant difference among the subareas of the west-central Seto

Inland Sea was observed in spring, summer and autumn for both Chl.*a* and Secchi depth ($p < 0.05$); no significant differences were observed in winter ($p > 0.05$). Generally, subarea Class 1 showed the highest Chl.*a* concentration, followed by Class 2 and Class 3 during spring, summer and autumn. By contrast, the highest Secchi depth was observed in subarea Class 3, followed by Class 2 and Class 1 in spring, summer and autumn. In winter, the large water mixing by the strong wind and the sea surface cooling could be responsible for the small regional difference in Chl.*a* and Secchi depth.

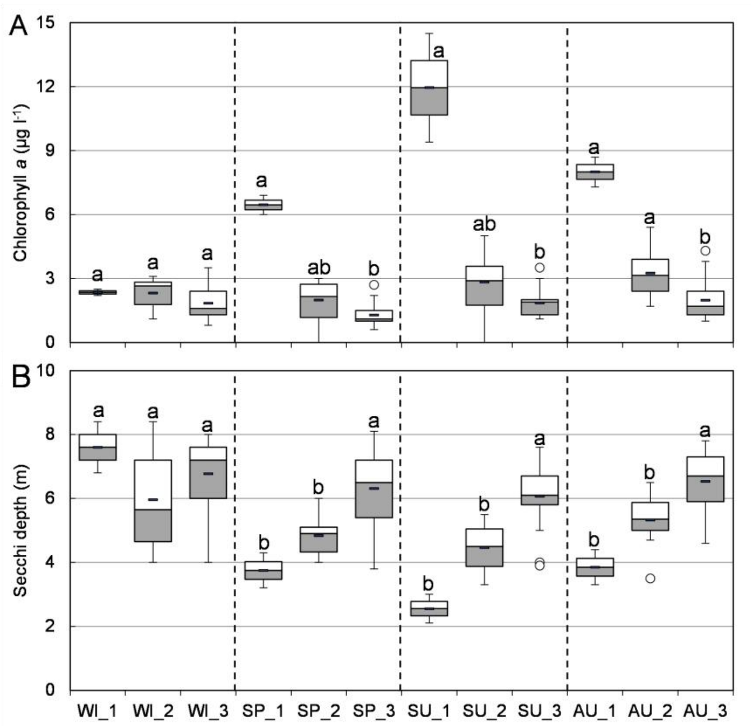

Figure 4.7 Seasonal mean chlorophyll a concentration and mean Secchi depth in different subareas of the west-central Seto Inland Sea. WI, SP, SU and AU = winter, spring, summer and autumn, respectively. 1, 2 and 3 = Class 1, Class 2 and Class 3, respectively (see Figure 4.6). "o" = the outlier by 1.5 interquartile range (IQR) rule. Within each season boxes with different letters (a, b) indicate significant differences ($p < 0.05$, Dunn's test) between different subareas.

The annual values in Chl.*a* and Secchi depth in different subareas of the west-central Seto Inland Sea during the past 35 years (1981–2015) are shown in Figures 4.8 and 4.9. Significant decreases in mean Chl.*a* concentration were observed during a specific season in the coastal regions (Class 1 and 2) and during several seasons in the offshore region (Class 3). In spring, the decreasing rate of mean Chl.*a* concentration expressed as a slope factor in Class 1 (0.177 $\mu g\ l^{-1}\ y^{-1}$) was significantly higher than those in Classes 2 and 3 (0.024–0.025 $\mu g\ l^{-1}\ y^{-1}$, $p < 0.05$).

Although large fluctuations in mean Chl.*a* were observed, the rates of decrease were also higher during summer (0.154 μg l^{-1} y^{-1}) and autumn (0.100 μg l^{-1} y^{-1}) in Class 1 than those in Classes 2 and 3.

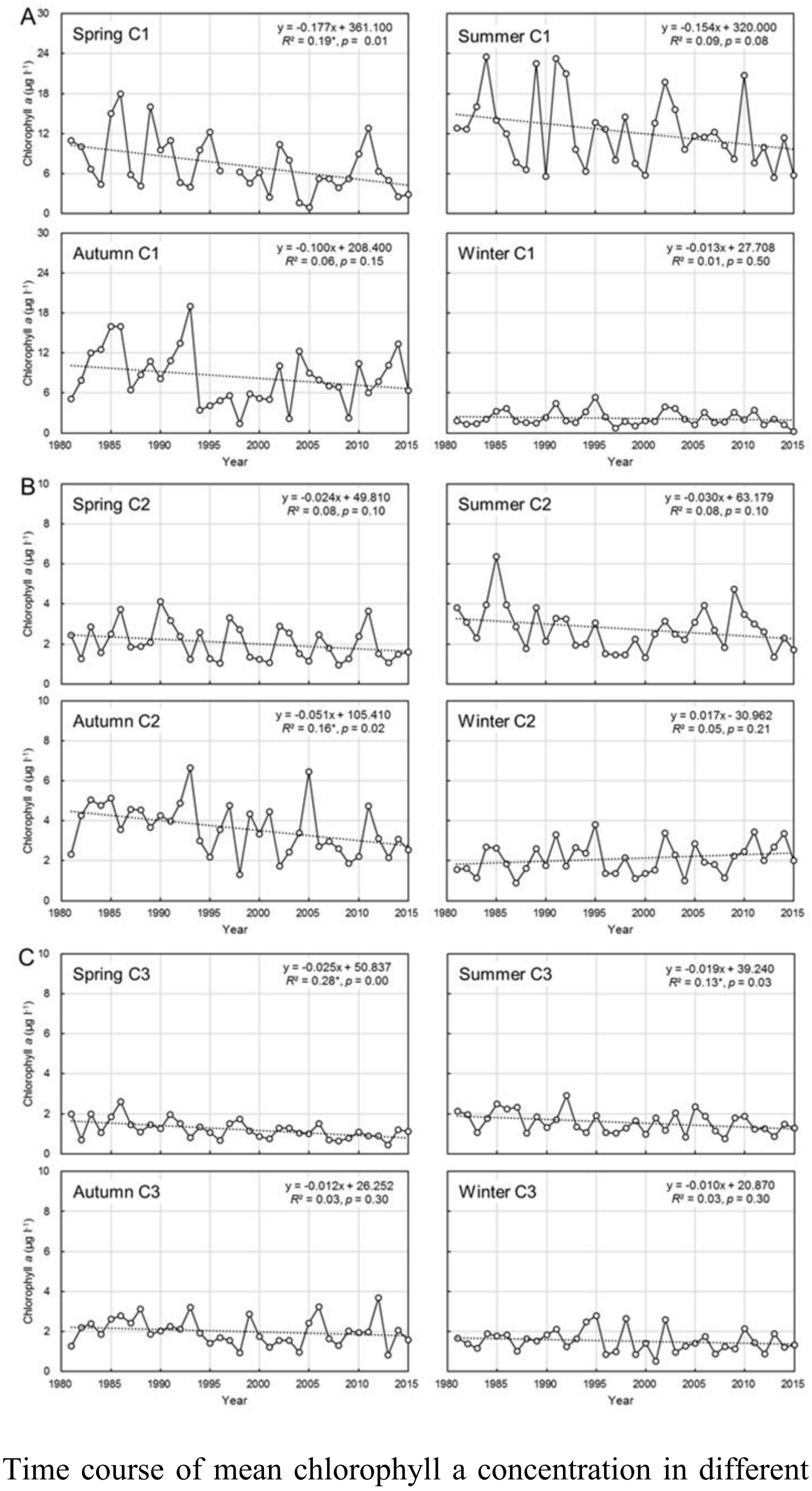

Figure 4.8 Time course of mean chlorophyll a concentration in different subareas of west-central Seto Inland Sea, 1981–2015. C1, C2, C3 = Classes 1, 2 and 3, respectively (see Figure 4.6). Note: * is $p < 0.05$; ** is $p < 0.01$

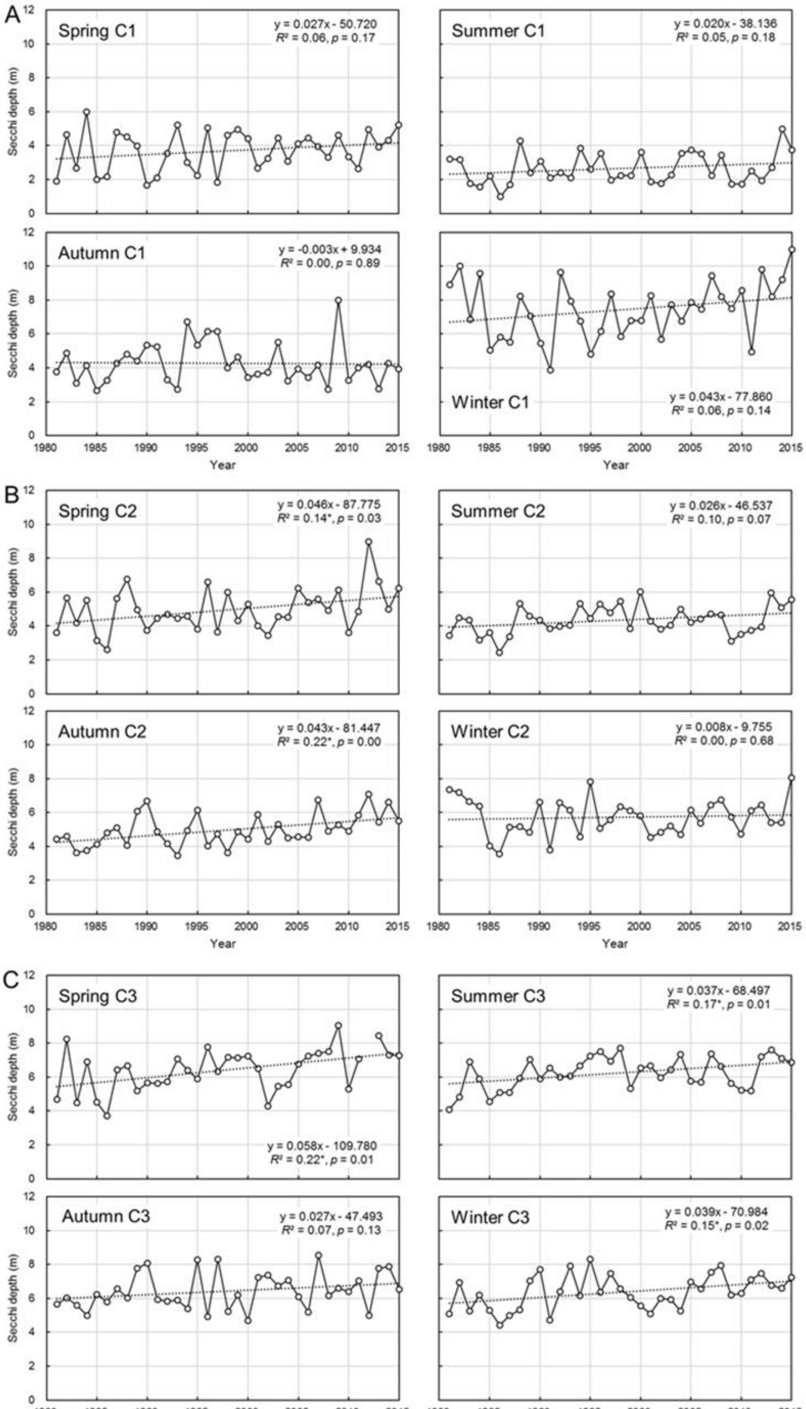

Figure 4.9 Time course of mean Secchi depth in different subareas of west-central Seto Inland Sea, 1981–2015. C1, C2, C3 = Classes 1, 2 and 3, respectively (see Figure 4.6). Note: * is p < 0.05; ** is p < 0.01

Secchi depth was observed to increase with time in most cases. Significant increase (p < 0.05) in mean Secchi depth was observed during several seasons in the regions of Class 2 and 3 (Figure 4.9). No significant difference was found in the rate of increase in mean Secchi depth among Classes 1–3 in all seasons, because of high fluctuation and low rates of increase. Moreover, Secchi depth is determined not only by phytoplankton concentration but also by other factors which will not change by eutrophication.

4.4 Discussion

Table 4.4 Nutrient loading (kg km^{-2} d^{-1}) from the surrounding land into the west-central Seto Inland Sea.

Area	Loading	Year							
		1979	1984	1989	1994	1999	2004	2009	Decrease (%)[a]
Hiroshima Bay	TN	31.6	30.7	32.6	28.7	25.9	24.0	22.6	28.71%
	TP	2.97	2.01	2.30	2.43	2.30	1.53	1.55	47.96%
Aki Nada	TN	10.8	9.4	9.4	10.2	9.4	9.4	9.2	14.48%
	TP	1.08	0.81	0.81	0.79	0.81	0.67	0.66	38.34%
Average	TN	22.9	21.8	22.9	21.0	19.0	17.9	17.0	25.76%
	TP	2.18	1.51	1.68	1.75	1.68	1.18	1.18	45.45%

[a] $Decrease(\%) = 100 \times (Load_{1979} - Load_{2009}) / Load_{1979}$

4.4.1 The relationship between nutrient load and Chl.a concentration in the west-central Seto Inland Sea

Chl.*a* concentration has decreased in the west-central Seto Inland Sea, although the extent of reduction has varied both seasonally and spatially. This may be a positive response to the implementation of TPLCS in this area. During the 30 years from 1979 to 2009, the TP and TN entering the west-central Seto Inland Sea from the land declined by 45.45% and 25.76%, respectively (Table 4.4). The mean Chl.*a* concentration in each classified area for 5-year intervals were plotted against TN and TP loadings from land during the corresponding time intervals to check the relationship between allochthonous nutrient loading and phytoplankton abundance (Figure 4.10). For example, the mean Chl.*a* concentration from 1981 to 1985 was paired with the nutrient loading in 1984. Class 1 was located in Hiroshima Bay and Class 2 was mainly located in Hiroshima Bay, so the mean Chl.*a* concentrations were paired with nutrient loads in Hiroshima Bay for Class 1 and 2. The mean Chl.*a* concentrations were paired with average nutrient loads in Hiroshima Bay and Aki Nada for Class 3. The results suggested that Chl.*a* may be impacted by the TN loading (R^2: 0.46–0.62) greater than TP loading (R^2: 0.05–0.21) throughout the west-central Seto Inland Sea. Although the decrease in Chl.*a* concentration with decrease in nutrient loading from the land was observed clearer in Classes 1 and 2 (facing the large sources of nutrients from rivers) than in Class 3, statistical significance was not observed in either case. Our result is consistent with a nutrient enrichment algal assay conducted by Lee et al. (1996), which reported that the growth of the entire phytoplankton community in Hiroshima Bay was stimulated by the addition of nitrogen.

In the west-central Seto Inland Sea, the molar ratios of DIN to DIP showed extremely high variations. It was lower than the Redfield ratio of 16 with some exceptions in the subareas of Class 2 and 3 and around 30 in the subarea of Class 1 (Table 4.5). Nutrient release from sediment and nutrient supply from the connecting waters should be considered as other sources. In nutrient release from sediment, greater amounts of phosphorus than nitrogen are known to be released and to enter the overlying waters, especially in the warmer seasons (Lee et al. 2000). In the nutrient supply from the connecting waters, DIN:DIP ratios in Iyo Nada, Bingo Nada and Hiuchi Nada were less than or around 16 in most cases. Consequently, the result that the Chl.*a* showed a better correlation with TN loading than with TP loading would be reasonable. Dissolved silicate is also an important nutrient for phytoplankton growth. In an investigation across the Seto Inland Sea it was proved not to be a limiting nutrient, except in Osaka Bay during 1994–2000 (Yanagi and Harashima 2003).

On the other hand, phosphorus is reported to control Chl.*a* concentration in Suo Nada, west of this study area in the Seto Inland Sea (Nishijima et al. 2016). The main differences between the water in this study, Hiroshima Bay and Aki Nada, and Suo Nada, were DIN:DIP ratios in water column and nutrients loadings from land. The DIN:DIP ratios in the water column ranged from 17.0 to 35.2 in the shallow area (less than 20 m). Those in nutrient loadings from the land ranged from 17.7 to19.0 after 1989 in Suo Nada. On the other hand, the DIN:DIP ratios in the water column ranged from 6.3 to 16.4, with one exception: the deep area connected to Iyo Nada. These results suggested that the shallow area near the coastline was strongly affected by nutrient loadings from land and a higher ratio than 16 of DIN:DIP in nutrient loading from land resulted in phosphorus limiting phytoplankton growth in Suo Nada. Not only the amount of nutrients supplied from land but also the ratio of DIN:DIP was found to control phytoplankton growth, especially in coastal areas.

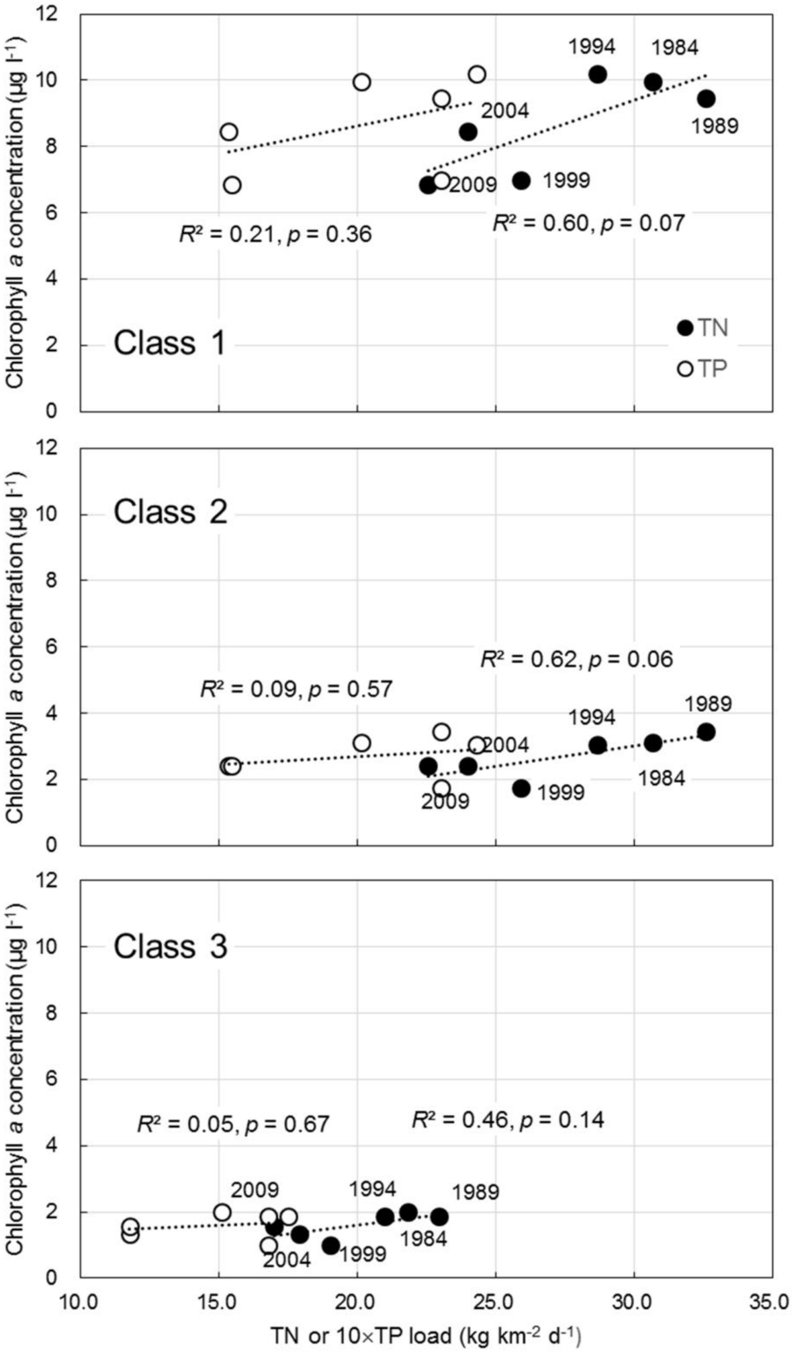

Figure 4.10 Relationship between total nitrogen (TN) and total phosphorus (TP) loading from land and mean chlorophyll a concentration in different subareas of the west-central Seto Inland Sea based on data from 15 observation sites in western central Seto Inland Sea, 1981–2000. Years in the figures are inserted for nitrogen plots. Dotted lines are linear regression lines fit to the TN or TP data. Class 1, 2 and 3 indicate the same regions as in Figure 4.6.

Table 4.5 Mean water quality in different regions of the west-central Seto Inland Sea. Error bounds are ± one standard deviation.

Area	Period	DIN	DIP	DIN:DIP	Secchi depth	Chl.*a*
		μM l^{-1}	μM l^{-1}		m	μg l^{-1}
Class 1	1981-1985	6.03±5.86	0.30±0.27	27±31	3.3±0.3	8.7±5.6
	1986-1990	9.18±7.87	0.44±0.35	33±43	3.2±0.4	7.7±6.2
	1991-1995	7.53±8.22	0.35±0.33	23±36	3.5±0.3	8.3±6.1
	1996-2000	8.15±5.33	0.43±0.31	25±17	3.9±0.4	5.8±5.1
	2001-2005	7.79±4.78	0.30±0.24	45±42	3.6±0.3	7.9±6.9
	2006-2010	6.10±4.44	0.27±0.24	36±30	3.7±0.3	6.2±4.3
	2011-2015	4.85±4.29	0.28±0.23	26±33	4.0±0.3	6.1±4.3
Class 2	1981-1985	3.14±2.61	0.26±0.21	19±20	5.3±0.2	3.3±3.1
	1986-1990	3.80±3.56	0.37±0.26	12±11	5.3±0.2	3.5±3.3
	1991-1995	3.76±3.08	0.37±0.35	12±11	5.2±0.1	3.1±2.2
	1996-2000	5.46±3.48	0.37±0.23	19±15	5.7±0.2	2.1±1.7
	2001-2005	5.56±3.61	0.27±0.18	27±25	5.3±0.2	2.6±2.0
	2006-2010	4.58±2.80	0.28±0.20	22±18	5.7±0.2	2.4±1.9
	2011-2015	3.01±2.33	0.29±0.20	12±6	6.3±0.2	2.7±2.2
Class 3	1981-1985	3.14±2.12	0.27±0.18	18±18	6.1±0.2	2.0±1.3
	1986-1990	3.80±2.08	0.37±0.21	10±8	6.3±0.2	1.9±1.4
	1991-1995	3.76±2.46	0.35±0.18	10±8	6.7±0.1	1.9±1.4
	1996-2000	5.46±2.82	0.35±0.20	14±8	7.0±0.2	1.4±1.2
	2001-2005	5.56±3.12	0.27±0.15	19±16	6.7±0.2	1.5±1.2
	2006-2010	4.58±2.12	0.27±0.15	16±12	7.1±0.2	1.6±1.2
	2011-2015	3.01±1.56	0.28±0.16	12±5	7.6±0.2	1.4±1.4

Table 4.6 Phytoplankton contribution to light attenuation in the classified areas of the west-central Seto Inland Sea.

Season	Class1	Class2	Class3
Spring	28.3%	22.1%	19.9%
Summer	35.2%	21.1%	12.6%
Autumn	28.4%	15.1%	14.6%
Winter	26.6%	10.3%	4.5%

Secchi depth in the west-central Seto Inland Sea has also improved over the past 35 years, but rates of increase were small (less than 0.05 m $year^{-1}$) and accompanied with large annual fluctuations. Secchi depth is influenced by multiple optical factors affecting light attenuation in the water column, including phytoplankton and other background factors such as sea water, tripton and CDOM (Christian et al. 2003, Devlin et al. 2008). In most parts of the west-central Seto Inland Sea, phytoplankton contribution to light attenuation was surprisingly limited, being less than 36% in Class 1 and less than 23% in Classes 2 and 3 (Table 4.6). Phytoplankton contribution to light attenuation in Classes 2 and 3 in the west-central Seto Inland Sea was less than that reported in Harima Nada, the Seto Inland Sea (27%, Yamaguchi et al. 2013).

Being more archipelagic than Harima Nada, the west-central Seto Inland Sea could support higher tripton levels in the offshore area, resulting in lower phytoplankton contribution to light attenuation. The reduction in Chl.*a* concentration in these areas was also modest, implying that the improvement in Secchi depth through decrease in Chl.*a* concentration via TPLCS may be limited in the west-central Seto Inland Sea.

4.4.2 Implications for future policy-making and management

The management of Seto Inland Sea has undergone a major and positive shift from water quality control to environmental remediation and restoration of habitat in the revision of Act on Special Measures concerning Conservation of the Environment of the Seto Inland Sea in 2015, which aimed at realizing a beautiful and bountiful sea (Nakai et al. 2018). Under the new management framework, restoration of seagrass and seaweed beds constituted an important part, which would rely much on the improvement of water clarity. This article emphasized the role of natural environmental conditions e.g. salinity or suspended solids in water as crucial for water quality, especially the water clarity. Considering the phytoplankton's low contribution to light attenuation in the west-central Seto Inland Sea, the improvement of water clarity via the TPLCS by decreasing phytoplankton concentration would be limited. Without our achievement, policy makers and environmental managers in the Seto Inland Sea may depend too much on water quality improvement through the TPLCS in seaweed and seagrass restoration. We should tackle not only natural increase of seaweed and seagrass by improvement of water quality but seaweed and seagrass bed construction by raising a bottom to improve light condition. These findings in the west-central Seto Inland Sea is expected to apply in other semi-enclosed waters receiving both substantial freshwater input and anthropogenic nutrient loads. Moreover, due to the highly variable natural condition in these regions, decadal time frames or flexible agenda should be used to allow significant or detectable improvements in coastal water quality.

4.5 Conclusions

This study identified salinity and distance from Honshu coastline to be the most definitive factors for Chl.*a* concentration and Secchi depth in the west-central Seto

Inland Sea, respectively, based on monitoring records for the period 2006–2015. Significant differences were observed among the subareas of the west-central Seto Inland Sea during spring, summer and autumn in both Chl.*a* concentration and Secchi depth, while no significant difference existed in winter. The large water mixing by the strong wind and the sea surface cooling during winter could be responsible for the small regional difference in Chl.*a* and Secchi depth.

The application of the TPLCS to the watershed of the west-central Seto Inland Sea since 1979 has resulted in a 45.45% reduction in TP loading and 25.76% reduction in TN loading from 1979 to 2009. The Chl.*a* concentration has decreased, although the extent of reduction varies both seasonally and spatially. In the innermost Hiroshima Bay (Class 1), mean Chl.*a* concentration underwent a significantly higher rate of decrease than other subareas of the west-central Seto Inland Sea during the spring of the past 35 years, while no significant difference in rate of decrease among the subareas was found in other seasons. Despite the largest Chl.*a* decrease in the innermost area of Hiroshima Bay, this area still endure high Chl.a concentration, especially in summer, due to the vulnerable characteristic of this area (Chapter 3, low salinity and water clarity, high stratification). This suggests that other intervention measures (e.g. seagrass restoration) should be taken simultaneously with terrestrial nutrient reduction to control the eutrophication and speed up the restoration of this area. Secchi depth in the west-central Seto Inland Sea also showed a trend of improvement over the past 35 years. However, the difference in increasing rates of mean Secchi depth among the subareas was insignificant in all seasons. Finally, considering the phytoplankton's low contribution to light attenuation in the west-central Seto Inland Sea, the influence of TPLCS on improvement in water clarity via decreasing phytoplankton concentration was limited.

4.6 References

Asaoka, S., A. Umehara, S. Otani, N. Fujii, T. Okuda, S. Nakai, W. Nishijima, K. Takeuchi, H. Shibata, and W. A. Jadoon. 2018. Spatial distribution of hydrogen sulfide and sulfur species in coastal marine sediments Hiroshima Bay, Japan. Marine pollution bulletin 133:891-899.

Belsley, D., E. Kuh, R. Welsh. 1980. Regression Diagnostics: Identifying Influential Data and Sources of Collinearity. Wiley Series in Probability and Mathematical Statistics. New York: John Wiley & Sons. pp. 11–16. ISBN 0-471-05856-4.

Carstensen, J., M. Sánchez-Camacho, C. M. Duarte, D. Krause-Jensen, and N. Marba. 2011. Connecting the dots: responses of coastal ecosystems to changing nutrient concentrations. Environmental science & technology 45:9122-9132.

Christian, D., and Y. P. Sheng. 2003. Relative influence of various water quality parameters on light attenuation in Indian River Lagoon. Estuarine, Coastal and Shelf Science 57:961-971.

Devlin, M., J. Barry, D. Mills, R. Gowen, J. Foden, D. Sivyer, and P. Tett. 2008. Relationships between suspended particulate material, light attenuation and Secchi depth in UK marine waters. Estuarine, Coastal and Shelf Science 79:429-439.

Duarte, C. M., A. Borja, J. Carstensen, M. Elliott, D. Krause-Jensen, and N. Marbà. 2015. Paradigms in the recovery of estuarine and coastal ecosystems. Estuaries and Coasts 38:1202-1212.

ESRI 2011. ArcGIS Desktop: Release 10. Redlands, CA: Environmental Systems Research Institute.

Greening, H., A. Janicki, E. T. Sherwood, R. Pribble, and J. O. R. Johansson. 2014. Ecosystem responses to long-term nutrient management in an urban estuary: Tampa Bay, Florida, USA. Estuarine, Coastal and Shelf Science 151:A1-A16.

Hara, Y. 1999. Calculation of population parameters using Richards function and application of indices of growth and seed vigor to rice plants. Plant production science 2(2): 129-135.

Hibino, T. and H. Matsumoto. 2006. Distribution of fluid mud layer in Hiroshima Bay and its seasonal variation. Journal of JSCE B **62**:348-359.

Hoshika, A., M. J. Sarker, S. Ishida, Y. Mishima, and N. Takai. 2006. Food web analysis of an eelgrass (*Zostera marina* L.) meadow and neighbouring sites in Mitsukuchi Bay (Seto Inland Sea, Japan) using carbon and nitrogen stable isotope ratios. Aquatic Botany 85:191-197.

Ishii, D., T. Yanagi. 2004. Origins and variable mechanisms of total phosphorus and total nitrogen concentrations in the Seto Inland Sea. Oceanography in Japan 13: 389–401 (in Japanese).

Japan Meteorological Agency. 2000. Guidelines for Marine Observations, Tokyo.

Kucharavy, D., & De Guio, R. 2015. Application of logistic growth curve. Procedia engineering, 131: 280-290.

Lam, F.C., C. T. Hung, D. G. Perrier. 1985. Estimation of variance for harmonic mean half-lives. J. Pharm. Sci. 74 (1):229–231.

Lee, I. and A. Hoshika. 2000. Seasonal variations in pollutant loads and water quality in Hiroshima Bay. Journal of Water Environment Society 23:367-373 (in Japanese with English abstract)

Lee, I., K. Fujita, Y. Takasugi and A. Hoshika. 2001. Numerical simulation of residual current and material transportation in Hiroshima Bay. Oceanography in Japan 10 (6):495–507 (in Japanese with English abstract).

Lee, Y. S., T. Seiki, T. Mukai, K. Takimoto, and M. Okada. 1996. Limiting nutrients of phytoplankton community in Hiroshima Bay, Japan. Water Research 30:1490-1494.

Ministry of the Environment of Japan, 2016. 2015 Annual Report on Pollutant Load Investigation and Pollutant Reduction Measures.

Nakai, S., Y. Soga, S. Sekito, A. Umehara, T. Okuda, M. Ohno, W. Nishijima, and S. Asaoka. 2018. Historical changes in primary production in the Seto Inland Sea, Japan, after implementing regulations to control the pollutant loads. Water Policy:wp2018093.

Nishijima, W., A. Umehara, T. Okuda, and S. Nakai. 2015. Variations in macrobenthic community structures in relation to environmental variables in the Seto Inland Sea, Japan. Marine pollution bulletin 92:90-98.

Nishijima, W., A. Umehara, S. Sekito, T. Okuda, and S. Nakai. 2016. Spatial and temporal distributions of Secchi depths and chlorophyll *a* concentrations in the Suo Nada of the Seto Inland Sea, Japan, exposed to anthropogenic nutrient loading. Science of The Total Environment 571:543-550.

Nishijima, W., A. Umehara, S. Sekito, F. Wang, T. Okuda, and S. Nakai. 2018. Determination and distribution of region-specific background Secchi depth based on long-term monitoring data in the Seto Inland Sea, Japan. Ecological Indicators 84:583-589.

Orth, R. J., T. J. Carruthers, W. C. Dennison, C. M. Duarte, J. W. Fourqurean, K. L. Heck, A. R. Hughes, G. A. Kendrick, W. J. Kenworthy, and S. Olyarnik. 2006. A global crisis for seagrass ecosystems. AIBS Bulletin 56:987-996.

R Core Team. R: A language and environment for statistical computing. 2015, Vienna, Austria.

Riemann, B., J. Carstensen, K. Dahl, H. Fossing, J. W. Hansen, H. H. Jakobsen, A. B. Josefson, D. Krause-Jensen, S. Markager, and P. A. Stæhr. 2016. Recovery of Danish coastal ecosystems after reductions in nutrient loading: a holistic ecosystem approach. Estuaries and Coasts 39:82-97.

Seiki, T., E. Date, and H. Izawa. 1991. Eutrophication in Hiroshima Bay. Marine pollution bulletin 23:95-99.

Takai, N., Y. Mishima, A. Yorozu, and A. Hoshika. 2002. Carbon sources for demersal fish in the western Seto Inland Sea, Japan, examined by δ13C and δ15N analyses. Limnology and Oceanography 47:730-741.

Williams, M. R., S. Filoso, B. J. Longstaff, and W. C. Dennison. 2010. Long-term trends of water quality and biotic metrics in Chesapeake Bay: 1986 to 2008. Estuaries and Coasts 33:1279-1299.

Yamaguchi, H., R. Katahira, K. Ichimi, and K. Tada. 2013. Optically active components and light attenuation in an offshore station of Harima Sound, eastern Seto Inland Sea, Japan. Hydrobiologia 714(1):49-59.

Yamamoto, T. 2003. The Seto Inland Sea—eutrophic or oligotrophic? Marine pollution bulletin 47:37-42.

Yanagi, T. and A. Harashima. 2003. Characteristics of dissolved inorganic phosphorus, nitrogen and silicate distributions in the Seto Inland Sea. Oceanography in Japan 12:565–572 (in Japanese with English abstract).

Zwietering, M. H., Jongenburger, I., Rombouts, F. M., & Van't Riet, K. 1990. Modeling of the bacterial growth curve. Applied and environmental microbiology, 56(6): 1875-1881

Chapter 5: Potential and impact of eelgrass bed recovery and expansion on phytoplankton growth through nutrient competition

5.1 Introduction

Eelgrass (*Zostera marina* L.) is widespread in northern hemisphere temperate coastal waters. Eelgrass beds are highly productive and support diverse faunal assemblages (Adams 1976, Orth et al. 1984) by providing ideal habitats for many commercial fishes and reducing the vulnerability of juveniles to piscivorous predators (Shoji et al. 2007). The ecosystem services provided by eelgrass beds keep them important for coastal management. Furthermore, *Z. marina* L. has been listed as a key indicator species for marine water quality in Europe (WFD, Europe Union 2009).

Eelgrass also takes in nutrients from the water and prevents excessive growth of phytoplankton in eutrophic coastal waters through the reduction of available nutrients. Excessive phytoplankton growth produces various environmental problems, such as red tides and sediment deterioration, and generally occurs in the warm season, which is also the growth period of many eelgrasses, including *Z. marina* L.

Despite its importance, the global distribution of eelgrass has declined by 1.4% per year over a 10-year period, as measured in 126 areas, from 1990–2000 because of anthropogenic and/or other pressures (IUCN 2018). In the Seto Inland Sea in central Japan, the eelgrass population has suffered a loss of about 70% over the last three decades of the 20th century, which has been mostly attributed to reclamation by coastal development, port construction activities and eutrophication (Komatsu 1997). Eutrophication can reduce eelgrass coverage directly by stimulating epiphytic algae and indirectly by restricting light penetration above the eelgrass bed canopy because of increased light absorption by phytoplankton (Lefcheck et al. 2018). A lot of effort has been expended to overcome eutrophication by reducing terrigenous anthropogenic nutrient loading globally; this is expected to aid the recovery of eelgrass beds because of a resulting increase in water clarity.

However, limitations on the recovery of eelgrass by reducing anthropogenic nutrient loading needs to be considered because light attenuation depends on phytoplankton as well as additional factors, such as other suspended particles and chromophoric dissolved organic matter. The impact of eutrophication on light transmittance is not severe even in some typical eutrophic enclosed seas, such as Tokyo Bay and Ise Bay in Japan (Wang et al. 2019). However, management plans for eutrophic coastal waters need to be constructed with knowledge about the potential for eelgrass recovery and extension through the improvement of optical conditions of the water column. Moreover, the impact of eelgrass recovery and expansion on the growth of phytoplankton after nutrient reduction should be understood.

Hiroshima Bay in the Seto Inland Sea, Japan, is an appropriate eutrophic coastal water body to assess the potential of eelgrass recovery and extension after improved water clarity through the reduction of anthropogenic nutrient loading. It is also an ideal location to assess the impact of eelgrass recovery and expansion on the growth of phytoplankton because there is available information on nutrient loading from land and open water (Ishii et al. 2004) and there has been intensive research in this area on water clarity (Nishijima et al. 2018), phytoplankton production (Nakai et al. 2018, Umehara et al. 2018) and sediment conditions (Asaoka et al. 2018).

The objectives of this study were to determine the maximum possible water clarity that could be reached after reducing anthropogenic nutrient loading and to evaluate the impact of eelgrass bed recovery and expansion on phytoplankton growth in the eutrophic northern Hiroshima Bay.

5.2 Materials and methods

5.2.1 Study site

The study area is located in the northern Hiroshima Bay, covering about 160 km^2 (Figure 5.1) with an average water depth of about 18 m. Itsukushima and Nomishima islands separate this area from the southern Hiroshima Bay and intensify the difference in hydrological conditions, abiotic and biotic environments between the north and the south (Fukushima et al. 2001, Umehara et al. 2018). Three major rivers, Ohta, Yahata and Seno River, with average discharges of 87, 2.3, and 2.4 m^3 s^{-1}, respectively, empty into the northern Hiroshima Bay. The water in this area is not easily exchanged because of the topographic characteristics. The apparent residence time of freshwater is around 30 d (Fukushima et al. 2001).

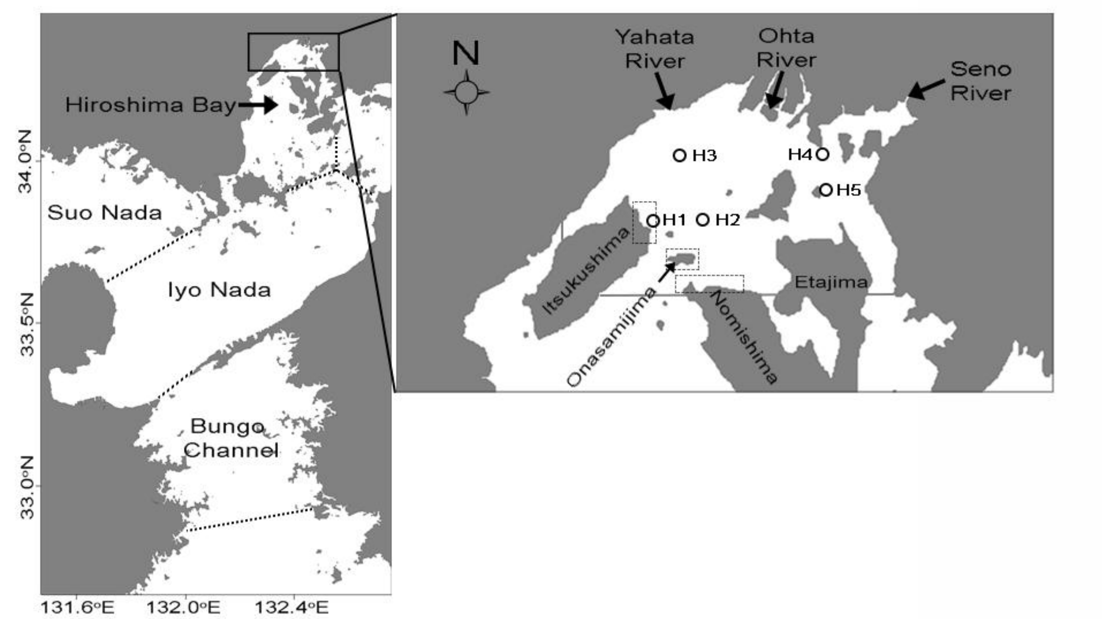

Figure 5.1 Location of the study area in northern Hiroshima Bay, Seto Inland Sea, Japan. Open circles indicate the monitoring sites.

5.2.2 Data sources

The monthly observed Secchi depths (SDs) and chlorophyll *a* (Chl.*a*) concentrations came from the Fisheries and Marine Technology Center, Hiroshima Prefectural Technology Research Institute. High-resolution water depth data of 50-m mesh were obtained from the Hydrographic and Oceanographic Department, Japan Coast Guard. Secchi depths with 450-m resolution were calculated based on monitoring data obtained from the Japanese Ministry of the Environment. The seagrass distribution map was provided by the Ministry of the Environment based on results from the fourth National Survey on the Natural Environment.

5.2.3 Estimation of potential improvement in Secchi depth

Background Secchi depth (BSD) was defined as a region-specific SD that excludes the contribution of phytoplankton (Nishijima et al. 2018) and was calculated for each monitoring site in each season of the 38-year sampling period. From the natural logarithm linear regressions of the standard deviation reciprocals [$ln(1/SD)$] plotted against the Chl.*a* concentrations, we calculated the y-intercepts as the reciprocals of the BSDs [$ln(1/BSD)$], i.e. $ln(1/SD)$, in the absence of phytoplankton effects (Nishijima et al. 2018). The reference Chl.*a* concentration was defined as the concentration that is only slightly influenced by anthropogenic nutrient loading. It was estimated based on the Chl.a concentration from an area offshore from the adjacent Aki Nada (Figure 5.1). The maximum possible Secchi depth (MPSD) was defined as the SD when the Chl.a concentration equals the reference Chl.a concentration. The reference Chl.a concentration was applied to the linear regression model of ln(1/SD) and Chl.a at each monitoring site to estimate the MPSDs (Figure 5.2).

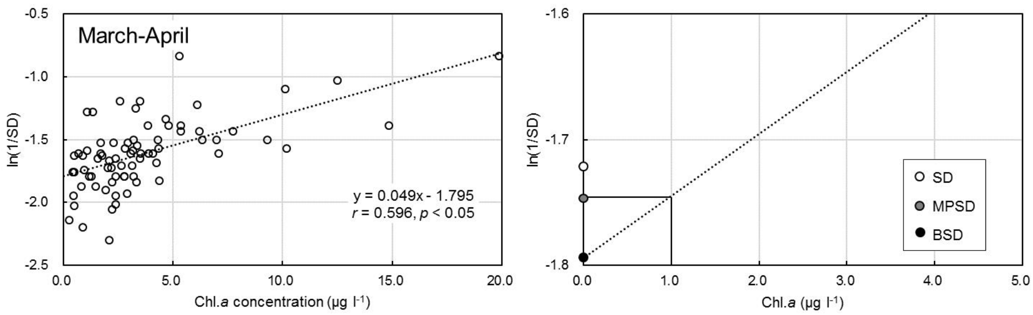

Figure 5.2 Estimation of maximum possible Secchi depth (MPSD at 1 μg l^{-1} of chlorophyll a (Chl.a)) and background Secchi depth (BSD) during March–April at a monitoring site (H3 in Figure 1) in northern Hiroshima Bay.

5.2.4 Estimation of the critical depth for eelgrass survival

The critical light intensity for eelgrass survival at the surface was estimated in three coastal areas: the northeast of Itsukushima, and parts of Nomishima and Onasamijima (Figure 5.1), where there is still natural coastline. The presence or absence of eelgrass was evaluated within each 50-m grid using the eelgrass distribution in these areas obtained from an investigation of seagrass beds and tidal flats (Setouchi NET). Then, the critical ratio of light intensity at the vegetation depth to the surface light intensity in the northern Hiroshima Bay was determined. The coefficient of water column light attenuation (K_d, m^{-1}) and the relative light intensity at the surface (I_z /I_0) was calculated as:

$$K_d = 0.15 + \frac{0.68}{SD} \quad \text{Eq. 1}$$

$$\frac{I_Z}{I_0} = \exp\left(-K_d \times Z\right) \quad \text{Eq. 2}$$

where SD is Secchi depth (m). I_0 and I_z is the irradiance at the water surface and water depth z (μmol m^{-2} s^{-1}).

Then the critical depth for eelgrass survival (Z_c, m) was calculated as follows:

$$Z_c = -\ln\left(I_Z/I_0\right)/K_d \quad \text{Eq. 3}$$

5.2.5 Estimation of chlorophyll a concentration

Monthly Chl.*a* concentrations (May–September) were calculated using a mathematical model developed by Kasamo et al. (2016) based on when intensive phytoplankton growth generally occurs.

The Princeton Ocean Model (POM), which is an oceanic general circulation model based on the 3D Navier-Stokes (primitive) equations under hydrostatic and Boussinesq assumptions, was used to develop our model. The POM was implemented in the Seto Inland Sea basin with a horizontal resolution of 2250 × 2250 m and 10 sigma-levels in the vertical. A detailed description of the model equations and its numerical algorithms can be found in Blumberg and Mellor (1978). The horizontal viscosity/diffusivity coefficients were estimated using the Smagorinsky. Simultaneously, the vertical viscosity/diffusivity coefficients were estimated following the model's turbulence closure scheme using Mellor and Yamada level 2.5 (Mellor and Yamada 1982). Water temperature and salinity at the initial conditions and the open boundaries were set based on JCOPE2 (Japan Coastal Ocean Predictability Experiment 2) reanalysis results (Miyazawa et al. 2009). The lower trophic level ecosystem model developed by Nakata (1993) and eelgrass (*Z. marina* L.) biomass model developed by Bocci et al. (1997) were then incorporated into our model.

In the eelgrass biomass model (Bocci et al., 1997), the stated variables were shoot biomass (S) [gdw m^{-2}], root and rhizome biomass (R) [g dw m^{-2}] and eelgrass nitrogen concentration (N) [mg N gdw^{-1}]. Verhagen and Nienhuis (1983) proposed to incorporate the effect of aging into an eelgrass biomass model to describe seasonal changes in biomass. We further added a limitation on growth rate (μ) [d^{-1}] by aging to the Bocci et al. (1997) model:

$$\frac{dS}{dt} = (\mu - trans - \Omega_S) \times S \quad \text{Eq. 4}$$

$$\frac{dR}{dt} = trans \times S - \Omega_S \times R \quad \text{Eq. 5}$$

$$\frac{dN}{dt} = uptakeS - \mu \times N \quad \text{Eq. 6}$$

$$\mu = MIMAX \times f(L) \times f(T) \times f(N) \times f(S) \times f(age) \quad \text{Eq. 7}$$

$$f(age) = 1 - 0.99 \times \frac{age - 129}{234 - 129} \qquad 129 < age \leq 234 \text{ (Julian day)} \quad \text{Eq. 8}$$

$$f(age) = 0.01 \qquad 234 < age \leq 304 \text{ (Julian day)} \quad \text{Eq. 9}$$

$trans = 0.25 \times \mu$ Eq. 10

$\Omega_S = 0.025 \times (0.098 + \exp(-4.690 + 0.2317T))$ Eq. 11

where *trans* is translocation from shoot to root and rhizome, Ω_S and Ω_R are respiration of shout, and root and rhizome, respectively (d^{-1}), *uptakeS* is mg gdw^{-1} h^{-1}, L is light (KJ m^{-2} d^{-1}), T is water temperature (°C), *age* is aging coefficient, *MIMAX* is maximum growth rate (0.06 d^{-1}).

5.2.6 Mapping and analysis

Mapping of the study area and geospatial analyses of water depths, SDs and seagrass distribution were performed using the geographical information system software ArcGIS 10.3 (ESRI, 2011). Inverse distance weighted interpolation was used to interpolate values at unsampled locations. Kruskal-Wallis ANOVA tests and subsequent Dunn's tests for multiple comparisons were used to compare SDs, MPSDs and BSDs in different periods. The Kruskal-Wallis and Dunn's tests were performed with R software (R Core Team, 2015) with $p < 0.05$ considered statistically significant.

5.3 Results

5.3.1 Water quality in the northern Hiroshima Bay

As shown in Table 5.1, water temperatures in the northern Hiroshima Bay showed an increasing trend during the eelgrass growth season (March–August). The bimonthly mean water temperatures at five monitoring sites were 11.6–11.9°C (March–April), 18.1–18.7°C (May–June) and 25.5–25.7°C (July–August). In contrast, salinity showed greater spatial variation and a decreasing trend over the same periods, dropping from 28.1–30.8 (March–April) to 22.1–25.6 (July–August). Similar to salinity, Chl.*a* concentrations in surface waters of the northern Hiroshima Bay also varied greatly by season and location. The values peaked in July–August (5.0–15.6 μg l^{-1}) and were lowest in March–April (3.0–4.8 μg l^{-1}). Secchi depth in the northern Hiroshima Bay ranged from 1.8 to 6.6 m with higher values in March–June (4.6–6.6 m) and lower values in July–August (2.1–3.8 m).

Table 5.1 Water quality parameters in northern Hiroshima Bay over different periods in 2009–2018. Values are presented as mean ± standard deviation.

Period	Site	Temp. (°C)	Salinity (-)	Chl.*a* (μg l^{-1})	SD (m)
March–April	H1	11.6 ± 1.4	29.9 ± 1.7	3.4 ± 1.8	6.0 ± 0.3
	H2	11.7 ± 1.4	29.8 ± 1.8	3.0 ± 1.3	6.6 ± 0.4
	H3	11.8 ± 1.7	28.1 ± 2.9	3.7 ± 3.1	5.6 ± 0.3
	H4	11.9 ± 1.6	28.4 ± 3.7	4.8 ± 3.4	4.6 ± 0.3
	H5	11.7 ± 1.5	30.8 ± 2.2	3.8 ± 2.5	6.0 ± 0.4
	Mean	11.7	29.4	3.7	5.7
May–June	H1	18.3 ± 2.3	29.6 ± 2.2	4.2 ± 2.4	4.2 ± 0.3
	H2	18.1 ± 1.8	29.2 ± 3.3	8.1 ± 3.6	4.5 ± 0.4
	H3	18.5 ± 1.8	27.4 ± 4.5	7.8 ± 7.3	3.2 ± 0.5
	H4	18.7 ± 2.1	28.5 ± 2.0	11.3 ± 6.7	2.7 ± 0.2
	H5	18.4 ± 2.0	30.4 ± 1.4	6.8 ± 5.6	4.4 ± 0.3
	Mean	18.4	29.0	7.6	3.6
July–August	H1	25.5 ± 2.3	25.6 ± 4.2	5.0 ± 2.8	3.3 ± 0.3
	H2	25.5 ± 2.2	25.1 ± 4.8	6.4 ± 4.5	3.2 ± 0.3
	H3	25.7 ± 2.5	22.1 ± 5.7	8.1 ± 4.4	2.5 ± 0.2
	H4	25.7 ± 2.1	22.2 ± 4.6	15.6 ± 8.5	1.8 ± 0.1
	H5	25.7 ± 2.2	25.5 ± 4.3	9.2 ± 6.6	2.7 ± 0.2
	Mean	25.6	24.1	8.9	2.6

Chl.*a* = chlorophyll *a*; SD = Secchi depth

5.3.2 BSD and MPSD distribution of northern Hiroshima Bay

Statistically reliable BSDs and MPSDs were obtained at all of the five monitoring sites during the eelgrass growing season. Figures 5.3 and 5.4 show the spatial distribution of SD, $MPSD_{0.5}$ and $MPSD_{1.0}$ (values at 0.5 μg l^{-1} and 1.0 μg l^{-1} Chl.*a*) and BSD during the eelgrass growth season in the northern Hiroshima Bay (Kruskal-Wallis test, p <0.05). All SD indicators decreased from March–April to July–August, indicating that background factors affected the light attenuation increase during this period. The difference between SD and $MPSD_{0.5}$ and $MPSD_{1.0}$ ranged from 0.0 to 0.7 m at each site. Moreover, the difference between BSD and $MPSD_{1.0}$ was small except for March–April. The largest increase in water clarity occurred in the southwestern part of the northern Hiroshima Bay, far away from the Ohta River estuary during May to August (Figure 5.5). These results indicated that phytoplankton did not strongly control water clarity, but background factors in this area, especially the inner part of the bay, were predominant. Therefore, improvements in water clarity from reducing terrigenous anthropogenic nutrient loading should not be expected.

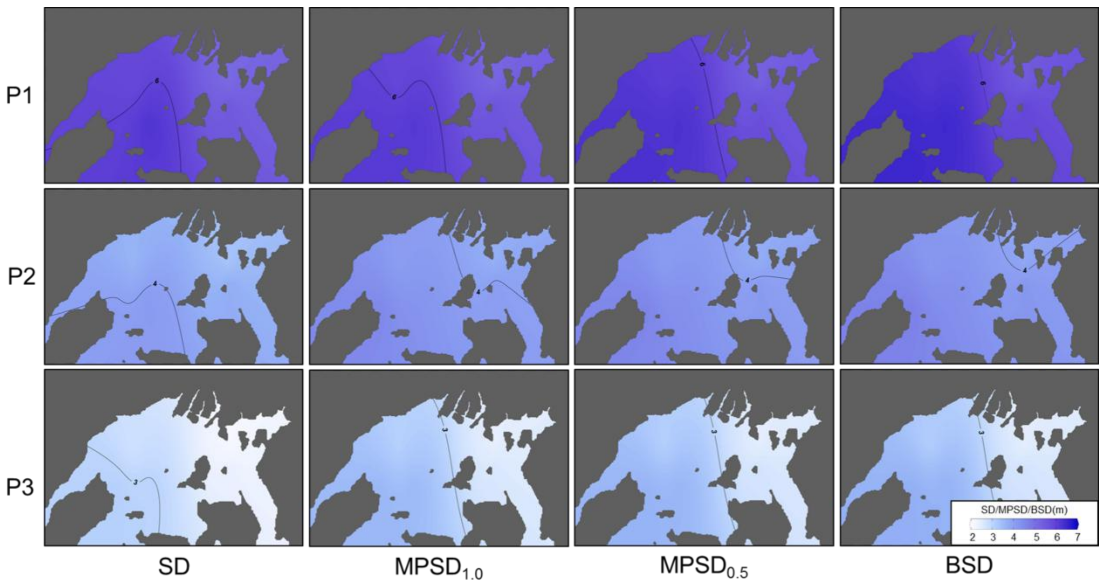

Figure 5.3 Spatial distribution of mean Secchi depth (SD), maximum possible Secchi depth ($MPSD_{1.0}$, $MPSD_{0.5}$) and background Secchi depth (BSD) in the northern Hiroshima Bay. P1, P2 and P3 correspond to March–April, May–June and July–August, respectively.

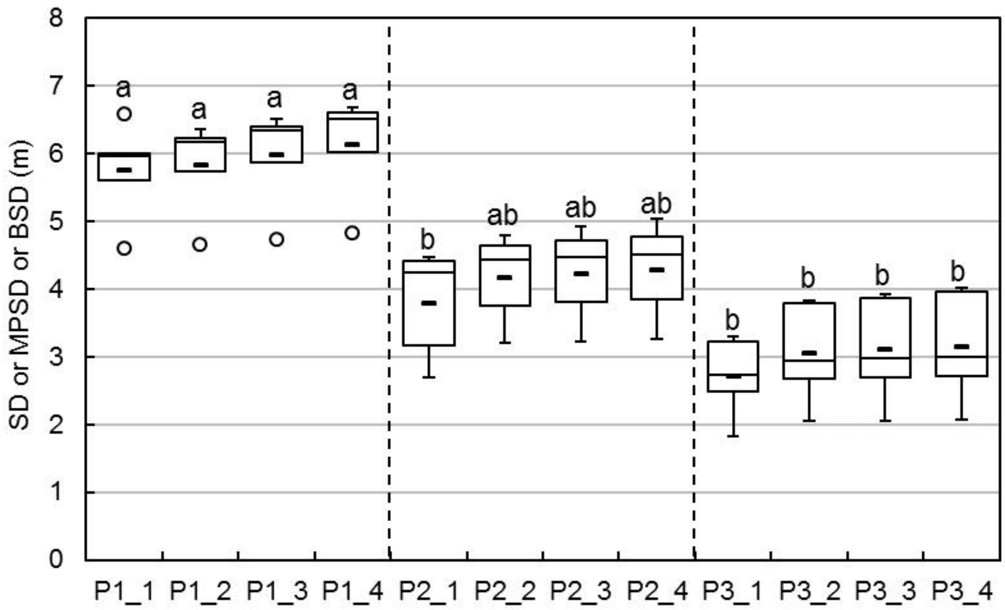

Figure 5.4 Bimonthly mean Secchi depth (SD), maximum possible Secchi depth ($MPSD_{1.0}$, $MPSD_{0.5}$) and background Secchi depth (BSD) in the northern Hiroshima Bay. P1, P2 and P3 = March–April, May–June and July–August, respectively. 1, 2 3 and 4 = SD, $MPSD_{1.0}$, $MPSD_{0.5}$ and BSD, respectively. o = the outlier by the 1.5 interquartile range rule. For the same parameters, boxes with different letters (a, b) indicate significant differences (p <0.05, Dunn's test) between different periods.

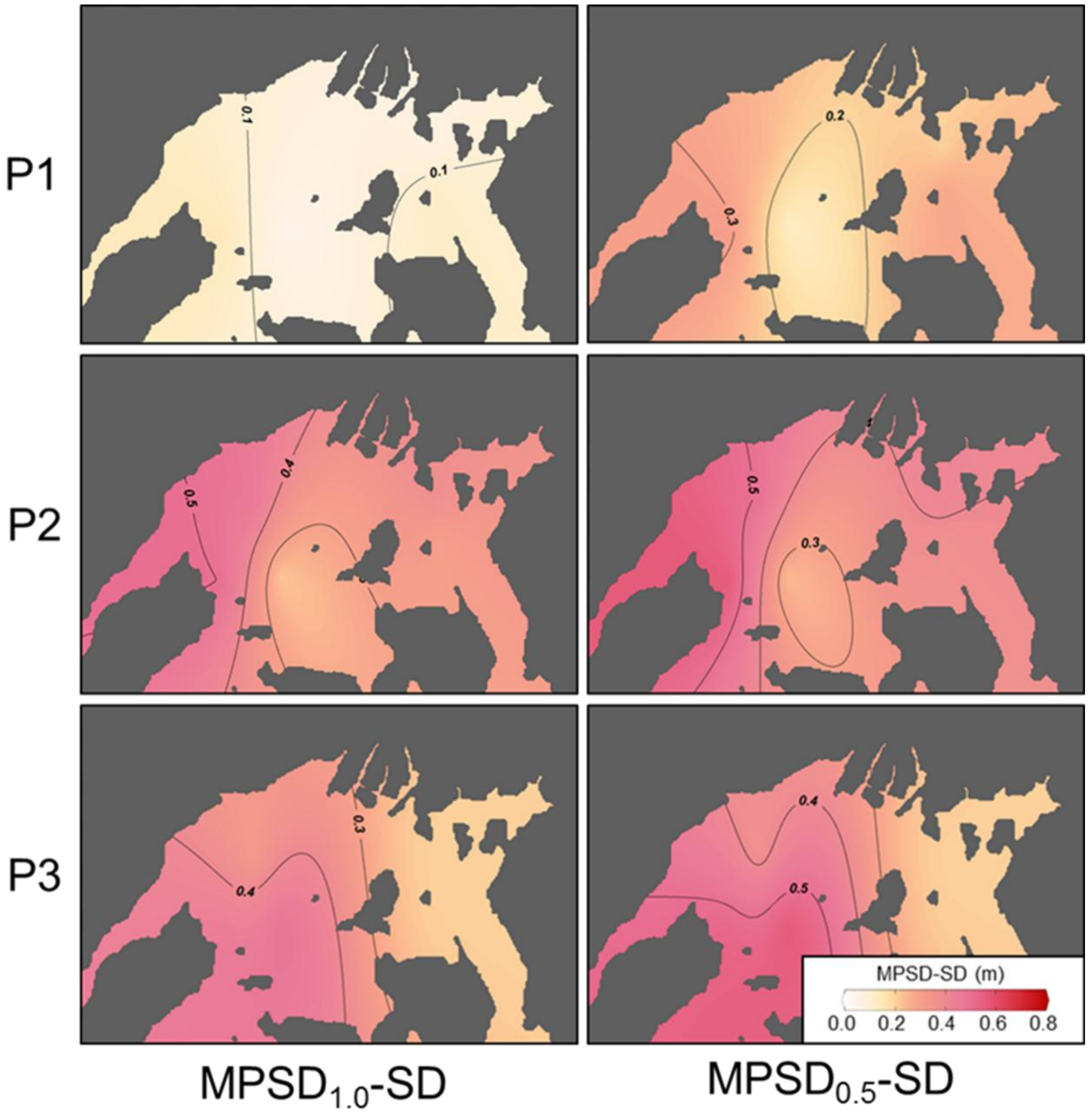

Figure 5.5 The differences between maximum possible Secchi depth ($MPSD_{1.0}$, $MPSD_{0.5}$) and current mean Secchi depth (SD) during 2009–2018 in the northern Hiroshima Bay. P1, P2 and P3 correspond to March–April, May–June and July–August, respectively.

5.3.3 Estimation of critical depth for eelgrass survival

In the selected areas where the natural coastline remains, eelgrass mainly grew at depths shallower than 6 m (Figure 5.6) and where relative light intensity at the surface was over 20% (Figure 5.7). The existence of eelgrass dramatically declined to less than 20% of areas with water depths greater than 6 m and further diminished in areas deeper than 11 m. No eelgrass was found when <5% of surface irradiance reaches the bottom (Figure 5.7). Therefore, the critical depth for eelgrass survival in this area is suggested to be 6 m.

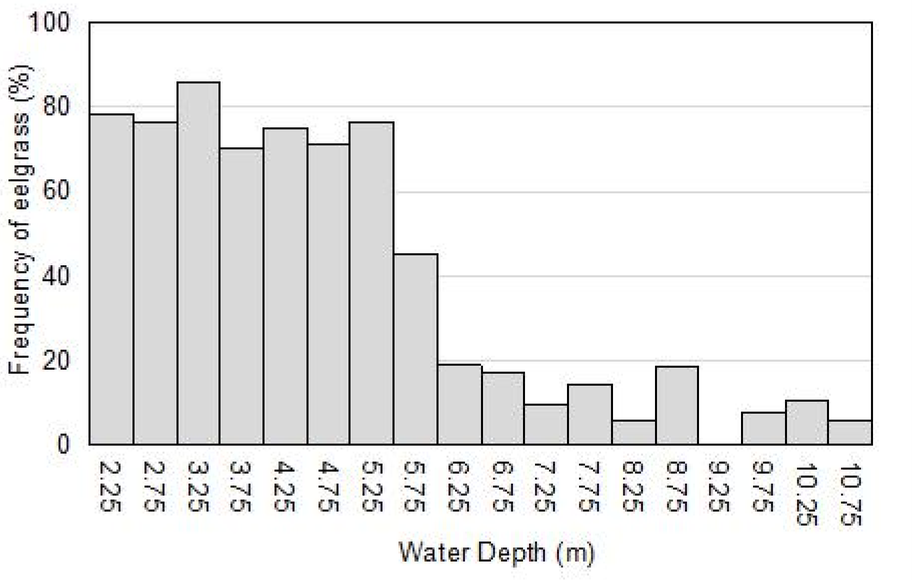

Figure 5.6 Depth distribution of eelgrass in selected areas (see Figure 5.1) of the northern Hiroshima Bay.

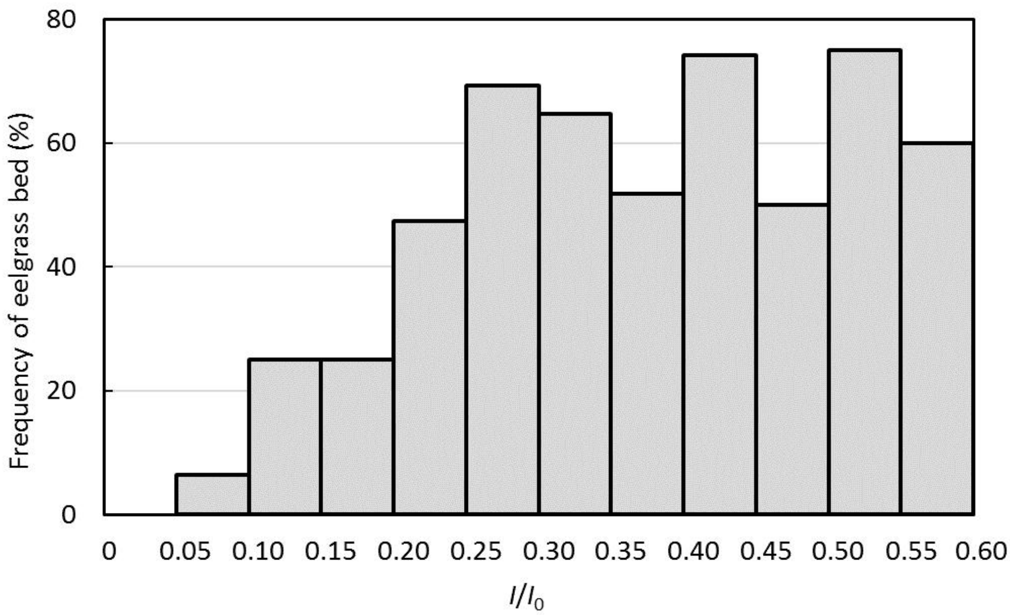

Figure 5.7 Changes in eelgrass survival with light availability (I/I_0) in selected areas (see Figure 5.1) of the northern Hiroshima Bay. I_0 and I correspond to the irradiance at the water surface and a different water depth.

5.3.4 Current and potential distribution of eelgrass in the northern Hiroshima Bay

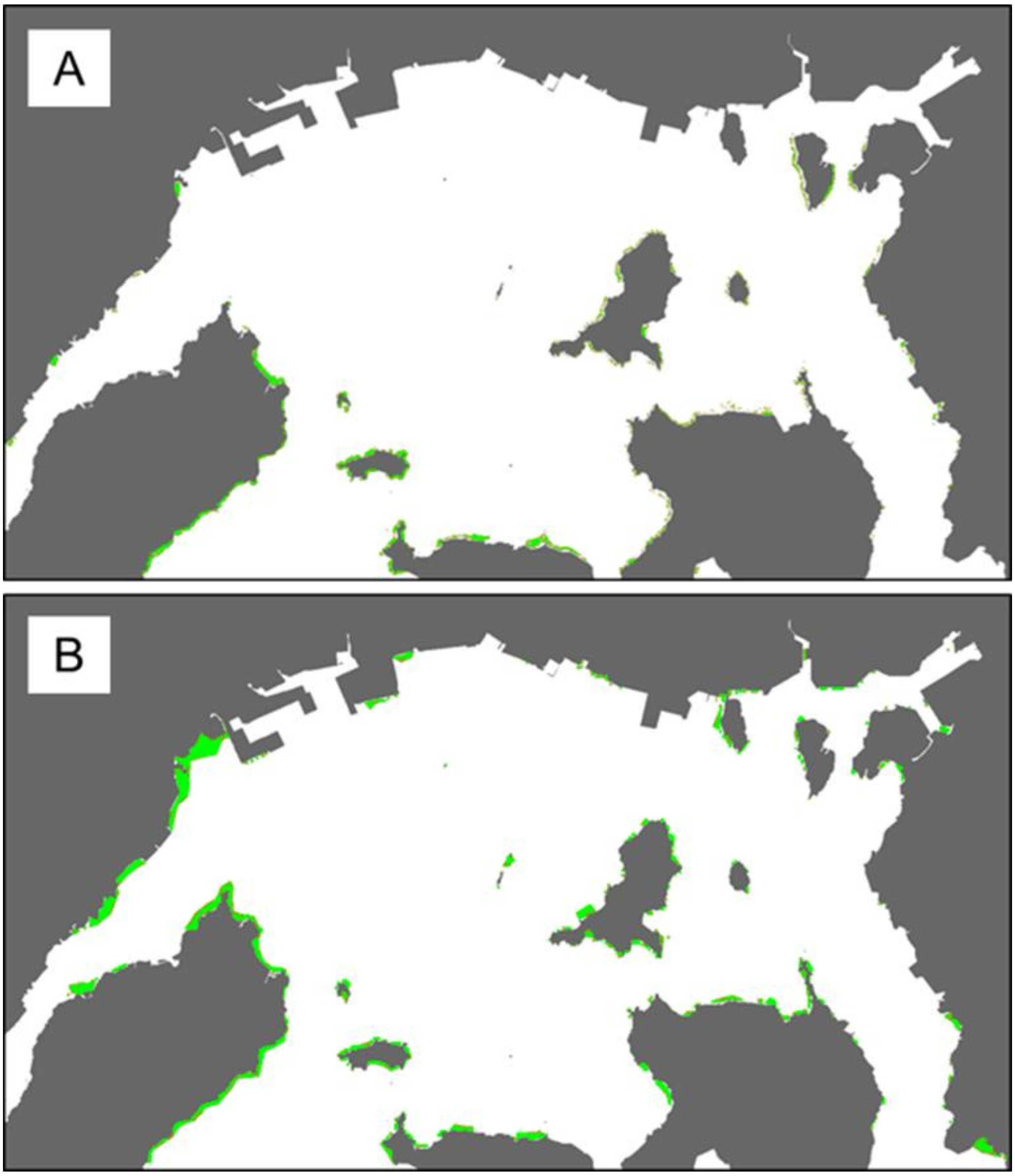

Figure 5.8 Current eelgrass distribution (A, 100 ha), and estimated eelgrass distribution derived from current light availability and light requirements of eelgrass (B, 373 ha) in the northern Hiroshima Bay.

The spatial distribution of eelgrass in the northern Hiroshima Bay is shown in Figure 8. Eelgrass mainly grows around the islands; the current total area of eelgrass beds in the study area is 100 ha (Figure 5.8A, Setouchi NET). However, the potential area for eelgrass growth, including the 100 ha of present eelgrass beds, estimated using only light availability (20% surface light) was 373 ha, which is around 2.4% of the study area (Figure 5.8B). Thus, the present area where eelgrass exists accounts for about 27% of the potential area. The expansion of eelgrass under different SD improvement scenarios was estimated to be 36 and 33 ha at $MPSD_{0.5}$ and $MPSD_{1.0}$ (May–June), respectively (Table 5.2). Although phytoplankton concentrations in this area could be reduced by less nutrient loading from land, a significant expansion of eelgrass beds by improving water clarity through phytoplankton decreases would not be expected.

Table 5.2 Expansion of eelgrass distribution (%) under different Secchi depth (m) improvement scenarios in northern Hiroshima Bay.

Scenarios		$MPSD_{1.0}$	$MPSD_{0.5}$	BSD
Current SD	Area	373		
March–April	Area	381	391	403
	Increase	8 (2.1%)	18 (4.8%)	30 (8.0%)
May–June	Area	406	409	419
	Increase	33 (8.8%)	36 (9.7%)	46 (12.3%)
July–August	Area	399	403	410
	Increase	26 (7.0%)	30 (8.0%)	37 (9.9%)

Note: values in parentheses indicate the percentage increase compared with a maximum potential area of 373 ha.
SD = Secchi depth; MPSD = maximum possible Secchi depth; BSD = bottom Secchi depth

5.3.5 Impact of eelgrass recovery and expansion on phytoplankton growth

There may be site-specific reasons, other than light availability, for a lack of eelgrass beds in a particular area. The significant decline of eelgrass beds in the Seto Inland Sea, which includes Hiroshima Bay, began after the 1960s when marine pollution and coastal reclamation occurred during rapid economic development. However, marine pollution is being addressed in the Seto Inland Sea by reducing the anthropogenic loading of chemical oxygen demand (COD) and nutrients from land. The loading of terrestrial COD, total nitrogen and total phosphorus into Hiroshima Bay was reduced from 83, 32 and 3.0 kg km^{-2} d^{-1}, respectively, in 1979 to 35, 22 and 1.3 kg km^{-2} d^{-1} in 2014, respectively (Setouchi NET). Therefore, eelgrass beds that had disappeared due to marine pollution are expected to naturally recover and areas where eelgrass had previously existed are good targets for artificial regeneration strategies, such as transplanting seeds or adult shoots (Park and Lee 2007, Bastyan and Cambridge 2008), to accelerate their recovery.

Eelgrass beds develop in coastal areas where a large amount of nutrients flow into the sea from river water, groundwater and municipal and industrial wastewater. Consequently, eelgrass uptakes nutrients where nutrient concentrations are relatively high and prevents excessive growth of phytoplankton. The impact of eelgrass recovery and expansion on phytoplankton growth from May to September was evaluated by the mathematical model under two scenarios: current eelgrass distribution (100 ha) and potential eelgrass distribution (370 ha) (Figure 5.9). Clear decreases in Chl.*a* concentrations after eelgrass expansion were observed in the northern and central parts of Hiroshima Bay from May to July. This improvement in Chl.*a* concentrations corresponded to 1.0 to 3.0 μg l^{-1} from 4.0 to 7.0 μg l^{-1}. However, the impact of eelgrass bed expansion decreased with time until August. No decrease in Chl.*a* was observed in September because of the decline in *Z. marina* L.

5.4 Discussion

Healthy marine coastal environments, particularly enclosed seas, are achieved through the control of excess phytoplankton by reductions in terrestrial nutrient loading. In general, vulnerable estuarine areas (Chapter 3, low salinity and Secchi depth) and healthy offshore areas are in close proximity in an enclosed sea, which affects strategies for overcoming severe eutrophic conditions. For example, it would not be appropriate to try to solve environmental problems occurring in limited coastal areas by reducing terrestrial nutrient loading because this affects the nutrient conditions in the entire water body and risks reducing the productivity of higher trophic levels, such as fish, as a result of production decline in lower trophic levels. Instead, a more appropriate strategy would be to prevent excessive phytoplankton growth by uptaking nutrients in the warm season near the coast with macroalgae (e.g., eelgrass). The macroalgae subsequently die and gradually discharge nutrients by decomposition in the cold season. These discharged nutrients support primary production in the cold season, but do not lead to excess growth of phytoplankton.

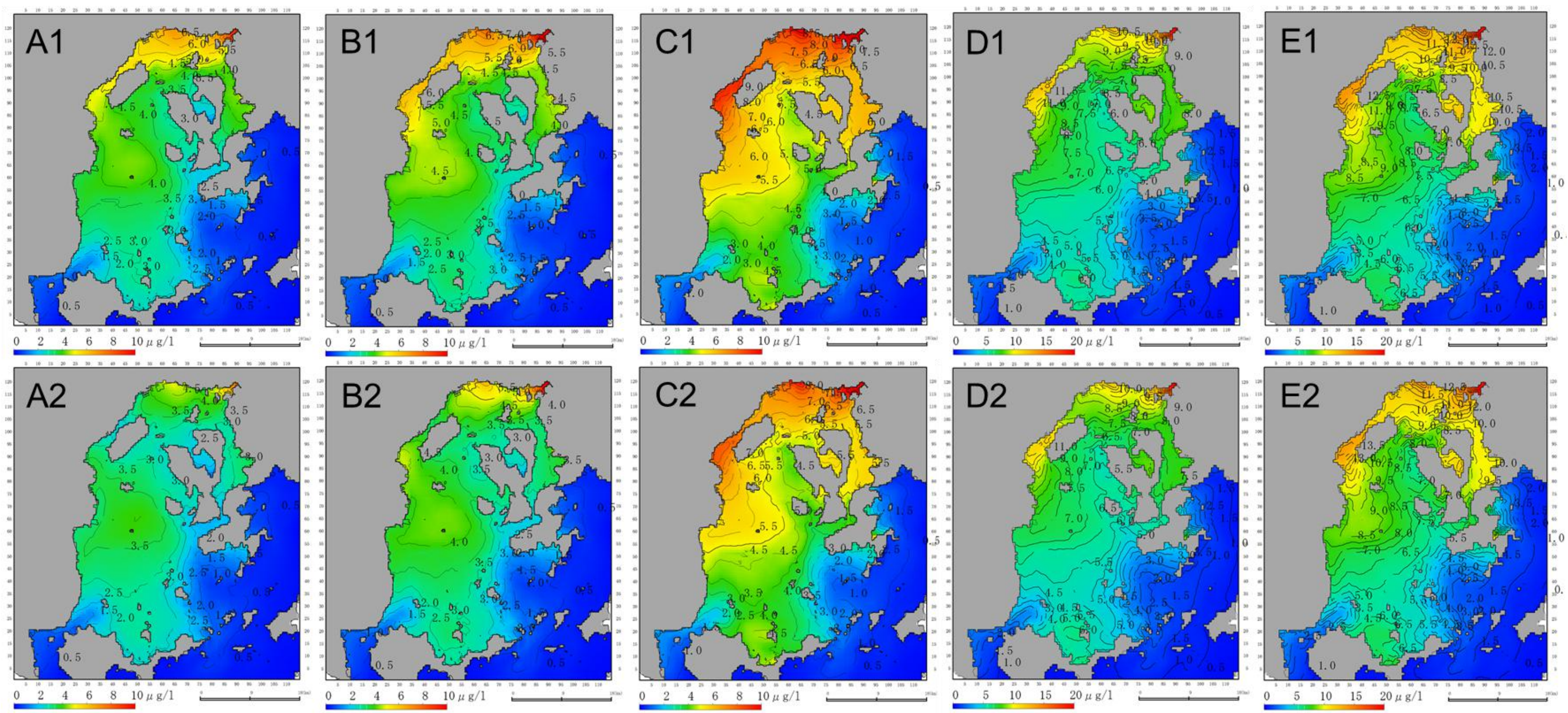

Figure 5.9 Contours of modeled chlorophyll *a* concentrations in current eelgrass areas (100 ha, top panels) and potential maximum eelgrass areas (373 ha, bottom panels) in May (A1 and A2), June (B1 and B2), July (C1 and C2), August (D1 and D2) and September (E1 and E2).

Z. marina L. is a suitable eelgrass for this purpose and is a common species growing on sandy-muddy sediments in temperate areas around the world, including Europe, North America and Asia (Lee et al. 2007). Despite only 2.4% of the northern Hiroshima Bay containing eelgrass beds, this study suggested that the recovery and expansion of *Z. marina* L. had a strong effect on phytoplankton growth through nutrient competition from May to August. Seagrasses, including *Z. marina* L. have nutrient storage strategies that include the uptake of nutrients when available and storage and then use of reserves when environmental conditions become suitable for plant growth. The maximum nitrogen content in the roots, rhizomes and leaves of *Zostera noltii* and *Cymodocea nodosa* were twice the minimum in the Mediterranean Sea (Kraemer and Mazzella 1999). Minimum nitrogen content persisted from June to July, indicating that stored nutrients were used for growth in the warm season; thus, there is a possibility to show strong nutrient uptake in the growing period when nutrient content is relatively low. Therefore, seagrass restoration represents an effective approach to control eutrophication or an approach that can be implemented simultaneously with terrestrial nutrient reduction in semi-enclosed seas, especially the estuarine area vulnerable to excessive phytoplankton growth and accumulate.

5.5 Conclusions

This study proposed a novel indicator for the MPSD, which was defined as the SD when the Chl.*a* concentration was equal to a reference Chl.*a* concentration. We used the MPSD and BSD to evaluate possible improvements in water clarity by reducing terrigenous anthropogenic nutrient loading. We found that phytoplankton largely did not control water clarity in this area and, therefore, improvements in water clarity could not be expected by reducing anthropogenic nutrient loading. The potential habitat of *Z. marina* L. is controlled by light availability; when the area with ≥20% surface irradiance was studied, *Z. marina* L. existed in 27% of the potential area (100 ha to 373 ha). The maximum recovery by SD improvements to the $MPSD_{0.5}$ was estimated at 36 ha. A modelling analysis on the impact of eelgrass recovery and expansion on phytoplankton growth from May to September found that improvements in Chl.*a* concentrations were achieved with concentrations decreasing to 1.0 to 3.0 μg l^{-1} from 4.0 to 7.0 μg l^{-1} from May to July. These findings could help us gain a better understanding of nutrient management in seagrass-vegetated semi-enclosed seas subjected to anthropogenic nutrient input.

5.6 References

Adams, S. M. 1976. The ecology of eelgrass, *Zostera marina* (L.), fish communities. I. Structural analysis. Journal of Experimental Marine Biology and Ecology 22:269−291.

Asaoka, S., A. Umehara, S. Otani, N. Fujii, T. Okuda, S. Nakai, W. Nishijima, K. Takeuchi, H. Shibata, and W. A. Jadoon. 2018. Spatial distribution of hydrogen sulfide and sulfur species in coastal marine sediments Hiroshima Bay, Japan. Marine pollution bulletin 133:891−899.

Bastyan, G. R., Cambridge, M. L. 2008. Transplantation as a method for restoring the seagrass *Posidonia australis*, Estuarine Coastal and Shelf Science 79:289−299.

Blumberg, A. F., and G. L. Mellor. 1978. A coastal ocean numerical model, in Mathematical Modelling of Estuarine Physics, Proc. Int. Symp., Hamburg.

Bocci, M., Coffaro, G., Bendoricchio, G., 1997. Modelling biomass and nutrient dynamics in eelgrass (*Zostera marina* L.): applications to the Lagoon of Venice (Italy) and Øresund (Denmark). Ecological modelling 102, 67−80.

ESRI 2011. ArcGIS Desktop: Release 10. Redlands, CA: Environmental Systems Research Institute.

Fukushima, T., T. Ishibashi, and A. Imai. 2001. Chemical characterization of dissolved organic matter in Hiroshima Bay, Japan. Estuarine, Coastal and Shelf Science 53:51−62.

IUCN 2018. The IUCN Red List of Threatened Species. Version 2018-1. <http://www.iucnredlist.org>. Downloaded on 05 July 2018.

Ishii, D. and T. Yanagi. 2004. Open ocean originated phosphorus and nitrogen in the Seto Inland Sea, Japan. Journal of Oceanography 60: 1001−1005.

Kasamo, K., Y. Shiraki, H. Shibaki and T. Yanagi 2016. Modeling of a spring larval Japanese anchovy (*Engraulis Japoneca*) flowing into Osaka Bay, Coastal, Proceedings of Coastal Engineering, JSCE, 72, 2, I_1381-I_1386 (in Japanese with English abstract).

Komatsu, T. 1997. Long-term changes in the Zostera bed area in the Seto Inland Sea (Japan), especially along the coast of the Okayama Prefecture. Oceanolica Acta 20:209−216.

Kraemer, G. P., Mazzella, L. 1999. Nitrogen acquisition, storage, and use by the co-occurring Mediterranean seagrasses *Cymodocea nodosa* and *Zostera noltii*, Marine Ecology Progress Series 183: 95−103.

Lee, K.-S., Park, S. R., Kim, Y. K. 2007. Effects of irradiance, temperature, and nutrients on growth dynamics of seagrasses: A review, Journal of Experimental Marine Biology and Ecology 350(1–2): 144–175.

Lefcheck, J. S., R. J. Orth, W. C. Dennison, D. J. Wilcox, R. R. Murphy, J. Keisman, C. Gurbisz, M. Hannam, J. B. Landry, and K. A. Moore. 2018. Long-term nutrient reductions lead to the unprecedented recovery of a temperate coastal region. Proceedings of the National Academy of Sciences 115:3658−3662.

Miyazawa, Y., Zhang, R., Guo, X., Tamura, H., Ambe, D., Lee, J.-S., Okuno, A., Yoshinari, H., Setou, T., Komatsu, K., 2009. Water mass variability in the western North Pacific detected in a 15-year eddy resolving ocean reanalysis. Journal of oceanography 65: 737−759.

Nakai, S., Y. Soga, S. Sekito, A. Umehara, T. Okuda, M. Ohno, W. Nishijima, and S. Asaoka. 2018. Historical changes in primary production in the Seto Inland Sea, Japan, after implementing regulations to control the pollutant loads. Water Policy 20:855−870.

Nakata, Kisaburo. 1993. Ecosystem model: its formulation and estimation method for unknown rate parameters. Journal of Advanced Marine Technology Conference 8:99−138 (in Japanese with English abstract).

Nishijima, W., A. Umehara, S. Sekito, F. Wang, T. Okuda, and S. Nakai. 2018. Determination and distribution of region-specific background Secchi depth based on long-term monitoring data in the Seto Inland Sea, Japan. Ecological Indicators 84:583−589.

Orth, R. J., K. L. Heck, and J. van Montfrans. 1984. Faunal communities in seagrass beds: a review of the influence of plant structure and prey characteristics on predator-prey relationships. Estuaries 7:339−350.

Park, J.-I., Lee, K.-S. 2007. Site-specific success of three transplanting methods and the effect of planting time on the establishment of Zostera marina transplants. Marine Pollution Bulletin 54:1238−1248.

R Core Team. R: A language and environment for statistical computing. 2015, Vienna, Austria.

Setouchi NET, Ministry of the Environment.
https://www.env.go.jp/water/heisa/heisa_net/setouchiNet/seto/index.html

Shoji, J., K. Sakiyama, M. Hori, G. Yoshida, and M. Hamaguchi. 2007. Seagrass habitat reduces vulnerability of red sea bream Pagrus major juveniles to piscivorous fish predator. Fisheries science 73:1281-1285.

Umehara, A., Asaoka, S., Fujii, N., Otani, S., Yamamoto, H., Nakai, S., Okuda, T., Nishijima, W., 2018. Biological productivity evaluation at lower trophic levels with intensive Pacific oyster farming of *Crassostrea gigas* in Hiroshima Bay, Japan. Aquaculture 495:311–319.

Verhagen, J. H. G. and P. H. Nienhuis. 1983. A simulation model of production, seasonal changes in biomass and distribution of eelgrass (Zostera marina) in Lake Grevelingen. Marine Ecology Progress Series 10:187-195.

Wang, F., Umehara, A., Nishijima, W., Nakai, S., 2019. Distribution of region-specific background Secchi depth in Tokyo Bay and Ise Bay, Japan, Ecological Indicators 98 : 397–408.

WFD CIS Guidance Document No. 20, 2009. Common Implementation Strategy for the Water Framework Directive (2000/60/EC), 46 pp

Chapter 6 Summary and Major Findings

1. Background Secchi depth is related to salinity and water depth in semi-enclosed seas and low background Secchi depths are generally observed in the inner regions adjacent to large rivers.
2. Phytoplankton's contributions to light attenuation are generally less than 40%.
3. Salinity, Secchi depth and water stability are the best factors to predict Chl.a concentration in the Seto Inland Sea.
4. Chl.a concentration and Secchi depth in the west-central Seto Inland Sea are mainly determined by salinity and distance to Honshu coast.
5. Eelgrass recovery is a good method to control the Chl.a concentration in northern Hiroshima Bay, reducing the Chl.a concentration by 1.0 to 3.0 μg l-1 from 4.0 to 7.0 μg l-1 from May to July.

List of Achievements

Original Papers

1. Nishijima, W., A. Umehara, S. Sekito, **F. Wang**, T. Okuda, and S. Nakai. 2018. Determination and distribution of region-specific background Secchi depth based on long-term monitoring data in the Seto Inland Sea, Japan. Ecological Indicators 84:583-589. (related to Chapter 2)
2. **Wang, F.**, A. Umehara, S. Nakai and W. Nishijima. 2019. Determination of region-specific background Secchi depth in Tokyo Bay and Ise Bay, Japan. Ecological Indicators 98: 397-408. (related to Chapter 2)
3. **Wang, F.**, A. Umehara, S. Nakai and W. Nishijima. 2019. Management of the west-central Seto Inland Sea, Japan: factors controlling the spatiotemporal distributions of chlorophyll a concentration and the Secchi depth. Water Policy. (related to Chapter 4)
4. Nishijima, W., **F. Wang**, Y. Uchida, A. Umehara, S. Nakai, K. Kasamo. Impact of eelgrass bed recovery and expansion on phytoplankton growth through nutrient competition. (Under Review, related to Chapter 5)

International Conferences

1. **Wang, F.**, A. Umehara, M. Ohno, S. Nakai and W. Nishijima. A new index for assessing phytoplankton growth potential in the Seto Inland Sea, Japan. The Third Asian Marine Biology Symposium, Kumamoto, Japan, Nov. 3 to 5, 2017. Oral Presentation (related to Chapter 3)
2. **Wang, F.**, A. Umehara, S. Nakai and W. Nishijima.. Determination of region-specific background Secchi depth in four temperate semi-enclosed seas, central Japan. 12th International Conference on the Environmental Management of Enclosed Coastal Seas, Pattaya, Thailand, Nov. 4 to 8, 2018. Oral Presentation (related to Chapter 2)
3. **Wang, F.**, A. Umehara, S. Nakai and W. Nishijima. Identification coastal zone vulnerable to phytoplankton growth in the Seto Inland Sea, Japan. The 9th International Conference on Marine Pollution and Ecotoxicology, Hong Kong, China, Jun. 10 to 14, 2019. Oral Presentation (related to Chapter 3)